UNIVERSIDAD AUTÓNOMA DE NUEVO LEÓN

FACULTAD DE CIENCIAS QUÍMICAS

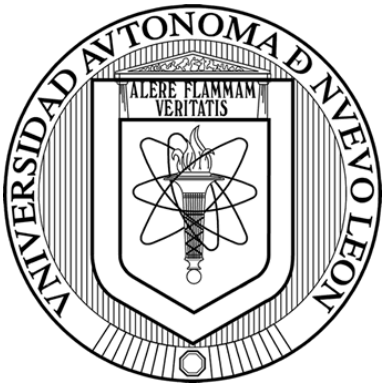

Synthesis and characterization of vinyl-oxadiazole derivatives and their *in-vitro* antifungal evaluation against drug-resistant fungi

Por:

LQI. MÓNICA EDITH ANAYA TAMEZ

Como requisito para obtener el grado de:

MAESTRÍA EN CIENCIAS CON ORIENTACIÓN EN FARMACIA

Mayo 2026

Synthesis and characterization of vinyl-oxadiazole derivatives and their *in-vitro* antifungal evaluation against drug-resistant fungi

Aprobación de la tesis

Dr. Francisco Guadalupe Avalos Alanís
Director de tesis

Dra. María del Rayo Camacho Corona
Comité tutorial

Dr. Eugenio Hernández Fernández
Co-director de tesis

Dra. Karla Ramírez Estrada
Comité tutorial

Dr. Efrén Ricardo Robledo Leal
Co-director de tesis

Dra. María Del Rosario González González
Comité tutorial

Dr. Javier Rivera de la Rosa
Subdirector de Posgrado

Acknowledgments

I would like to thank Universidad Autónoma de Nuevo León and Facultad de Ciencias Químicas, Universidad Autónoma de Nuevo León for the facilities and help provided to complete this project. I would also like to thank SECIHTI for the scholarship granted (CVU No. 1342471). I would like to thank Brigham Young University for the research done there. The Michaelis group receive me with open arms, answering every question and helping me with every challenge presented along the way. I would like to especially thank Emma and Karson for learning everything I had to teach them.

I would like to express my deepest gratitude to my advisor Dr. Francisco Avalos and my co-advisor Dr. Eugenio Hernández for their infinite patient while guiding through my classes and the project. I would also like to extend my gratitude to my tutorial committee, Dra. María del Rayo Camacho, Dra. Karla Ramírez and Dra. María Del Rosario González for all the valuable comments that helped shape this work.

I would like to express my deepest appreciation to the research group, Organic Synthesis Group, and all the friends I made during my time there. I´m certain that without them, my time in the laboratory would have been very boring and frustrating. My greatest thanks to Efren, Osvaldo, Tadeo, Martín and Luis for being by my side since the start of undergraduate studies. Other names (that if I don't include people will be sad) in no particular order are: Leydy, David, Keyel, Jabnia, Felipe, Torres, Adolfo.

Finally, I would like to thank my family, especially my parents and siblings, for all their support and kindness. Also, my 4 dogs who I love very much.

Resumen

Mónica Edith Anaya Tamez
Universidad Autónoma de Nuevo León
Facultad de Ciencias Químicas

Fecha de Graduación: Junio 2026

Título del Estudio: **Synthesis and characterization of vinyl-oxadiazole derivatives and their *in-vitro* antifungal evaluation against drug-resistant fungi**

Número de páginas: 91

Área de Estudio: Farmacia

Candidato para el grado de Maestría en Ciencias con Orientación en Farmacia

Propósito y Método de Estudio: En los últimos años las Infecciones Fúngicas Invasivas (IFI) han aumentado de gran manera en número y rapidez, principalmente por el aumento de resistencia de los hongos hacia los medicamentos actualmente accesibles. Por lo tanto, en este proyecto se realizó la síntesis y caracterización de ocho nuevos derivados de vinil-oxadiazol, la evaluación de su hepatotoxicidad *in vitro* contra células HepG2 y la evaluación de actividad antifúngica contra *Lomentospora prolificans* y *Scedosporium apiospermum in vitro*.

Contribuciones y Conclusiones: Se realizó la síntesis, caracterización estructural y determinación de la citotoxicidad *in vitro* de ocho nuevos derivados de vinil oxadiazol, obteniendo rendimientos químicos de 20-42% y porcentajes de viabilidad entre 89-98%. Los derivados de oxadiazol no presentaron actividad antifúngica contra *Lomentospora prolificans* y *Scedosporium apiospermum in vitro* a 700 µg/mL o concentraciones menores por lo que se rechaza la hipótesis presentada.

Dr. Francisco Guadalupe Avalos Alanís	Dr. Eugenio Hernández Fernández	Dr. Efrén Ricardo Robledo Leal
Director de tesis	Co-director de tesis	Co-director de tesis

Summary

Mónica Edith Anaya Tamez
Universidad Autónoma de Nuevo León
Facultad de Ciencias Químicas

Graduation Date: June, 2026

Study's Title: **Synthesis and characterization of vinyl-oxadiazole derivatives and their in-vitro antifungal evaluation against drug-resistant fungi**

Number of pages: 91

Candidate for MSc. Pharmacy degree

Study's Field: Pharmacy

Purpose and Study Methods: In the last years, the numbers of Invasive Fungal Infections (IFI) have greatly increased. One of the principal reasons for this is the increased of resistance towards commercial drugs in the fungi. For this reason, project presents the synthesis and characterization of eight new vinyl-oxadiazole, the evaluation of hepatotoxicity against the HepG2 cell line and antifungal activity against resistant *Lomentospora prolificans* and *Scedosporium apiospermum in vitro*.

Contributions and preliminary conclusions: The synthesis, structural characterization and *in vitro* cytotoxicity determination of eight new vinyl oxadiazole derivatives were carried out for their possible application as antifungal agents against drug-resistant fungi, obtaining chemical yields of 20-42% and viability percentages between 89-98%. The oxadiazole derivatives did not show activity against resistant *Lomentospora prolificans* and *Scedosporium apiospermum in vitro* at 700 µg/mL or lower concentrations. As a result, the hypothesis presented is rejected.

Dr. Francisco Guadalupe Avalos Alanís	Dr. Eugenio Hernández Fernández	Dr. Efrén Ricardo Robledo Leal
Thesis Director	Thesis Co-director	Thesis Co-director

Synthesis and characterization of vinyl-oxadiazole derivatives and their *in-vitro* antifungal evaluation against drug-resistant fungi

Presented by:

LQI. Mónica Edith Anaya Tamez

The present research project was done at Laboratorio de Química Industrial, of Centro de Laboratorios Especializados (CELAES) of Facultad de Ciencias Químicas, UANL, under the supervision of Dr. Francisco Guadalupe Avalos Alanís, Dr. Eugenio Hernández Fernández and Dr Efrén Ricardo Robledo Leal, with resources given by Secretaría de Ciencia, Humanidades, Tecnología e Innovación (SECIHTI) with the projects CF-2023-I-1693 and FARMC-105526-FGAA-24/08 and scholarship 1342471.

Table of contents

List of Schemes

List of Figures

List of Tables

List of Appendices

List of abbreviations

Amb	Amphotericin B
bs	Broad singlet
C. albicans	*Candida albicans*
C. auris	*Candida auris*
CO_2	Carbon dioxide
CYP51	Lanosterol 14α-demethylase
D_2O	Deuterium
DMSO	Dimethyl sulfoxide
d	Doublet
EMEM	Eagle's minimum essential medium
eq	Equivalent
EtOH	Ethanol
EtOAc	Ethyl acetate
Flz	Fluconazole
Hz	Hertz
Hex	Hexane
HRMS	High-resolution mass spectrometry
HUVEC	Human umbilical vein endothelial cells
HCl	Hydrochloric acid
FT-IR,	Infrared spectroscopy
IFI	Invasive fungal infections
L. prolificans	*Lomentospora prolificans*
µg	Microgram
µL	Microlitre
µM	Micromolar
MW	Microwave

mL	Milliliter
mm	Millimeter
MIC	Minimum inhibitory concentration
m	Multiplet
DCC	*N*,*N*-dicyclohexylcarbodiimide
NMP	*N*-methyl-2-pyrrolidone
^{13}C NMR	Nuclear magnetic resonance of Carbon-13
^{1}H NMR	Nuclear magnetic resonance of Hydrogen
KN_3	Potassium azide
q	Quartet
S. apiospermum	*Scedosporium apiospermum*
S. aurantiacum	*Scedosporium aurantiacum*
S. boydii	*Scedosporium boydii*
S. boydii	*Scedosporium boydii*
S. minutisporium	*Scedosporium minutisporium*
s	Singlet
$NaHCO_3$	Sodium bicarbonate
NaOH	Sodium hydroxide
SAR	Structure activity relationship
TLC	Thin-layer chromatography
t	Triplet
Vor	Voriconazole
WHO	World Health Organization

1. Introduction

1.1. Fungi

Fungi are one of the seven biological kingdoms. With fossils from around one billion years and an estimated between 11.7 and 13.2 million species, fungi constitute one of the oldest and diverse groups of eukaryotic microorganisms on earth (1,2).

Fungi are eukaryotic, heterotrophic (they do not produce photosynthesis), osmotrophic (they absorb their food, they digest it externally), and reproduce by means of spores (3). Depending on the organism, it can be unicellular or multicellular, and its morphology can vary based on the mode of cellular division. They can grow either as yeast or as filamentous fungi (4).

1.1.1. Filamentous fungi

Filamentous fungi, commonly called mold, are one of the two big groups that divide true fungi. They grow by the extension of hypha. The hypha is a vegetative organ in fungi in charge of many things, mainly to explore the surroundings and to assimilate the nutrients in the environment (3,4). They can grow with or without a wall division (called septum), branching itself repeatedly as the spread, forming complex arrangements known as mycelium (4,5).

1.1.2. Pathogenic Fungi

The human body is not an exception for the ubiquity of fungi. They are part of the microflora inside the body and can exist in equilibrium with its host without causing major problems. In a healthy person, fungi are usually not a match for the human immune system, but under certain conditions they can become infectious (6,7).

Superficial infections are the most common type of fungal infections. Skin, nails and hair are the first contact the body has with environmental fungi, and even with the many barriers they must protect its host (including a specialized immune system), some fungi have evolved ways to avoid them and colonize the skin (6,8,9). Subcutaneous infections can also happen, most cases through penetrating trauma, but tend to stay localized to the site of inoculation (10). In healthy individuals, the risk doesn't go beyond

these types of fungal infections, but when the immune system is compromised, fungi can colonize deep tissue and become invasive (11).

1.2. Invasive Fungal Infections

Invasive Fungal Infections (IFI) occur when the fungus is isolated from blood and other sterile sites, and it's deep seeded in a specific organ. Not all pathogenic fungi can become invasive, but those who do must be able to endure and grow at the human body temperature, reach and penetrate tissue. Invasive fungi are usually opportunistic and cause infections when the host defenses are down. The list of life-threatening opportunistic fungi increases each year and is now larger than ever (12).

IFI are serious infections, with high mortality rates and long treatment times. Medicine in low- and middle-income countries is usually hard to come by (13). They are one of the leading causes of infections in the intensive care unit and contribute up to 50% of mortality among people living with HIV (14,15). In the last decade, they have risen due to the increased number of patients undergoing immunosuppression therapies (12,16).

Reliable and quick diagnosis are changeling, especially in developing or lower income countries, as they involve high costs, special infrastructure and tests are not easily available (15). A study conducted in México in 2025 showed that most HIV-dedicated health care centers in the country did not have the capacity to diagnose IFI, and rapid tests were frequently unavailable (15).

Due to the rising problem, in 2022, the World Health Organization (WHO) issue the first fungal priority pathogen list as a tool to encourage research focus towards IFI and facilitate international coordination to prevent and combat IFI. Nineteen different fungi were ranked and grouped into three categories (critical, high and medium priority group) depending on different criteria like number of deaths, annual incidences and antifungal resistance, this last one having the highest importance weight at the moment of ranking. From the list, *Lomentospora prolificans* and *Scedosporium* spp have the highest antifungal resistance, making them a priority by the WHO even though they have the lowest incidence between the fungi in the list. Besides their high resistance, they present other problems like almost no studies or data, low preventability, moderate access to diagnosis

and low availability and affordability of treatments. All these characteristics renders them a growing global health threat (13).

1.2.1. Lomentospora prolificans

The genus *Lomentospora* was proposed in 1974, when *Lomentospora prolificans* was isolated from greenhouse soil in Belgium. Since then, the name suffered changes through the years (17). In 1984 it was synonymized to *Scedosporium inflatum*, in 1991 the species returned to its original name, *Scedosporium prolificans* and finally, in 2014 after enough evidence of distinguishable morphology was found, *Lomentospora* was established as a new genus with *Lomentospora prolificans* as the only species (18–20).

L. prolificans exhibits a global distribution, with a significant preference for dry climate countries such as Southern USA, European regions such as Spain and Australia. This last one presented around 8 times more cases per million population than the average number of all countries (21). The fungus can be isolated principally from the soil, but has appeared in other sources such as cattle dang, sewage, polluted waters, plants and decaying organic matter (22,23).

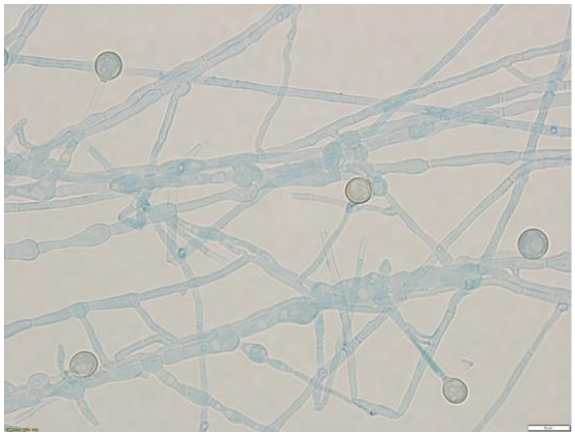

Figure 1. *Lomentospora prolificans*-induced Invasive Fungal Sinusitis (24), CC BY SA 4.0.

Reports of invasive *L. prolificans* infections started around 1984 in both immunocompetent and immunocompromised patients (25). Patients with conditions such as malignancy, cystic fibrosis and solid organ transplantation (especially hematopoietic stem cell transplant) are the biggest risk group. Invasive lomentosporiosis show a mortality rate close to 47%. Early diagnosis is difficult, and treatment is often delayed

because of this (26). After the initial infection, dissemination is frequent (around 80% of all cases), in this case, the mortality rate can go up to 87%, as mentioned by Konsoula *et al* (21,22,27).

Since its discovering, *L. prolificans* showed an intrinsic resistance against most antifungal drugs, making the treatment a big challenge. Voriconazole has presented the best *in vitro* activity against it, and it's suggested as the first-line monotherapy with successful outcomes between 25% and 66%. Combination therapy has proved to increase 28-day survival, the increase rate depending on the combination. The most popular combinations being amphotericin B with pentamidine, amphotericin B with voriconazole, and voriconazole with terbinafine (21,22).

Due to the high mortality rates, lack of studies and extremely high resistance to commercial antifungal drugs, and rarity of infections, the World Health Organization has ranked this pathogen as a medium priority in the fungal priority pathogens list, in order to promote research on it (13).

1.2.2. Scedosporium

Scedosporium spp is a fungal genus all around the globe, although different species can be found in different regions (21). The name of the genus was proposed in 1911 by Saccardo, P.A., who, while isolating a case of eumycetoma, described the fungus found as *Monosporium apiospermum* but with morphological similarities with *Monosporium acremonioides*. The name was then validated in 1919 as *Scedosporium apiospermum* instead of *Monosporium* (28).

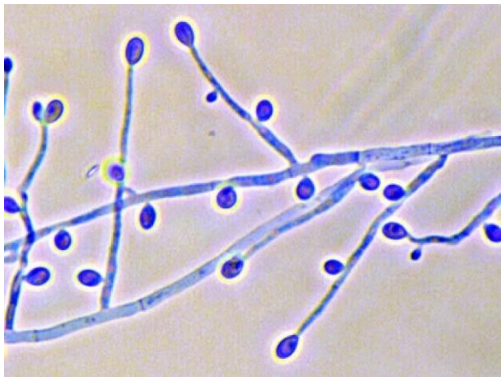

Figure 2. *Scedosporium apiospermum* conidiophores and conidia (29), CC BY SA 4.0.

Scedosporium species are soil saprophytes (decomposing microorganisms), mostly found in temperate climates and not so much in the tropical countries (30). At the same time, correlation has been found with diesel fuel concentration and *Scedosporium* spp. abundance, so they are more likely to be found in cities with high population density (31).

In the matters of medicine, *S. boydii*, *S. apiospermum*, *S. aurantiacum* and *S. minutisporium* are the most reported species of *Scedosporium*, infecting people all around the world. The last one is the second most colonizing filamentous fungi in patients with cystic fibrosis (21,28,30). The countries with most reported cases have been United States, Australia, Germany, India, Spain and Japan (21). In Mexico, *S. apiospermum* and *S. boydii* have been identified in the soil of a wide range of places (32).

As is the rule with opportunistic pathogens, the biggest group at risk for invasive *Scedosporium* infections are immunocompromised patients. Solid organ transplant and hematological disease treatments are usually the biggest risk factors. The most common mode of infection is by traumatic inoculation (surgery or intravenous drug injection for example) or by aspiration of contaminated water. Victims of tsunamis, earthquakes or near drowning situations have been detected as a high-risk group for invasive scedosporiosis (21,32). Infections in patients with hematological malignancy and advanced HIV infection can also happen (31).

Mortality rates for infections can go as high as 42-46%, with some studies (WHO and Cortez *et al*) claiming a mortality rate of over 75% (13,33–35). After initial colonization, dissemination is common. Central nervous system infections can appear in case of high dissemination and are most common in near drawing victims (31). Other complications related to scedosporiosis are allergic bronchopulmonary mycoses, skin manifestations (necrotic papules and hemorrhagic bullae), muscle, joint, bone infections, and endocarditis and other intravascular infections (31).

Besides voriconazole, the most common antifungal drugs for IFI are not effective against *Scedosporium* spp., and show a high minimum inhibitory concentration for the species. For this reason, monotherapy with voriconazole is presented as the first-line

antimycotic drug against scedosporiosis (21,28). Combination therapy can be done with amphotericin B or echinocandins, as increase efficacy has been proved, but due to toxicity caused by the drugs or by pre-existing organ damage, is not recommended unless necessary (21,32).

Due to the high mortality rates, lacking on preventive measures, lack of studies and extremely high resistance to commercial antifungal drugs, and rarity of infections, the World Health Organization has ranked this pathogen as a medium priority in the fungal priority pathogens list, to promote research on it (13).

Table 1 shows a comparison between *Scedosporium* spp. and Lomen*tospora prolificans*.

Table 1. Comparison between *Lomentospora prolificans* and *Scedosporium* spp.

	Lomentospora prolificans	*Scedosporium* spp.
Location	Dry climate countries across the globe	Ubiquitous
Mortality rate (%)	47-87	42-46
First line medication	Voriconazole	Voriconazole
Resistance to	No current licensed antifungal has *in vitro* activity	Amphotericin B, itraconazole, isavuconazole and echinocandins
Rank in the WHO in the FPP.	Medium Priority	Medium priority

1.3. Azole Antifungals

1.3.1. Current Antifungals

In modern times there are five types of antifungals in the market; Polyenes, pyrimidine analogs, allylamines, echinocandins and azole derivatives (**Figure 3**) (36). Each type is used in specific cases, nevertheless, azole derivatives are preferred to the other types, as they are still active against most fungi infections while remaining safe to the patients.

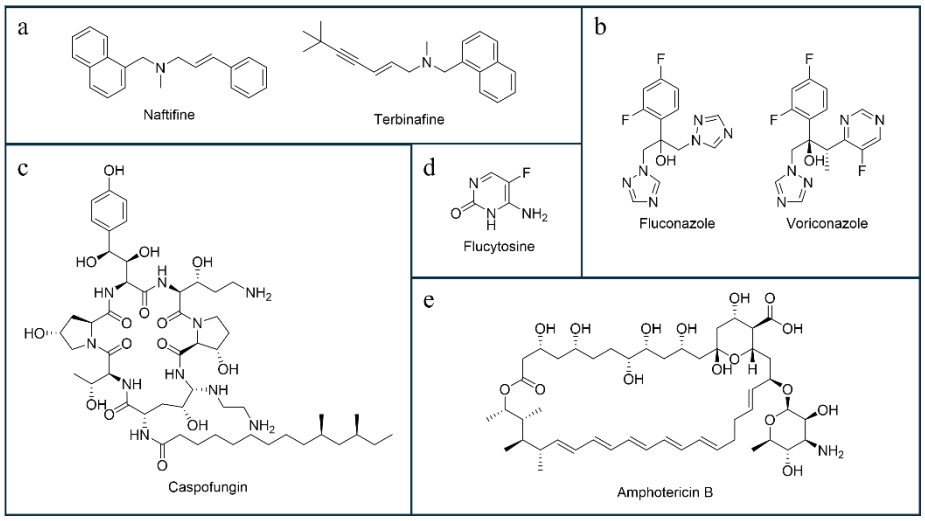

Figure 3. Commercial examples of a) allylamine, b) azole, c) echinocandin, d) pyrimidine, and e) polyene antifungals.

Despite the wide range of antifungals, their unregulated use in medicine, agriculture (crops protection), wood industry (timber preservation) and livestock is leading to global increase of antifungal resistance (36) Intrinsic resistance and acquired multidrug resistance are reducing treatment options, stressing the need for new and better antifungals.

1.3.2. Azole derivatives

The azole derivatives englobe both the triazole and the tetrazole derivatives. They are the most widespread end employes type of antifungals among all the types, due to their activity and low toxicity compared to other groups. Voriconazole is usually the drug of choice even before amphotericin B. Azole derivatives are associated with high rate of resistance due to their fungistatic activity, but even then, their safety margin makes them more popular than other types of antifungals. Examples of azole derivative drugs in the market are fluconazole and voriconazole (**Figure 4**) (37).

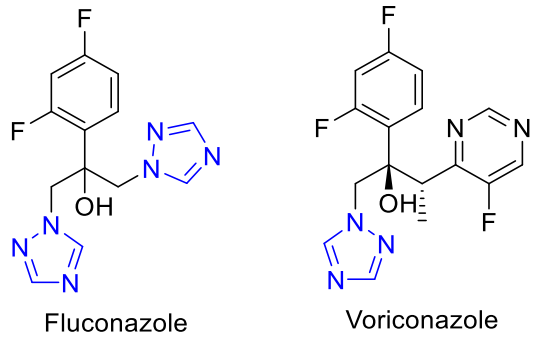

Figure 4. Fluconazole and voriconazole structures.

1.3.3. Action mechanisms

Azole antifungals work by the inhibition of the enzyme lanosterol 14α-demethylase (CYP51) (**Figure 5**). The enzyme is involved in the third reaction of the ergosterol biosynthesis in fungi. Ergosterol is an important sterol in fungi in charge of regulating the membrane, its fluidity and cellular responses (38).

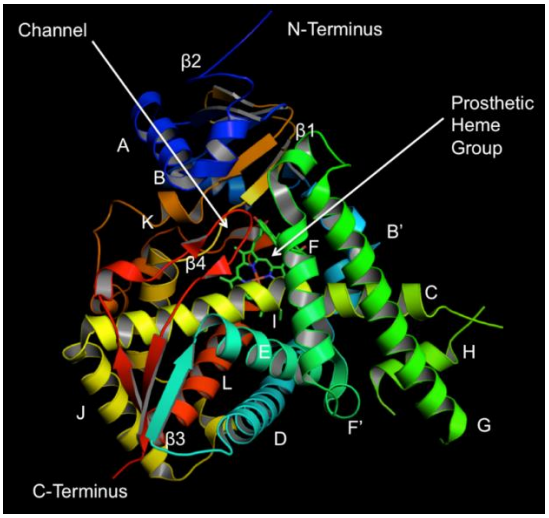

Figure 5. Structure of lanosterol 14 α-demethylase (CYP51) (39) CC BY SA 4.0.

1.3.4. Structure

An azole is a five-member heterocycle containing one or more nitrogen atoms in its structure, different azoles have been used in drugs though history. The first generation of azole antifungals had an imidazole ring in its structure. Due to high hepatoxicity, the second generation changed the imidazole ring for a triazole, which greatly lowered the side-effects, and was not changed until the fourth generation. This last generation changed

the triazole ring for a tetrazole in the hopes that the change could resolve the drug-drug interactions problem caused by human CYP3A4 enzyme inhibition (40,41).

A pattern can be seen, were the higher the number of nitrogen atoms in the ring (**Figure 6**), (and by consequence, the lower the basicity of the ring) the higher the selectivity against the human CYP450 enzymes is (lower toxicity). Other azole derivatives such as the oxadiazole ring have lower basicity than the tetrazole ring. Structure Activity Relationship (SAR) studies have proven this, along with use of amines and heteroaromatic groups in the side chain can enhance activity by making hydrophobic and hydrogen-bonding interactions with the enzyme (40).

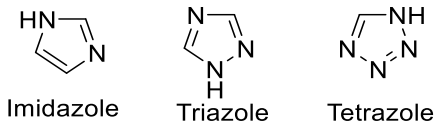

Figure 6. Structure of the imidazole, triazole and tetrazole ring.

1.3.5. Toxicity

The toxicity of azole derivatives lies mostly in the liver and doesn't generally show other side-effects. They don't present any incidence of cardiac disorder. They are associated with a lower incidence in general disorders (including pyrexia, weight loss, chills, etc.), renal, urinary, respiratory, thoracic, mediastinal and skin disorders than amphotericin B (42).

1.3.6. Resistance

Resistance to azole derivatives was reported in late 80´s, when systemic active azoles were introduced to the market (43). One of the most reported causes of azole resistance is the use of broad-spectrum azole fungicides in agriculture. USA use of azole fungicide raised more than 400% from 2006 to 2016 (3, 000 metric tons per year) and is reported than China uses approx. 10 times that amount (30, 000 metric tons per year) (44,45).

Antifungal resistance is presented by change in the effect of the drug-target interaction. The primary mechanism of resistance presented against azoles is the increase of effluxed

drug in the fungal cell, which can be a result of increased expression of efflux pumps, or duplication chromosomes associated with efflux genes (43,44,46).

Another mechanism of resistance is the mutation in the drug target, such as the mutation of the lanosterol 14α-demethylase to prevent azole binding, mutation in the promoter region to increase the formation of the enzyme, increasing the intracellular concentration (45–47).

2. Background

As awareness of the problem that IFIs presents grows, new studies are made to overcome the knowledge gap. These studies offer new perspectives on the use of oxadiazoles as antifungal agents for their future use in medicine; and were used as foundation for the present project.

2.1.Antifungal Properties

In 2011, Sadek B. *et al.* (48) synthesized a series of oxazole, oxadiazole, tetrazole, and thiazole derivatives, all containing 4-hydroxyphenyl as a substituent. The *in vitro* antimicrobial activity of the compounds was evaluated against different microorganisms including *Aspergillus niger* (*A. niger*). Compounds **A1-6** showed good antifungal activity against *A. niger* (25 μg/mL) and the best antimicrobial activity among the six derivatives, with a MIC six to eight times lower than the oxazole, tetrazole, and thiazole derivatives (150-200 μg/mL), see **Figure 7**.

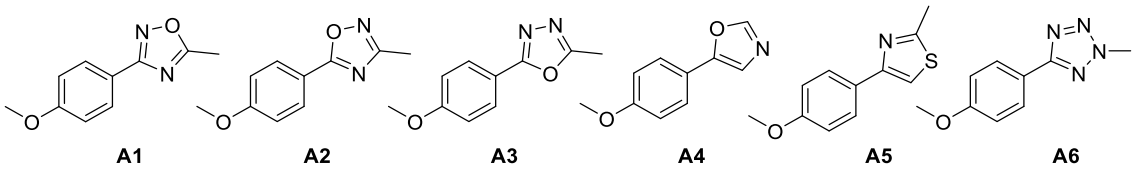

Figure 7. Oxazole, oxadiazole, tetrazole, and thiazole derivatives **A1-6** with antifungal activities against *Aspergillus niger*.

In 2013, Ningaiah S. *et al.* (49) developed a series of twenty-one pyrazolyl-1,2,4-oxadiazole and pyrazoline amidoxime derivatives, and their *in vitro* antioxidant, antimicrobial, and anti-inflammatory activities were determined. Antifungal activity, based on the measurement of the inhibition zone, against *A. niger* and *A. flavus* was determined using fluconazole as the reference drug. Oxadiazoles **B1-3** showed the best antifungal activity against *A. flavus* (at 50 μg/mL) with inhibition zones of 15 ± 0.12 mm, 14 ± 0.15 mm, and 16 ± 0.13 mm respectively, similar values to fluconazole (16 ± 0.18 mm), see **Figure 8**. In general, the activity of the compounds with the substituent on the *para* position in the ring was close to 40% more active against the mentioned fungi. Oxadiazoles **B1**, **B4,** and **B5** showed the best antifungal activity against *A. niger* with a MIC of 5 μg/mL, the same that fluconazole.

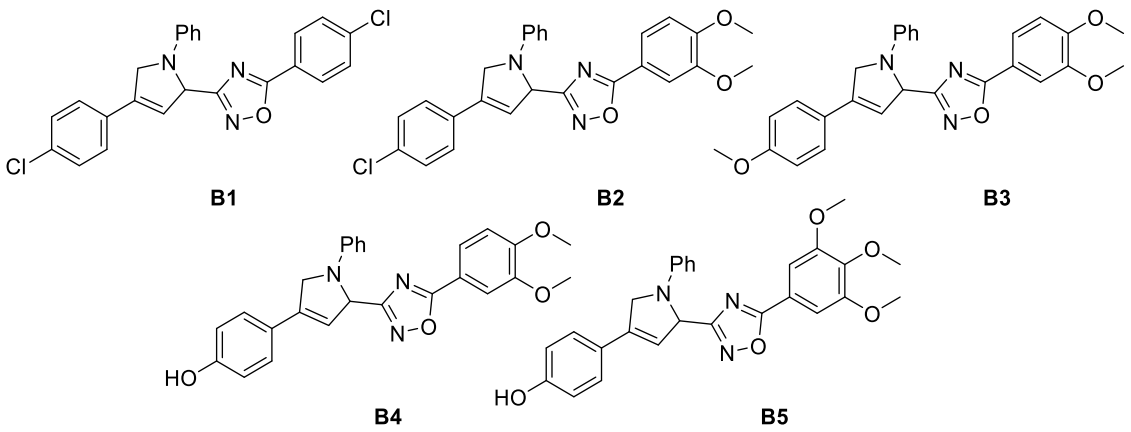

Figure 8. Oxadiazole derivatives **B1-5** with antifungal activities against *Aspergillus niger* and *Aspergillus flavus*.

In 2019, Rodrigues-Vendramini *et al.* (50) evaluated the *in vivo* cytotoxicity and antifungal activity of compounds **C1** and **C2** against nine isolates of *Paracoccidioides spp*), shown in **Figure 9**. The MIC ranged from 1 to 32 µg/mL for compound **C1** and 8 µg/mL for compound **C2** for all the isolates. *In vivo* toxicity assays showed no differences in the body weight of the mice, the hematological profile, and the macroscopic analysis of the organs after two weeks. Histopathological analysis showed no significant difference between the two compounds and itraconazole (reference drug) in the reduction of fungal cells present in the histological lung section.

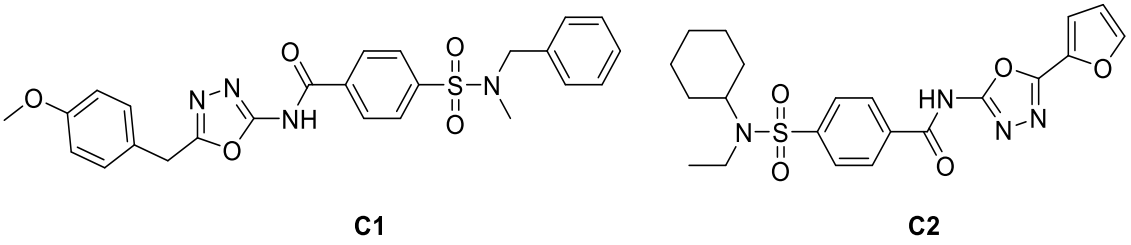

Figure 9. Oxadiazole derivatives **C1-2** with antifungal activities against *Paracoccidioides* spp.

In 2019, Greiner-Capoci *et al.* (51), seeing Rodrigues-Vendramini results, determined the *in vitro* cytotoxicity and antifungal activity of compounds **C1** and **C2** against *Candida albicans*. The first analysis was done at different concentrations (0.5–256 µg/mL) in two cell lines (Vero and HUVEC) of the two oxadiazoles and showed no significant cytotoxicity for compound **C1** and an IC_{50} at 256 and 128 µg/mL for the

HUVEC cell line for compound **C2**. The antifungal analysis showed a MIC of 32 µg/mL for both compounds, about a quarter of their IC_{50}, making them safe for use at their MIC.

In 2020, Das R. *et al.* (52) synthesized a series of eight chloro-aryl-oxadiazole derivatives and analyzed their antifungal activity against *C. albicans* and *A. niger,* shown in **Figure 10**. Derivatives **D1-3** showed the best antifungal activity with a zone of inhibition of 22 - 23 mm for *C. albicans* and 23 - 25 mm for *A. niger*. Miconazole was used as reference drug and exhibited a zone of inhibition of 26.3 ± 0.47 mm and 28 ± 0.86 mm, respectively. Compound **D1** also showed an MIC of 12.5 µg/mL, lower than miconazole (25 µg/mL), while **D2** and **D3** showed the same MIC as the reference.

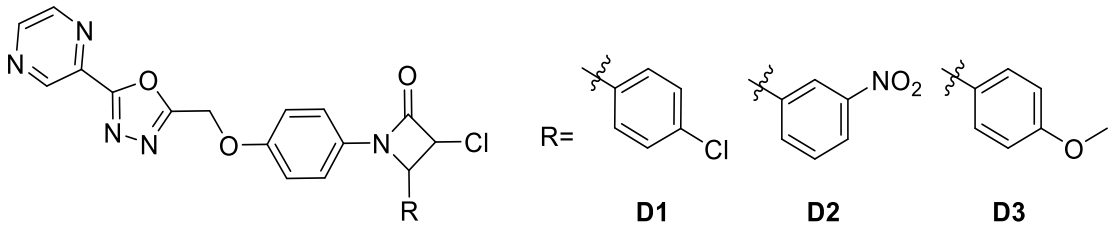

Figure 10. Chloro-aryl-oxadiazole derivatives **D1-3** with antifungal activities *Candida albicans* and *Aspergillus niger*.

In 2022, Hamdy R. *et al.* (53) synthesized a series of fifteen oxadiazole derivatives and analyzed their antifungal activity against *C. albicans* and *C. auris,* shown in **Figure 11**. Compounds **E1**, **E2**, **E3,** and **E4** showed great antifungal activity as they significantly inhibited the growth of *C. albicans* by 57%, 83%, 99%, and 80%; and C. *auris* by 86%, 85%, 99%, and 40%, respectively, at the screening dose of 100 µg/mL. The MIC_{50} ranged from 0.5 to 10 µM compared to fluconazole (25 ± 0.12 µM) for *C. albicans*, and from 0.8 to 30 µM compared to fluconazole (600 ± 0.45 µM) for *C. auris*.

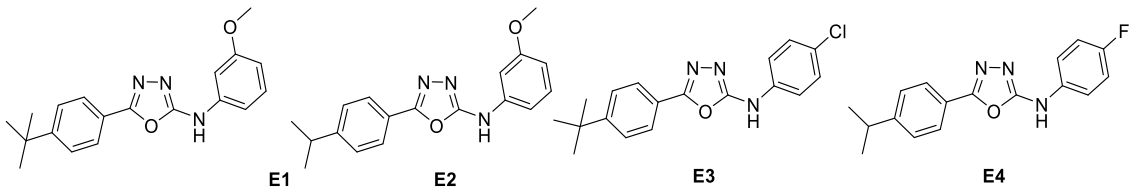

Figure 11. Oxadiazole derivatives **E1-4** with antifungal activity against *Candida albicans* and *Candida auris*.

2.2.Synthesis

1,3,4-oxadiazoles have been synthesized in a variety of ways across the years. Cyclocondensations using a carbonyl group and hydrazides, oxidative cyclization of hydrazones, dehydrative cyclization of diacyl hydrazides and Huisgen's rearrangement with tetrazoles and activated carboxylic acids are a few examples (**Figure 12**).

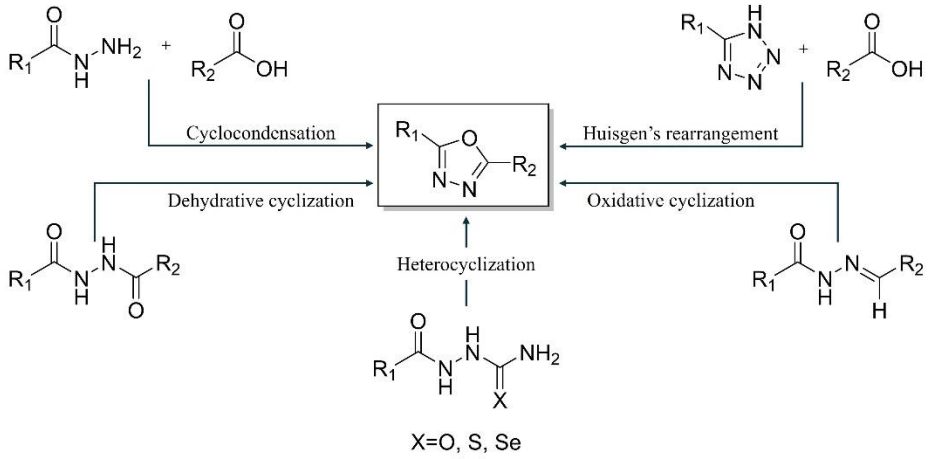

Figure 12. Possible methods for the preparation of 1,3,4-oxadiazoles (54).

Dehydrative cyclization of diacyl hydrazides has been the most popular way to prepare 1,3,4-oxadiazoles is, however, these reactions need strong conditions and reagents like $SOCl_2$, SOF_2, $POCl_3$ or P_2O_5. While chemical yields are often good, the use of toxic or environmental hazard reagents is the principal reason why other ways to synthesize oxadiazoles are on the rise (55,56). The use of tetrazoles as an has been proposed as an alternative to synthetize 1,3,4-oxadiazoles showing good chemical yields and the option to use greener coupling agents and solvents like DCC and EtOH or ACN (57,58).

2.3.Critical Analysis

As shown in the studies mentioned beforehand, oxadiazole derivatives show a high potential for their use in novel antifungal agents. However, studies on these derivatives have been made almost only in *Candida* and *Aspergillus* species. While these fungi are guilty of most fungal infections, the lack of fungal diversity in the studies creates a big knowledge gap when medical treatment is planned for rarer mold infections. To overcome this problem, the present project decided to evaluate the antifungal effect against

uncommon but medically important molds, due to their previously mentioned resistance (*Lomentospora prolificans* and *Scedosporium apiospermum*).

2.4.Hypothesis

At least one of the vinyl-oxadiazole derivatives will exhibit greater antifungal activity than the reference drug, voriconazole, against drug-resistant strains of *Scedosporium apiospermum* and *Lomentospora prolificans*.

2.5.Objectives

2.5.1. General Objectives

To synthesize vinyl-oxadiazole derivatives **6a-h** and to evaluate their cytotoxicity and *in vitro* antifungal activity against drug-resistant *Scedosporium apiospermum* and *Lomentospora prolificans*.

2.5.2. Specific Objectives

1. To synthesize the phenyl tetrazole **2**.
2. To synthesize the cinnamic acid derivatives **5a**-**h**.
3. To synthesize the vinyl-oxadiazole derivatives **6a**-**h**.
4. To structurally characterize compounds **2**, **5a**-**h**, **6a**-**h** by means of infrared spectroscopy (FT-IR), nuclear magnetic resonance of hydrogen and carbon-13 (^{1}H and ^{13}C NMR) and high-resolution mass spectrometry (HRMS).
5. To evaluate the cytotoxicity *in vitro* of the compounds against the HepG2 cell line (liver cells) using the CellTiter-Blue (resazurin) colorimetric technique.
6. To evaluate the antifungal susceptibility *in vitro* of the compounds **6a**-**h** against drug-resistant fungi (S*cedosporium apiospermum* and *Lomentospora prolificans*).

3. Materials and Methods

3.1.Instruments

The organic synthesis was carried out in Laboratorio de Química Industrial (Centro de Laboratorios Especializados, FCQ-UANL) and in the Department of Chemistry and Biochemistry (Brigham Young University, Provo). The equipment employed included the microwave reactor Anton Paar Monowave 300. Melting points were registered using an Electrothermal Mel-Temp apparatus and are uncorrected. Thin-layer chromatography (TLC) was performed with coated commercial silica gel plates (silica gel 60 F254, E. Merck). Compounds were revealed using UV lamps (254 and 365 nm, Spectroline). The biologic studies were conducted in the Department of Chemistry and Biochemistry (Brigham Young University, Provo) and Laboratorio de Micología y Fitopatología (FCB-UANL).

The structural characterization of the compounds was carried out in the following Laboratories: Nuclear Magnetic Resonance and Hight resolution Mass Spectrometry (HRMS) (Ezra Taft Benson building at Brigham Young University, Utah, USA) and Infrared Spectroscopy (Laboratorio de Análisis instrumental FCQ-UANL).

Proton nuclear magnetic resonance (^{1}H-NMR) and Carbon-13 nuclear magnetic resonance (^{13}C-NMR) data was acquired on a Bruker 500 MHz spectrometer. Chemical shifts (δ) are reported in ppm (parts per million). Signals are reported as follows: s (singlet), bs (broad singlet), d (doublet), t (triplet), q (quartet), m (multiplet). Coupling constants were expressed as (*J*) and reported in Hertz (Hz). Infrared spectra were acquired with an ATR-FT-IR Perkin Elmer Spectrum-One. HRMS data was acquired with an Agilent, 6210 TOF. Cell count was performed with a Countess 3 Automated Cell Counter. Fluorometric assay data was adquired on a BioTek Synergy Neo2 Hybrid Multimode Reader.

All reagents were acquired from Sigma-Aldrich and Combi Blocks and were used without prior treatment or purification.

3.2.Synthetic methodology

The synthesis of the vinyl-oxadiazoles **6a-h** followed a three-step process shown in **Scheme 1**.

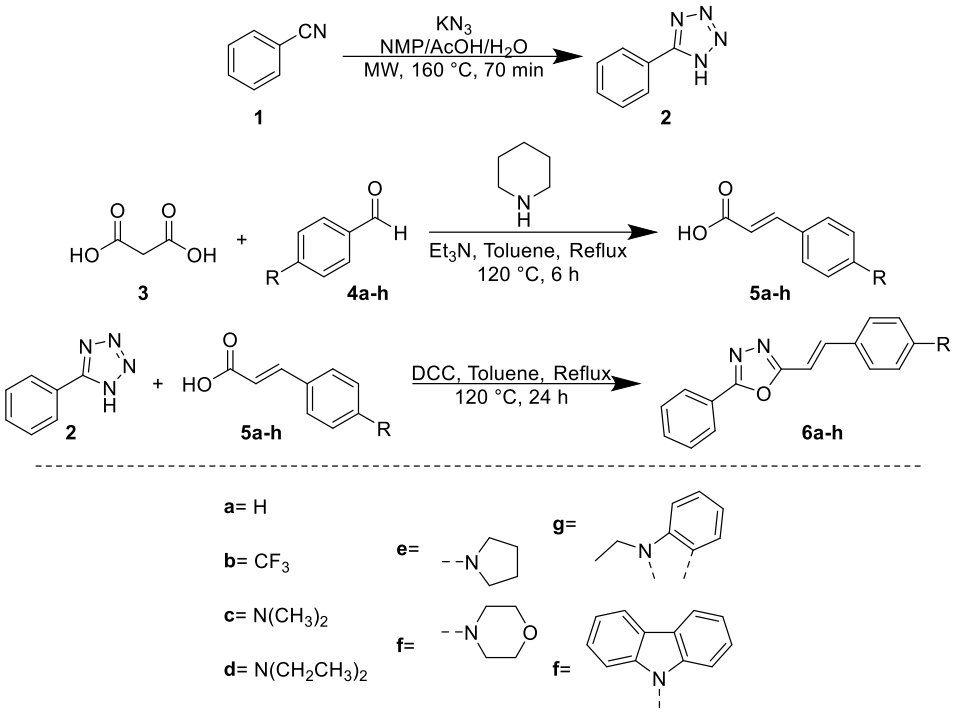

Scheme 1. Synthetic route to obtain vinyl-oxadiazole derivatives **6a-h**.

*3.2.1. Synthesis of 5-phenyl-1H-tetrazole **2***

In a G-30 microwave vessel, provided with a magnetic stirrer, 1 eq of benzonitrile and 1.2 eq of KN_3 (potassium azide) were added, along with 5 mL of N-methyl-2-pyrrolidone (NMP), 3 mL of distilled water, and 2 mL of acetic acid. The mixture was heated for 70 minutes at 160 ºC under microwave (MW) irradiation. The reaction progress was monitored by TLC using Hexane (Hex):Ethyl Acetate (EtOAc) 7:3 v/v. When the reaction was completed, it was basified in a beaker using a saturated $NaHCO_3$ (sodium bicarbonate) solution until it reached pH 10. The resulting mixture was extracted three times with 20 mL of ethyl acetate (3 x 20 mL). The aqueous phase was acidified with HCl (hydrochloric acid) until precipitation. The solid obtained was filtered and rinsed with cold water and dried.

*3.2.2. Synthesis of Cinnamic acid derivatives **5c-h***

In a round-bottom flask, provided with a magnetic stirrer, 1 eq of malonic acid **3**, 1.5 eq of triethylamine, and 30 mL of toluene as reaction medium were added. The mixture was heated at 100 °C for 30 minutes. Next, 0.2 eq of piperidine and 0.8 eq of the corresponding aldehyde **4c-h** were added, and the mixture was placed under reflux for 6 hours. The progress of the reaction will be monitored by TLC using Hex:EtOAc (7:3 v/v). After the completion of the reaction, 30 mL of NaOH (sodium hydroxide) aqueous solution (pH 12) was added to the flask and placed in stirring for 30 minutes. The resulting mixture was extracted three times with 10 mL of distilled water (3 x 10 mL). The aqueous phase was acidified with HCl 12 M until precipitation. The solid obtained was filtered and washed with cold water and dried. Cinnamic acids **5a** and **5b** were not synthetized and brought instead.

3.2.2.1. Synthesis of (*E*)-3-(4-(dimethylamino)phenyl)acrylic acid **5c**

Following the general procedure, in a round-bottom flask, provided with a magnetic stirrer, 1.0051 g of malonic acid **3**, 2 mL of triethylamine, and 30 mL of toluene as reaction medium were added. After 30 minutes 190 µL of piperidine and 1.146 g of 4-(dimethylamino)benzaldehyde **4c** were added.

3.2.2.2. Synthesis of (*E*)-3-(4-(diethylamino)phenyl)acrylic acid **5d**

Following the general procedure, in a round-bottom flask, provided with a magnetic stirrer, 1.0029 g of malonic acid **3**, 2 mL of triethylamine, and 30 mL of toluene as reaction medium were added. After 30 minutes 190 µL of piperidine and 1.362 g of 4-(diethylamino)benzaldehyde **4d** were added.

3.2.2.3. Synthesis of (*E*)-3-(4-morpholinophenyl)acrylic acid **5e**

Following the general procedure, in a round-bottom flask, provided with a magnetic stirrer, 1.0038 g of malonic acid **3**, 2 mL of triethylamine, and 30 mL of toluene as reaction medium were added. After 30 minutes 190 µL of piperidine and 1.469 g of 4-(pyrrolidin-1-yl)benzaldehyde **4e** were added.

3.2.2.4. Synthesis of (*E*)-3-(4-(pyrrolidin-1-yl)phenyl)acrylic acid **5f**

Following the general procedure, in a round-bottom flask, provided with a magnetic stirrer, 0.9982 g of malonic acid **3**, 2 mL of triethylamine, and 30 mL of toluene as reaction medium were added. After 30 minutes 190 µL of piperidine and 1.346 g of 4-morpholinobenzaldehyde **4f** were added.

3.2.2.5. Synthesis of (*E*)-3-(9-ethyl-9H-carbazol-3-yl)acrylic acid **5g**

Following the general procedure, in a round-bottom flask, provided with a magnetic stirrer, 0.9971 g of malonic acid **3**, 2 mL of triethylamine, and 30 mL of toluene as reaction medium were added. After 30 minutes 190 µL of piperidine and 2.084 g of 4-(9*H*-carbazol-9-yl)benzaldehyde **4g** were added.

3.2.2.6. Synthesis of (*E*)-3-(4-(9H-carbazol-9-yl)phenyl)acrylic acid **5h**

Following the general procedure, in a round-bottom flask, provided with a magnetic stirrer, 1.0032 g of malonic acid **3**, 2 mL of triethylamine, and 30 mL of toluene as reaction medium were added. After 30 minutes 190 µL of piperidine and 1.715 g of 9-ethyl-9*H*-carbazole-3-carbaldehyde **4h** were added.

3.2.3. Synthesis of vinyl-oxadiazole derivatives ***6a-h***

In a round-bottom flask, provided with a magnetic stirrer, 1.0 eq of phenyl-tetrazole **2**, 1.5 eq of the corresponding cinnamic acids **5a-h**, 1.1 eq of N,N-dicyclohexylcarbodiimide (DCC), and 30 mL of toluene were added. The mixture was placed under reflux for 24 hours with constant stirring. The progress of the reaction was monitored by TLC using Hex:EtOAc (7:3 v/v). Once the reaction was complete, the solvent was evaporated under reduced pressure, 10 mL of ethanol (EtOH) was added, and the mixture was left in the fridge overnight. The precipitate obtained was filtered, washed with EtOH and dried.

3.2.3.1. Synthesis of (*E*)-2-phenyl-5-styryl-1,3,4-oxadiazole **6a**

Following the general procedure, in a round-bottom flask, provided with a magnetic stirrer, 1.1846 g of phenyl-tetrazole **2**, 0.4924 g of (*E*)-Cinnamic acid **5a**, 0.7665 g of DCC, and 30 mL of toluene were added.

3.2.3.2. Synthesis of (*E*)-2-phenyl-5-(4-(trifluoromethyl)styryl)-1,3,4-oxadiazole **6b**

Following the general procedure, in a round-bottom flask, provided with a magnetic stirrer, 0.8118 g of phenyl-tetrazole **2**, 0.5044 g of (*E*)-3-(4-(trifluoromethyl)phenyl)acrylic acid **5b**, 0.5253 g of DCC, and 30 mL of toluene were added.

3.2.3.3. Synthesis of (*E*)-dimethyl-4-(2-(5-phenyl-1,3,4-oxadiazol-2-yl)vinyl)aniline **6c**

Following the general procedure, in a round-bottom flask, provided with a magnetic stirrer, 0.9178 g of phenyl-tetrazole **2**, 0.5058 g of (*E*)-3-(4-(dimethylamino)phenyl)acrylic acid **5c**, 0.5939 g of DCC, and 30 mL of toluene were added.

3.2.3.4. Synthesis of (*E*)-diethyl-4-(2-(5-phenyl-1,3,4-oxadiazol-2-yl)vinyl)aniline **6d**

Following the general procedure, in a round-bottom flask, provided with a magnetic stirrer, 0.8004 g of phenyl-tetrazole **2**, 0.4944 g of (*E*)-3-(4-(diethylamino)phenyl)acrylic acid **5d**, 0.5179 g of DCC, and 30 mL of toluene were added.

3.2.3.5. Synthesis of (*E*)-4-(4-(2-(5-phenyl-1,3,4-oxadiazol-2-yl)vinyl)phenyl)morpholine **6e**

Following the general procedure, in a round-bottom flask, provided with a magnetic stirrer, 0.7524 g of phenyl-tetrazole **2**, 0.5088 g of (*E*)-3-(4-morpholinophenyl)acrylic acid **5e**, 0.4868 g of DCC, and 30 mL of toluene were added.

3.2.3.6. Synthesis of (*E*)-2-phenyl-5-(4-(pyrrolidin-1-yl)styryl)-1,3,4-oxadiazole **6f**

Following the general procedure, in a round-bottom flask, provided with a magnetic stirrer, 0.8078 g of phenyl-tetrazole **2**, 0.4963 g of (*E*)-3-(4-(pyrrolidin-1-yl)phenyl)acrylic acid **5f**, 0.5227 g of DCC, and 30 mL of toluene were added.

3.2.3.7. Synthesis of (*E*)-2-(2-(9-ethyl-9H-carbazol-3-yl)vinyl)-5-phenyl-1,3,4-oxadiazole **6g**

Following the general procedure, in a round-bottom flask, provided with a magnetic stirrer, 0.6615 g of phenyl-tetrazole **2**, 0.5015 g of (*E*)-3-(9-ethyl-9H-carbazol-3-yl)acrylic acid **5g**, 0.4281 g of DCC, and 30 mL of toluene were added.

3.2.3.8. Synthesis of (*E*)-2-(4-(9H-carbazol-9-yl)styryl)-5-phenyl-1,3,4-oxadiazole **6h**

Following the general procedure, in a round-bottom flask, provided with a magnetic stirrer, 0.5601 g of phenyl-tetrazole **2**, 0.4921 g of (*E*)-3-(4-(9H-carbazol-9-yl)phenyl)acrylic acid **5g**, 0.3624 g of DCC, and 30 mL of toluene were added.

3.3. Cytotoxicity evaluation

The toxicity evaluation was conducted performing a viability assay with CellTiter-Blue, using the Hep G2 [HEPG2] cell line (liver).

3.3.1. Vinyl oxadiazole solutions

Vinyl-oxadiazoles **6a-h** were dissolved in a mix of sterile Dimethyl sulfoxide (DMSO):HCl (1M) 1:1 to make a 10 mM stock solution. The stock solution was then diluted with Eagle's Minimum Essential Medium (EMEM) to make 100, 150 and 200 μM solutions of each compound.

3.3.2. Cell preparation

Hep G2 cells were incubated in EMEM (38°C, 5% carbon dioxide, CO_2) until they reached a high confluency (around 70%). The cells were passed to 5 mL of media and counted, then diluted until a final concentration of 120 000 cells/mL. In a 96 microplate, 100 μL of the cell solution was added to the wells, to get a final concentration of 5 000 cells per well (around 80% confluency). The cells were then incubated for 36 hours, when they were ready to be drugged.

3.3.3. Cell treatment

The cell media was disposed and 100 μL of the respective oxadiazole derivative (**6a**-**h**) solution was added. Besides the oxadiazole solutions, solutions of sterile DMSO

($1x10^5$ μM), a mixture of DMSO ($5x10^4$ μM):HCl ($4x10^3$ μM) 1:1, voriconazole (100, 150 and 200 μM), Arsenic Trioxide ($5x10^4$ μM), and EMEM were added as positive, negative and blank controls respectively.

3.3.4. Cell Fluorescence

Cell viability was taken using a CellTiter-Blue assay, which is based on the enzymatic reduction of resazurin in the mitochondria (by dehydrogenases and cytochromes) to highly fluorescent resorufin (59,60). Sixteen hours after the cell treatment, 20 μL of CellTiter-Blue was added to each well. Fluorescence was measured after 2 hours using an excitation wavelength of 560 nm and emission wavelength of 590 nm.

3.4. Antifungal activity evaluation

The antifungal activity evaluation was conducted using the broth macrodilution method for MIC determination established by the CLSI M38 (61).

3.4.1. Vinyl oxadiazole solutions

Vinyl-oxadiazoles **6a**-**h** were dissolved in DMSO to make a 10000 μg/mL stock solution. The stock solution was then diluted with DMSO and a 30% Tween 80 solution to make 7000, 5120, 2560, 1280, 640, 320, 160, 80, 40 and 20 μg/mL solutions of each compound.

3.4.2. Inoculum preparation

Conidia were collected adding 3 mL of saline solution to a seven days culture of the corresponding mold (*S. apiospermum* or *L. prolificans*) and scraping with a sterile swab. After 5 minutes, the supernatant was transferred to a falcon tube, and the conidia concentration was determined using a Neubauer chamber. The solution was adjusted to obtain a final concentration of 0.4-5 $x10^4$ UFC (conidia) /mL.

3.4.3. Antifungal activity evaluation

In a 2 mL snap cap tube 900 μL of the conidia solution was added along with 100 μL of the respective oxadiazole derivative (**6a**-**h**) solution, diluting the concentration 1:10, achieving final concentrations of 700, 512, 256, 128, 64, 32, 16, 8, 4 and 2 μg/mL, with a

final DMSO concentration of <2% and Tween 80 <2.5%. Voriconazole (16 to 1.25 µg/mL), fluconazole (64-1.25 µg/mL), and amphotericin B (8-0.25 µg/mL) were used as control.

The MIC values were determinate by triplicate, after 48 h incubation (35 °C without stirring) as the lowest concentration able to inhibit all fungal grow (determinate by eye).

3.5. Waste Disposal

Waste management and disposal was done following the regulations of the Departamento de Medio Ambiente y Seguridad (FCQ-UANL), see **Table 2**.

Table 2. Waste disposal classification**.**

Residue	Container
Aqueous solutions	A
Inorganic solids	B
Organic non-halogenated solutions	C
Organic halogenated solutions	D
Toxic, carcinogenic organic solutions	E_{org}
Toxic, carcinogenic inorganic solutions	E_{inorg}
Precious metal solutions	F
Organic solids	G
Oxidants	H
Absorbent materials that were in contact with chemicals, latex gloves	Industrial waste
Empty glassware that was in contact with chemicals	Impregnated glass
Empty plastic material that was in contact with chemical substances	Impregnated plastics

4. Results and Discussion

4.1.Organic Synthesis

The synthesis of the vinyl-oxadiazoles **6a-h** followed a three-step process. First, the phenyl tetrazole **2** was formed in a Huisgen cycloaddition with benzonitrile and potassium azide as starting materials, assisted by MW irradiation. Secondly, a series of cinnamic acid derivatives, **5a-h**, were synthesized by Knoevenagel condensation. Finally, the phenyl tetrazole reacted with the cinnamic acid derivative assisted by MW irradiation, to afford the corresponding vinyl-oxadiazole **6a-h** showed in **Figure 13**.

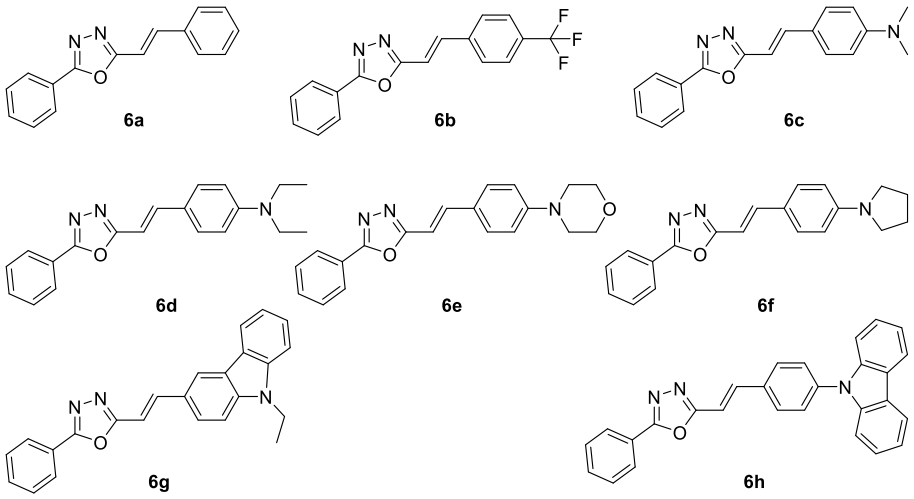

Figure 13. Oxadiazole derivatives **6a-h**.

4.1.1. Synthesis of Phenyl Tetrazole 2

For the synthesis of phenyl tetrazole **2**, a mixture of benzonitrile and potassium azide was heated for 70 minutes at 160 ºC under MW irradiation (**Scheme 2**).

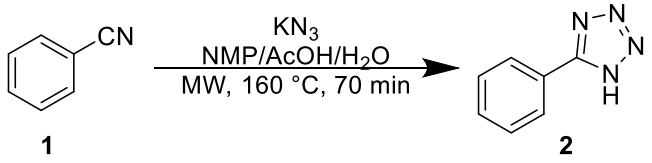

Scheme 2. Synthetic route to obtain phenyl tetrazole **2**.

After the reaction was completed, it was basified using a saturated $NaHCO_3$ solution until it reached pH 10. The resulting mixture was extracted three times with 20 mL of ethyl acetate (3 x 20 mL). The aqueous phase was acidified with HCl until a white

solid precipitated. The solid was filtered, rinsed with cold water and dried. The product was obtained as a white cotton-like solid, with a chemical yield of 85%.

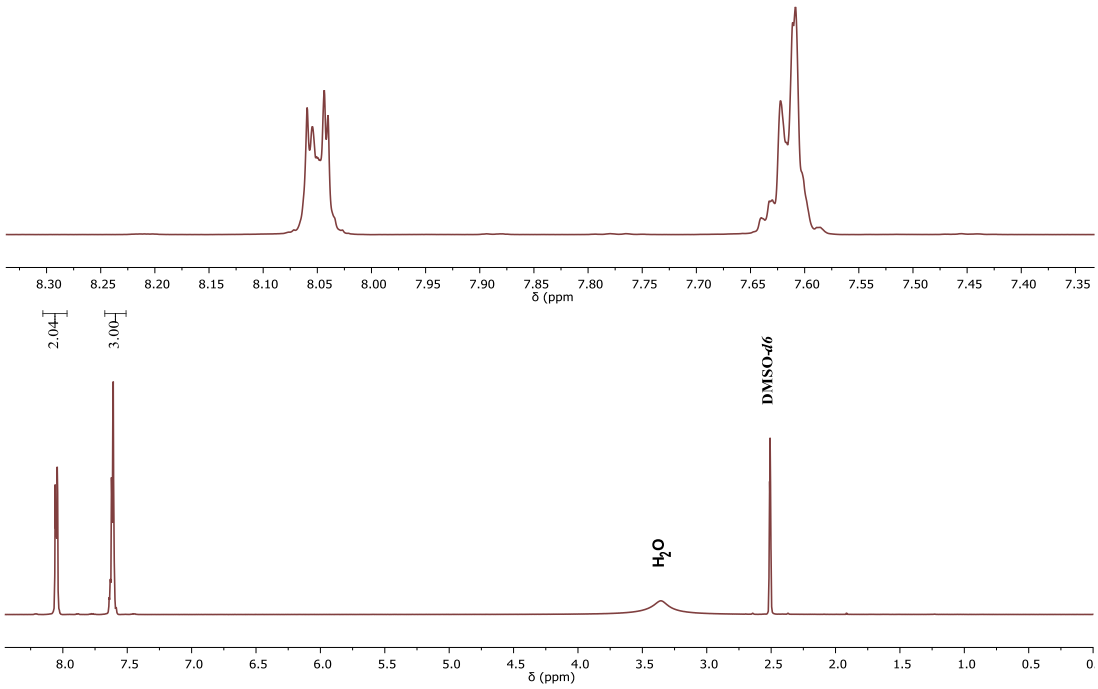

Figure 14. NMR ^{1}H (500 MHz, DMSO-*d*6) of 5-phenyl-1H-tetrazole **2**.

The product was characterized by FT-IR, NMR ^{1}H and ^{13}C and HRMS, confirming the structure of the phenyl-1H-tetrazole. The ^{1}H NMR spectrum (**Figure 14** and **Table 3**) shows a doublet of doublets around 8 ppm (2H) that corresponds with protons 1. The signals around 7.6 ppm integrate 3 protons and it's a signal overlap between protons 3, 2 and 2′. The singlet at 7.62 ppm (corresponding to proton 3) integrates to 1H and has a coupling constant of 6.95 Hz with protons 2 and 2′. It does not show the coupling with proton 1 which can be explained due to the overlap and the resolution of the instrument. The signal at 7.61 ppm (corresponding to protons 2 and 2′) integrates to 2H and has a multiplicity similar to a double signal (not a doublet). This signal has a coupling constant of 1.80 Hz, consistent with the proton located in the meta position relative to 2 (2′). The amino hydrogen doesn't appear in the spectrum; this can be explained by proton exchange with any deuterium (D_2O) present in the solvent.

Table 3. NMR ^{1}H of 5-phenyl-1*H*-tetrazole **2** (500 MHz, DMSO-*d*6).

	Proton	δ (ppm)	Multiplicity	Integration	*J* (Hz)
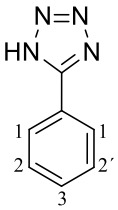	1	8.10-7.99	dd	2 H	7.43 2.27
	2	7.61	d	2 H	6.95 1.80
	3	7.62	s	1 H	6.95

*4.1.2. Synthesis of cinnamic acid derivatives **5a-h***

For the synthesis of the cinnamic acids derivatives, a mixture of the corresponding aldehyde, malonic acid, triethyl amine and piperidine were refluxed in toluene for 6 h (**Scheme 3**).

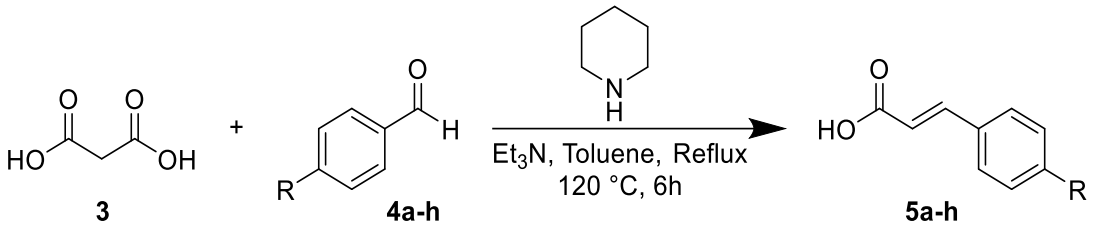

Scheme 3. Synthetic route to obtain cinnamic acid derivatives **5a-h**.

After the reaction was complete, it was basified with a solution of NaOH and stirred for 30 minutes. The resulting mixture was extracted three times with 10 mL of distilled water (3 x 10 mL). Finally, the aqueous phase was acidified with HCl 12 M until precipitation, and the solid obtained was filtered, rinsed with cold water and dried.

Six different cinnamic acid derivatives were synthetized. All of them were obtained as solids, with colors variating from white, yellow, orange and brown, and chemical yields from 39% to 80%. All solids were characterized by FT-IR, NMR ^{1}H and ^{13}C and HRMS confirming the desired structure (**Table 4**).

Table 4. Yield, R.F. and HRMS characterization of compounds **5a-h**.

	Appearance	Yield	R.F. (Hex:AcOEt 7:3)	Theoretical Mass: *m/z*	Exact Mass: *m/z*
5a	White	Commercial	-	-	-
5b	Beige	Commercial	-	-	-
5c	Yellow	54.30%	0.18	192.1019	192.0974
5d	Orange	63.70%	0.19	220.1332	220.1322
5e	Yellow	79.10%	0.06	234.1125	234.1116
5f	Brown	39.60%	0.25	218.1176	218.1169
5g	Light Yellow	61.10%	0.12	266.1176	266.1172
5h	Beige	80.63%	0.19	314.1176	314.1139

The ^{1}H NMR spectrum of molecule **5e** (**Figure 16**) (**Table 5**) shows two doublet of doublets corresponding to the morpholine protons in the aliphatic area, each signal integrating to 4 protons. The reason for the multiplicity not being a triplet as expected is the gauche arraignment due to the shape of the chair, **Figure 15**. The change of the positions in the conformers makes it so the protons are not chemical equivalent. At the same time, the multiplicity of the signals depends on the %anti/gauche in the sample. It is established in the literature that a 20/80 mixture presents coupling constants of 6.2 and 4.2 Hz, similar to the ones obtained in **5e**. Due to the resolution of the instrument, however, the doublet of doublets is not appreciated, with a shape more alike to a triplet signal (62). In the aromatic area, four signals can be seen. The signals in 6.98 and 6.18 ppm show a coupling constant of 15.8 Hz and an integration of 1 proton, both the constant and the protons correspond to the vinyl signals and demonstrate a trans geometry. The remaining signals, 7.32 and 6.18 have a coupling constant of 8.8 Hz characteristic of the aromatic ring, the integration for 1 proton also corroborates it.

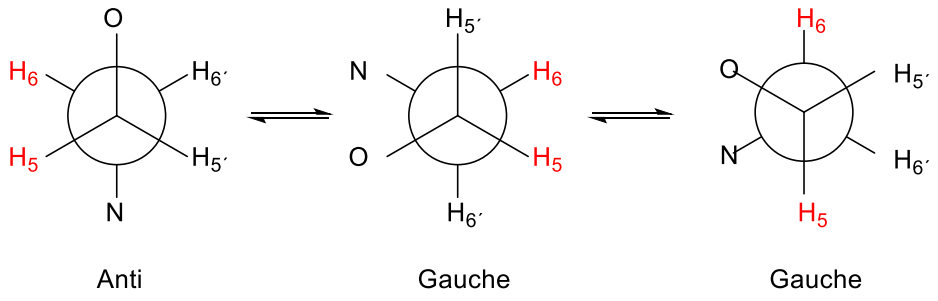

Figure 15. Anti and gauche configuration for the morpholine ring in **5e**.

Table 5. NMR ^{1}H of cinnamic acid **5e** (500 MHz, DMSO-*d6*).

	Proton	δ (ppm)	Multiplicity	Integration	*J* (Hz)
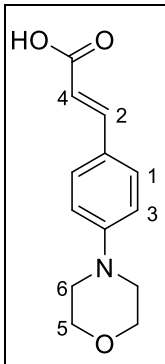	1	7.32	d	2 H	8.8
	2	6.98	d	1 H	15.8
	3	6.89	d	2 H	8.8
	4	6.18	d	1 H	15.8
	5	3.73	dd	4 H	6.0, 3.6
	6	3.11	dd	4 H	6.0, 3.6

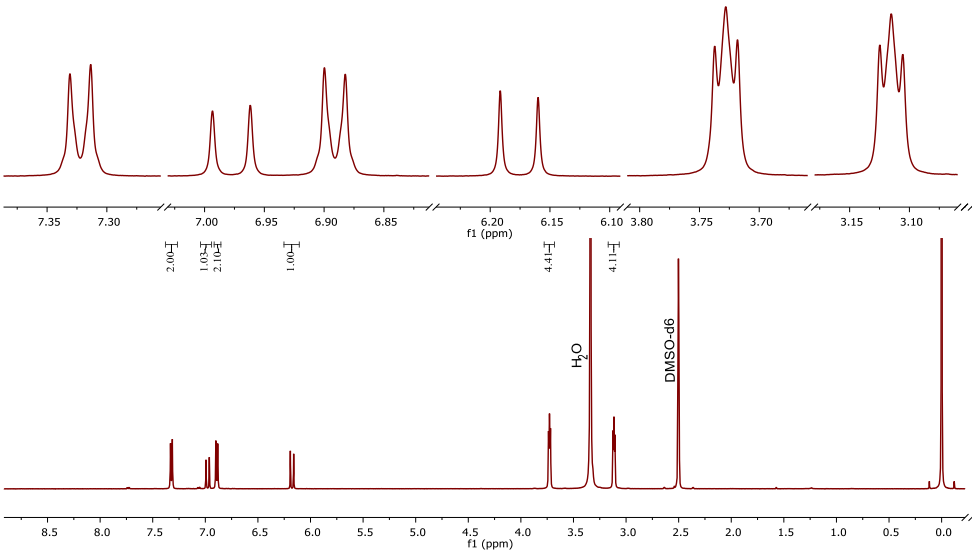

Figure 16. NMR ^{1}H (500 MHz, DMSO-*d6*) of (*E*)-3-(4-morpholinophenyl)acrylic acid **5e**.

*4.1.3. Synthesis of vinyl-oxadiazole derivatives **6a-h***

For the synthesis of the cinnamic acids derivatives, a mixture of the corresponding cinnamic acid (**5a-h**), phenyl tetrazole **2** and DCC were refluxed in toluene for 24 h (**Scheme 4**).

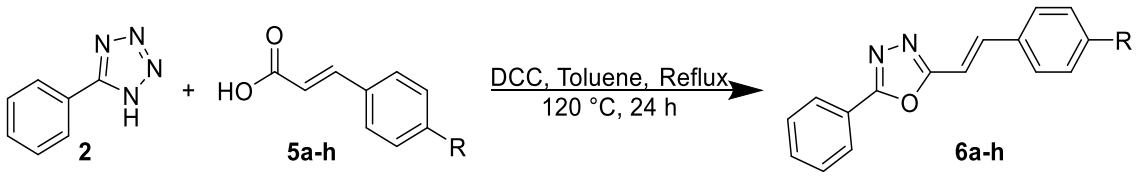

Scheme 4. Synthetic route to obtain vinyl-oxadiazole derivatives **6a-h**.

After the reaction was completed, the solvent was rotovaporated and 15 mL of EtOH was added to the round bottom flask and cooled in the fridge overnight so the vinyl-oxadiazole could precipitate. All solids were filtered and rinsed with cold EtOH. Finally, the vinyl-oxadiazole was recrystallized in EtOH.

Eight different vinyl-oxadiazole derivatives were synthetized. All of them were obtained as solids, with colors variating from white, yellow, orange and brown, and chemical yields from 20% to 42%. All solids were characterized by FT-IR, NMR ^{1}H and ^{13}C and HRMS confirming the desired structure (**Table 6**).

Table 6. Yield, R.F. and HRMS characterization of compounds **6a-h**.

	Appearance	Yield	R.F. (Hex:AcOEt 7:3)	Theoretical Mass: *m/z*	Exact Mass: *m/z*
6a	White	29.20%	0.59	249.1022	249.1006
6b	Beige	21.40%	0.58	317.0896	317.0873
6c	Yellow	41.30%	0.37	292.1444	292.1423
6d	Orange	37.10%	0.43	320.1757	320.1733
6e	Yellow	38.90%	0.21	334.155	334.1526
6f	Brown	35.90%	0.43	318.1601	318.1573
6g	Light Yellow	38.20%	0.51	366.1601	366.1575
6h	Beige	41.20%	0.34	414.1601	414.1571

The ^{1}H NMR spectrum of molecule **6e** (**Figure 17**) presented all the signals corresponding to the cinnamic acid previously analyzed (**5e**), in addition of two signals in the aromatic area corresponding to the phenyl protons from the tetrazole (**Table 7**). The vinyl signals, shown in 7.50 and 6.88 ppm have a similar coupling constant to its precursor (16.4 Hz), this confirm that the trans geometry didn't change between reactions.

Table 7. ^{1}H NMR (500 MHz, $CDCl_3$) of vinyl-oxadiazole **6e**.

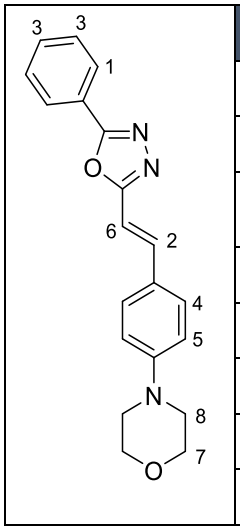

Proton	δ (ppm)	Multiplicity	Integration	J (Hz)
1	8.05	dd	2 H	7.5, 2.0
2	7.50	d	1 H	16.3
3	7.48 – 7.45	m	3 H	-
4	7.45	d	2 H	7.1
5	6.90	d	2 H	8.7
6	6.88	d	1 H	16.3
7	3.83	dd	4 H	6.0, 3.6
8	3.20	dd	4 H	6.0, 3.6

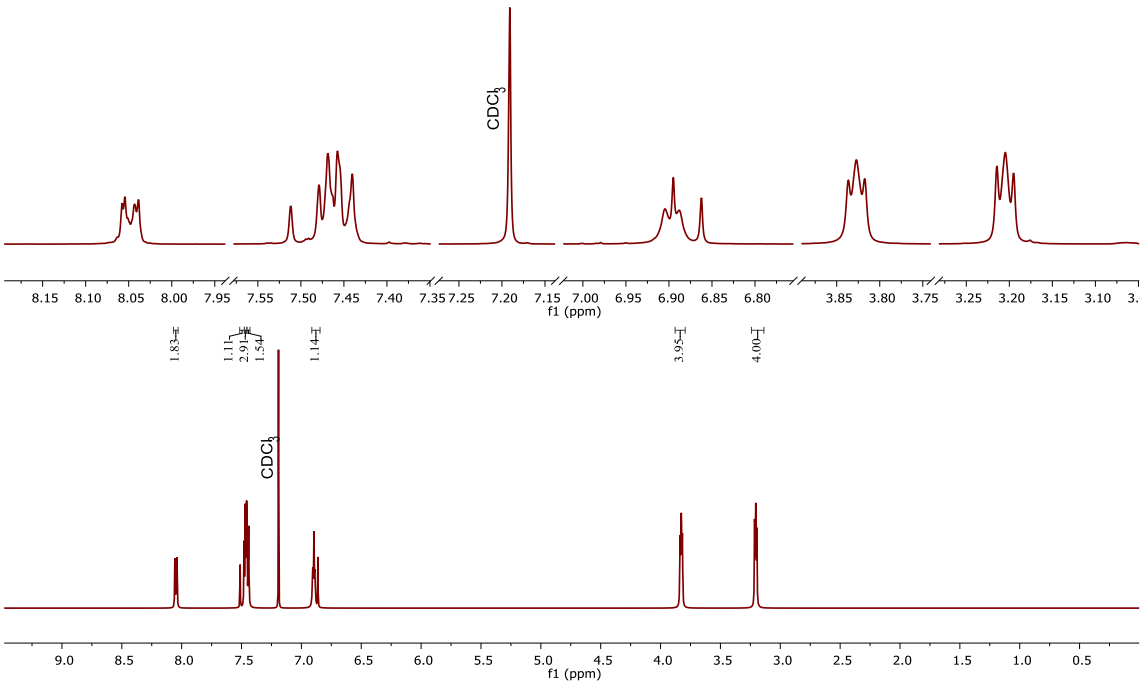

Figure 17. ^{1}H NMR (500 MHz, $CDCl_3$) of (*E*)-4-(4-(2-(5-phenyl-1,3,4-oxadiazol-2-yl)vinyl)phenyl)morpholine **6e**.

4.1.4. Toxicity evaluation

The viability tests in the eight synthesized compounds against the HepG2 cell line (liver) were done using the CellTiter-Blue (resazurin) colorimetric technique.

The azole hepatotoxicity in antifungal drugs is well established in the literature, as they show low selectivity to other metalloenzymes provoking drug-drug interactions and liver toxicity (63). True to this, the voriconazole (Vor) used as reference (100, 150 and 200 μM) showed a high toxicity against the liver cell line.

On the other hand, the oxadiazoles used in the assay (**6a-h**) showed a decrease of viability around 89% and 98% (**Figure 18)**. Gruber S. *et al*. (64) establishes a substance as toxic when it lowers the cell viability to 70% or lower. Given that none of the oxadiazoles presented enough diminution of cell viability, they can be labeled as non-toxic.

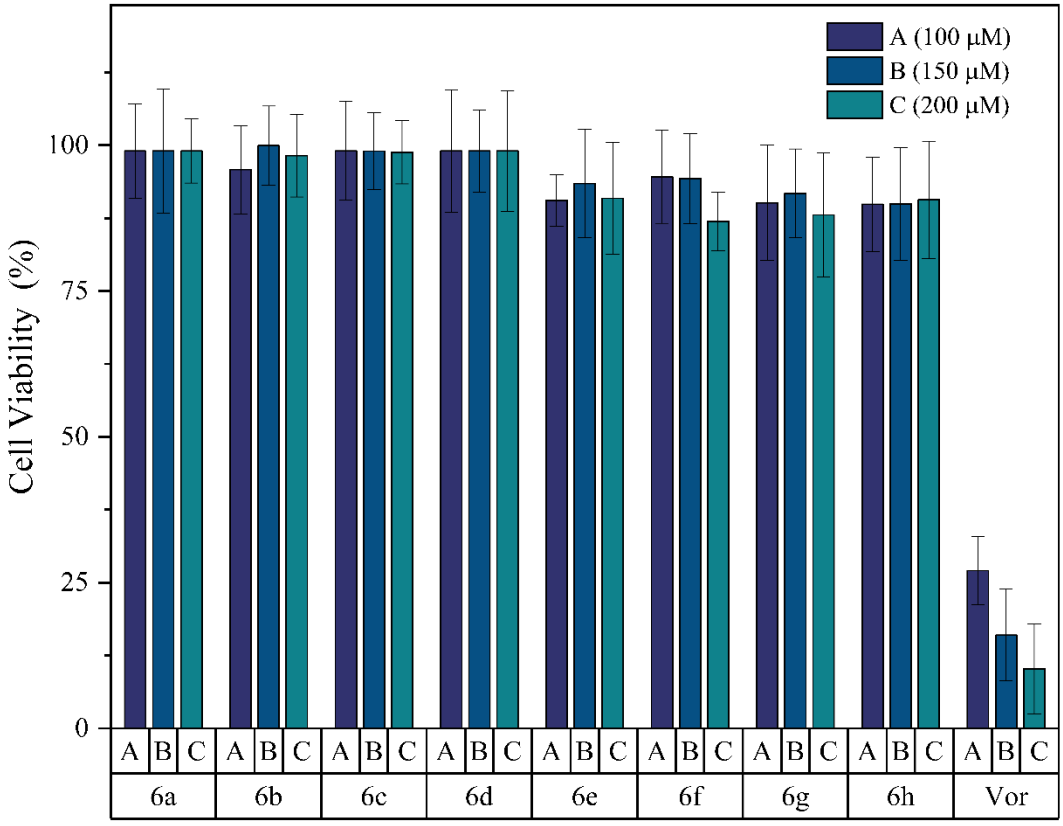

Figure 18. Cell viability percentage of compounds **6a-h** against the HepG2 cell line, using the CellTiter-Blue (resazurin) colorimetric technique.

The difference in toxicity between the voriconazole and the oxadiazole derivatives **6a-h** could be justified due to an increase in selectivity caused by the change in the metal-binding group. In 2014, Hoekstra, W. *et al*. (63) observed that changing the metal binding group in the voriconazole to one with lower-affinity for heme-iron (tetrazole instead of

triazole) greatly increased the selectivity towards Lanosterol 14 alpha-demethylase (CYP51A1) rather than human CYP enzymes such as CYP3A4. The iron affinity of the metal binding group is strongly associated with its basicity, and given that the oxadiazole group is less basic than the tetrazole and the triazole is reasonably to link this property to the decrease in toxicity shown by derivatives **6a-h**.

4.1.5. Antifungal evaluation

The antifungal evaluation was done using the using the broth macrodilution method for MIC determination established by the CLSI M38. The assays were reviewed after 48 h and 72 h and done by triplicate (**Figure 19**). MICs are presented in **Table 8**. All compounds, **6a-h**, showed no activity against *L. prolificans* and *S. apiospermum*. Testing at higher concentrations was not possible due to the solubility of the compounds.

Table 8. Minimum inhibitory concentration (MIC) of *Lomentospora prolificans* and *Scedosporium apiospermum*.

Lomentospora prolificans		*Scedosporium apiospermum*	
Compound	MIC (μg/mL)	Compound	MIC (μg/mL)
6a	>700	**6a**	>700
6b	>700	**6b**	>700
6c	>128*	**6c**	>128
6d	>128*	**6d**	>128
6e	>700	**6e**	>700
6f	>700	**6f**	>700
6g	>700	**6g**	>700
6h	>700	**6h**	>700
Vor	8	Vor	4
Flz	>64	Flz	32
AmB	>16	AmB	>16

Due to the low quantity of compounds **6c and **6d** the highest concentration used in the assay was 128 μg/mL*

Neither the CLSI nor the EUCAST (European Committee on Antimicrobial Susceptibility Testing) have official MIC breakpoints for rare molds such as *L. prolificans* and *S. apiospermum*, but the EUCAST offer breakpoints for other fungi particularly different species of *Aspergillus*. Taking these values as reference, Both *L. prolificans* and *S. apiospermum* showed resistance to fluconazole (Flz) (MIC >16 μg/mL), voriconazole

(Vor) (MIC >1 μg/mL), and amphotericin B (AmB) (MIC >1 μg/mL) (65). These results coincide with the literature, as other works, included Kirchhoff *et al*. report resistance shown by *L. prolificans* to echinocandins, polyenes and azole antifungals, with voriconazole having the lowest MIC between the three types of antifungals (66). On the other hand, Mello *et al*. reported resistance shown by *S. apiospermum* to allylamines, echinocandins, polyenes antifungals and limited resistance to azole derivatives, with voriconazole and posaconazole having the lowest MIC between the four types of antifungals (67).

The high resistance of both molds has been reported in the literature before, as they pose intrinsic resistance to azoles (**6a**-**h**, voriconazole and fluconazole), and echinocandins (amphotericin B) (68,69).

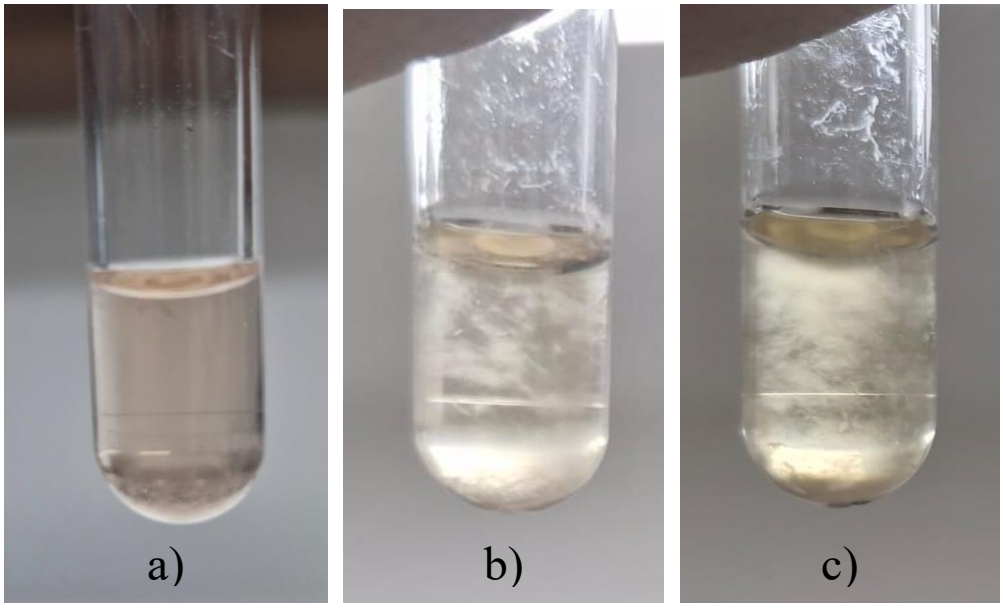

Figure 19. *Scedosporium apiospermum* growth with **6a** at 700 μg/mL after a) 24 h, b) 48 h and c) 72 h.

In his work, Hamdy *et al*. worked with highly similar compounds to the ones in this work (**Figure 10**). He determined the interactions of **E3** and CYP51 via molecular docking, discovering important hydrophobic (Leu-88, Tyr-118, Pro-230, Phe-228, Phe-380 and Tyr-132) and π-π stacking interactions (His-377, Phe-233) with key amino acid residuals. The interactions presented were made mostly by the rings presented to the sides

of the oxadiazole. Seeing the similitude between Hamdy work and this one, it is logical to expect the same interactions were made between **6a-h** and CYP51 presented in *L. prolificans* and *S. apiospermum*, however, the lack of activity presented suggests the opposite (53).

Even though the intrinsic resistance of *L. prolificans* and *Scedosporium* spp have not been extensively studied, it is believed that the amino acid substitutions in Cyp51 (in *L. prolificans* and *Scedosporium*) are one of the reasons for this resistance. In his work, Wu *et al*. sequenced the Cyp51 gene of 21 *L. prolificans* clinical isolates, founding an identity of 86.6% with *S. apiospermum*, on the other hand, the identity with Cyp51 of *Aspergillus fumigatus* was only 54.8%. They also identified several azole resistance intrinsic amino acid residues in Cyp51 (of *L. prolificans*) reported to be associated with azole resistance in *A. fumigatus* (70). As aspergillosis and candidiasis are around 90% of all fungal infections (Aspergillosis being 75% of all mold infections), it is comprehensible that *Aspergillus* and *Candida* Cyp51 are the ones used to design new antifungal candidates, however these designs do not account for the differences in *L. prolificans* and *Scedosporium* Cyp51 (71,72).

Another intrinsic resistance mechanism showed by *L. prolificans* and *Sedosporium.* spp. is biofilm formation. Kirchhoff *et al*. in their work, detected the formation of biofilm in *L. prolificans* strains and determined the MIC of voriconazole in three different biofilm development stages; prior adhesion (0 h), after adhesion (2 h and in mature biofilm (48 h) The MIC obtained for voriconazole was 8 times greater in the mature biofilm stage than in the other two stages (66).

Mello *et al*. also detected the formation of biofilm in all *L. prolificans* and *Scedosporium* spp. strains after collecting 21 clinical isolates. They obtained the MIC of voriconazole against *L. prolificans* and *S. apiospermum* 72 h-biofilm, obtaining MICs greater than 256 μg/mL for both fungi (67). In a following work, Mello *et al*. determinate the importance of efflux pump activity in *L. prolificans* and *S.* spp resistance using the efflux pump inhibitor PaβN. After the inhibition, they found that the MIC of voriconazole against *S. apiospermum*, *S. minutisporum* and *S. aurantiacum* decreased 2, 8 and 2 times respectively when the assay was made in RPMI medium; on the other hand, when the

assay was done with *L. prolificans*, the MIC decreased more than 64 times. This indicates the importance of efflux pumps in *L. prolificans* as a resistance mechanism. A future experiment with a efflux pump inhibitor could determine if the lack of activity of compounds **6a**-**h** is related to this resistance mechanism (73).

The structural differences between the oxadiazoles in Hamdy´s work and **6a**-**h** could also be another reason for their low activity. The amino substituents and the vinyl group could be interfering or showing low interactions with the amino acid residuals in Cyp51. To confirm this, computational studies would be beneficial, however there is no assembly for *L. prolificans* or *Scedosporium* Cyp51 in the Protein Data Bank.

The lack of information regarding the resistance mechanisms and protein structure of rare molds like *L. prolificans* or *Scedosporium* is a big limitation in the search of new and better antifungal drugs. A better understanding of the limitations of this work will be achieved as more research is conducted.

5. Conclusions

- Phenyl tetrazole **2** was obtained via Huisgen´s cycloaddition obtaining a chemical yield of 85%. The structure was confirmed by FT-IR, ^{1}H-NMR, ^{13}C-NMR and HRMS.
- The cinnamic acid derivatives **5a**-**h** were obtained via Knoevenagel reaction obtaining chemical yields between 39% and 80%. The structures were confirmed by FT-IR, ^{1}H-NMR, ^{13}C-NMR and HRMS.
- The vinyl-oxadiazole derivatives **6a**-**h** were obtained via Huisgen´s rearrangement obtaining chemical yields between 39% and 80%. The structures were confirmed by FT-IR, ^{1}H-NMR, ^{13}C-NMR and HRMS.
- The cytotoxicity of the compounds **6a**-**h** was determined against the cell line HepG2 (liver cells) obtaining cell viabilities between 89% and 98% at 100, 150 and 200 μM, demonstrating no hepatotoxicity *in vitro*.
- Compounds **6a**-**h** showed no activity against the azole and polyene-resistant fungi *Scedosporium apiospermum* and *Lomentospora prolificans* at 700 μg/mL or less and higher concentrations could not be used due to the low solubility of the compounds in water and ethanol.
- Due to none of the vinyl-oxadiazole derivatives exhibited greater antifungal activity than voriconazole, against drug-resistant strains of *Scedosporium apiospermum* and *Lomentospora prolificans*, the hypothesis presented is rejected

5.1. Future Perspective

- Because compounds **6a**-**h** showed no toxicity, they could be used in another areas, such as bioimaging (they present fluorescent properties not discussed in this work).
- The use of computational tools like molecular docking to determinate the interactions between **6a**-**h** and Cyp51 to make the necessary modifications in the structure to obtain a greater antifungal activity.

- The addition of functional groups capable of helping with the solubility of the oxadiazoles in water (carboxylic acids, alcohols, etc.).

6. Bibliography

1. Loron CC, François C, Rainbird RH, Turner EC, Borensztajn S, Javaux EJ. Early fungi from the Proterozoic era in Arctic Canada. Nature. 2019 Jun 22;570(7760):232–5. doi:10.1038/s41586-019-1217-0

2. Hyde KD. The numbers of fungi. Fungal Divers. 2022 May 30;114(1):1–1. doi:10.1007/s13225-022-00507-y

3. Kendrick B. The Fifth Kingdom. 4th ed. Indianapolis; 2017.

4. Powers-Fletcher M V., Kendall BA, Griffin AT, Hanson KE. Filamentous Fungi. Microbiol Spectr. 2016 May 6;4(3). doi:10.1128/microbiolspec.dmih2-0002-2015 PubMed PMID: 27337469.

5. Webster J, Weber R. Introduction to Fungi. 3rd ed. Cambridge University Press; 2007. doi:10.1017/CBO9780511809026

6. Kavanagh K. Fungi. Kavanagh K, editor. Wiley; 2011. doi:10.1002/9781119976950

7. Pérez JC. Fungi of the human gut microbiota: Roles and significance. International Journal of Medical Microbiology. 2021 Apr 1;311(3). doi:10.1016/j.ijmm.2021.151490 PubMed PMID: 33676239.

8. Nguyen A V., Soulika AM. The dynamics of the skin's immune system. International Journal of Molecular Sciences. MDPI AG; 2019. doi:10.3390/ijms20081811 PubMed PMID: 31013709.

9. Kaushik N, Pujalte GGA, Reese ST. Superficial Fungal Infections. Primary Care - Clinics in Office Practice. W.B. Saunders; 2015. p. 501–16. doi:10.1016/j.pop.2015.08.004 PubMed PMID: 26612371.

10. Hay RJ. Subcutaneous Mycoses. In: Hunter's Tropical Medicine and Emerging Infectious Diseases. Elsevier; 2020. p. 653–8. doi:10.1016/B978-0-323-55512-8.00083-1

11. Firacative C. Invasive fungal disease in humans: Are we aware of the real impact? Mem Inst Oswaldo Cruz. 2020;115(9):1–9. doi:10.1590/0074-02760200430 PubMed PMID: 33053052.

12. Kwarteng Owusu S. Invasive fungal infections. African Journal of Thoracic and Critical Care Medicine. 2022 Sep 19;3(1):100–1. doi:10.7196/AJTCCM.2022.v28i3.264

13. Sati H, Alastruey-Izquierdo A, Morrissey O. WHO fungal priority pathogens list to guide research, development and public health action. 2022.

14. Shoham S, Marwaha S. Invasive Fungal Infections in the ICU. Journal of Intensive Care Medicine. 2010. p. 78–92. doi:10.1177/0885066609355262 PubMed PMID: 19955115.

15. Corzo-Leon DE, Martinez-Rivera N, Martin-Onraet A, Piñeirua-Menendez A. Access to diagnostic testing for invasive fungal diseases and other opportunistic infections in Mexican health care centers caring for patients living with HIV. BMC Health Serv Res. 2025 Dec 1;25(1). doi:10.1186/s12913-025-12405-5 PubMed PMID: 39966809.

16. Xess I, Pagano L, Dabas Y. Invasive Fungal Infections 2021. Journal of Fungi. 2022 Jul 22;8(8):760. doi:10.3390/jof8080760

17. Hennebert BGD. Lomentospora prolificans, a new hyphomycete from greenhouse soil. Mycotaxon. 1974;1:45–50.

18. Malloch D, Salkin IF. A new species of Scedosporium associated with osteomyelitis in humans. Mycotaxon. 1984;21:247–55. doi:10.5962/p.418847

19. Gueho E, Hoog G de. Taxonomy of the medical species of Pseudallescheria and Scedosporium. J Mycol Med. 1991;1:3–9.

20. Lackner M, de Hoog GS, Yang L, Ferreira Moreno L, Ahmed SA, Andreas F, et al. Proposed nomenclature for Pseudallescheria, Scedosporium and

related genera. Fungal Divers. 2014 Sep 23;67(1):1–10. doi:10.1007/s13225-014-0295-4

21. Hoenigl M, Salmanton-García J, Walsh TJ, Nucci M, Neoh CF, Jenks JD, et al. Global guideline for the diagnosis and management of rare mould infections: an initiative of the European Confederation of Medical Mycology in cooperation with the International Society for Human and Animal Mycology and the American Society for Microbiology. Lancet Infect Dis. 2021 Aug;21(8):e246–57. doi:10.1016/S1473-3099(20)30784-2

22. Konsoula A, Tsioutis C, Markaki I, Papadakis M, Agouridis AP, Spernovasilis N. Lomentospora prolificans: An Emerging Opportunistic Fungal Pathogen. Microorganisms. MDPI; 2022. doi:10.3390/microorganisms10071317

23. Konsoula A, Agouridis AP, Markaki L, Tsioutis C, Spernovasilis N. Lomentospora prolificans Disseminated Infections: A Systematic Review of Reported Cases. Pathogens. MDPI; 2023. doi:10.3390/pathogens12010067

24. Kakuno S, Imoto W, Teranishi Y, Kakeya H. Lomentospora prolificans-induced Invasive Fungal Sinusitis. Internal Medicine. 2023;62(18):2761–2. doi:10.2169/internalmedicine.1074-22 PubMed PMID: 36642520.

25. Wilson CM, O'rourke EJ, Mcginnis MR, Salkin IF. Scedosporium inflatum: Clinical Spectrum of a Newly Recognized Pathogen. J Infect Dis. 1990;161:102–7.

26. Sato K, Hayashi T, Ishizaki T, Yoshida M, Watanabe A. Disseminated Lomentospora prolificans infection that could have been predicted: A case report. IDCases. 2024 Jan 1;37. doi:10.1016/j.idcr.2024.e02046

27. Dong M, Pearce F, Singh N, Lin ML. A case of Lomentospora prolificans endophthalmitis treated with the novel antifungal agent Olorofim. J Ophthalmic Inflamm Infect. 2024 Dec 1;14(1). doi:10.1186/s12348-024-00393-2

28. Abrantes RA, Refojo N, Hevia AI, Fernández J, Isla G, Córdoba S, et al. Scedosporium spp. From clinical setting in Argentina, with the proposal of the new pathogenic species scedosporium americanum. Journal of Fungi. 2021 Mar 1;7(3):1–16. doi:10.3390/jof7030160

29. scedosporium.

30. Rougeron A, Giraud S, Alastruey-Izquierdo A, Cano-Lira J, Rainer J, Mouhajir A, et al. Ecology of Scedosporium Species: Present Knowledge and Future Research. Mycopathologia. 2018 Feb 1;183(1):185–200. doi:10.1007/s11046-017-0200-2 PubMed PMID: 28929280.

31. Ramirez-Garcia A, Pellon A, Rementeria A, Buldain I, Barreto-Bergter E, Rollin-Pinheiro R, et al. Scedosporium and Lomentospora: An updated overview of underrated opportunists. Medical Mycology. Oxford University Press; 2018. p. S102–25. doi:10.1093/mmy/myx113 PubMed PMID: 29538735.

32. Neoh CF, Chen SCA, Lanternier F, Tio SY, Halliday CL, Kidd SE, et al. Scedosporiosis and lomentosporiosis: modern perspectives on these difficult-to-treat rare mold infections. Clinical Microbiology Reviews. American Society for Microbiology; 2024. doi:10.1128/cmr.00004-23 PubMed PMID: 38551323.

33. Gunasekaran K, Amoah K, Rahi MS, Rudolph D. A RARE CASE OF PULMONARY SCEDOSPORIUM IN AN IMMUNOCOMPETENT ADULT. Chest. 2020 Oct;158(4):A355. doi:10.1016/j.chest.2020.08.352

34. Gupta S, Knapik S. Chronic Invasive Pulmonary Scedosporium apiospermum Infection in an Immunocompetent Host. Chest. 2010 Oct;138(4):109A. doi:10.1378/chest.10905

35. Cortez KJ, Roilides E, Quiroz-Telles F, Meletiadis J, Antachopoulos C, Knudsen T, et al. Infections caused by Scedosporium spp. Clin Microbiol

Rev. 2008 Jan;21(1):157–97. doi:10.1128/CMR.00039-07 PubMed PMID: 18202441.

36. Vanreppelen G, Wuyts J, Van Dijck P, Vandecruys P. Sources of Antifungal Drugs. Journal of Fungi. MDPI; 2023. doi:10.3390/jof9020171

37. Bouz G, Doležal M. Advances in Antifungal Drug Development: An Up-To-Date Mini Review. Pharmaceuticals. 2021 Dec 16;14(12):1312. doi:10.3390/ph14121312

38. Song L, Wang S, Zou H, Yi X, Jia S, Li R, et al. Regulation of Ergosterol Biosynthesis in Pathogenic Fungi: Opportunities for Therapeutic Development. Microorganisms. 2025 Apr 10;13(4):862. doi:10.3390/microorganisms13040862

39. 1024px-Structure_of_lanosterol_14_α-demethylase_(CYP51).

40. Shafiei M, Peyton L, Hashemzadeh M, Foroumadi A. History of the development of antifungal azoles: A review on structures, SAR, and mechanism of action. Bioorganic Chemistry. Academic Press Inc.; 2020. doi:10.1016/j.bioorg.2020.104240 PubMed PMID: 32906036.

41. Smith EB. History of antifungals. J Am Acad Dermatol. 1990 Oct;23(4):776–8. doi:10.1016/0190-9622(90)70286-Q

42. Yang YL, Xiang ZJ, Yang JH, Wang WJ, Xu ZC, Xiang RL. Adverse Effects Associated With Currently Commonly Used Antifungal Agents: A Network Meta-Analysis and Systematic Review. Frontiers in Pharmacology. Frontiers Media S.A.; 2021. doi:10.3389/fphar.2021.697330

43. Bell AS. Major Antifungal Drugs. In: Comprehensive Medicinal Chemistry II. Elsevier; 2007. p. 445–68. doi:10.1016/B0-08-045044-X/00216-9

44. Fisher MC, Alastruey-Izquierdo A, Berman J, Bicanic T, Bignell EM, Bowyer P, et al. Tackling the emerging threat of antifungal resistance to

human health. Nat Rev Microbiol. 2022 Sep 1;20(9):557–71. doi:10.1038/s41579-022-00720-1 PubMed PMID: 35352028.

45. Perlin DS, Rautemaa-Richardson R, Alastruey-Izquierdo A. The global problem of antifungal resistance: prevalence, mechanisms, and management. The Lancet Infectious Diseases. Lancet Publishing Group; 2017. p. e383–92. doi:10.1016/S1473-3099(17)30316-X PubMed PMID: 28774698.

46. Maillard JY. Does the use of topical azoles have an impact on antifungal resistance? Journal of Antimicrobial Chemotherapy. 2025 Aug 4. doi:10.1093/jac/dkaf270

47. Li Y, Hind C, Furner-Pardoe J, Sutton JM, Rahman KM. Understanding the mechanisms of resistance to azole antifungals in Candida species. JAC-Antimicrobial Resistance. Oxford University Press; 2025. doi:10.1093/jacamr/dlaf106

48. Sadek B, Fahelelbom KMS. Synthesis, characterization, and antimicrobial evaluation of oxadiazole congeners. Molecules. 2011 Jun;16(6):4339–47. doi:10.3390/molecules16064339 PubMed PMID: 21613975.

49. Ningaiah S, Bhadraiah UK, Keshavamurthy S, Javarasetty C. Novel pyrazoline amidoxime and their 1,2,4-oxadiazole analogues: Synthesis and pharmacological screening. Bioorg Med Chem Lett. 2013 Aug 15;23(16):4532–9. doi:10.1016/j.bmcl.2013.06.042 PubMed PMID: 23850201.

50. Rodrigues-Vendramini FAV, Faria DR, Arita GS, Capoci IRG, Sakita KM, Caparroz-Assef SM, et al. Antifungal activity of two oxadiazole compounds for the paracoccidioidomycosis treatment. PLoS Negl Trop Dis. 2019 Jun 1;13(6). doi:10.1371/journal.pntd.0007441 PubMed PMID: 31163021.

51. Capoci IRG, Sakita KM, Faria DR, Rodrigues-Vendramini FAV, Arita GS, de Oliveira AG, et al. Two New 1,3,4-Oxadiazoles With Effective Antifungal

Activity Against Candida albicans. Front Microbiol. 2019 Sep 12;10. doi:10.3389/fmicb.2019.02130

52. Das R, Mehta DK. Evaluation and Docking Study of Pyrazine Containing 1, 3, 4-Oxadiazoles Clubbed with Substituted Azetidin-2-one: A New Class of Potential Antimicrobial and Antitubercular. Drug Res. 2021 Jan 1;71(1):26–35. doi:10.1055/a-1252-2378 PubMed PMID: 33027823.

53. Hamdy R, Hamoda AM, Al-Khalifa M, Menon V, El-Awady R, Soliman SSM. Efficient selective targeting of *Candida* CYP51 by oxadiazole derivatives designed from plant cuminaldehyde. RSC Med Chem. 2022 Sep 29;13(11):1322–40. doi:10.1039/D2MD00196A

54. Luczynski M, Kudelko A. Synthesis and Biological Activity of 1,3,4-Oxadiazoles Used in Medicine and Agriculture. Applied Sciences. 2022 Apr 8;12(8):3756. doi:10.3390/app12083756

55. Chen J, Lou Z, Jin H, Ding C, Zhang G. Synthesis of 1,3,4-Oxadiazoles from 1,2-Diacylhydrazines Using SO2F2 as a Simple and Practical Cyclization Reagent. Synlett. 2025 May 26;36(08):1017–20. doi:10.1055/a-2489-7481

56. Kudelko A, Jasiak K, Ejsmont K. Study on the synthesis of novel 5-substituted 2-[2-(pyridyl)ethenyl]-1,3,4-oxadiazoles and their acid-base interactions. Monatsh Chem. 2015;146(2):303–11. doi:10.1007/s00706-014-1355-x

57. Green L, Livingstone K, Bertrand S, Peace S, Jamieson C. UV-Induced 1,3,4-Oxadiazole Formation from 5-Substituted Tetrazoles and Carboxylic Acids in Flow. Chemistry - A European Journal. 2020 Nov 20;26(65):14866–70. doi:10.1002/chem.202002896 PubMed PMID: 32786060.

58. Mayder DM, Tonge CM, Hudson ZM. Thermally activated delayed fluorescence in 1,3,4-oxadiazoles with π-extended donors. Journal of

Organic Chemistry. 2020 Sep 4;85(17):11094–103. doi:10.1021/acs.joc.0c00908

59. Promega. CellTiter-Blue ® Cell Viability Assay Instructions for Use of Products G8080, G8081 and G8082 [Internet]. 2023 Jul. Available from: www.promega.com

60. Czekanska EM. Assessment of Cell Proliferation with Resazurin-Based Fluorescent Dye. In: Methods in Molecular Biology. Humana Press Inc.; 2011. p. 27–32. doi:10.1007/978-1-61779-108-6_5 PubMed PMID: 21468965.

61. Pemán Javier, Martín-Mazuelos Estrella, Rubio Calvo MCarmen. Métodos estandarizados por el CLSI para el estudio de la sensibilidad a los antifúngicos (documentos M27-A3, M38-A y M44-A). In: Guía Práctica de Identificación y Diagnóstico en Micología Clínica. 2nd ed. Revista Iberoamericana de Micologia; 2010.

62. Hans Reich's Collection. NMR Spectroscopy: The AA'BB' Pattern [Internet]. 2020. Available from: https://organicchemistrydata.org/hansreich/resources/nmr/?page=05-hmr-15-aabb%2F

63. Hoekstra WJ, Garvey EP, Moore WR, Rafferty SW, Yates CM, Schotzinger RJ. Design and optimization of highly-selective fungal CYP51 inhibitors. Bioorg Med Chem Lett. 2014 Aug 1;24(15):3455–8. doi:10.1016/j.bmcl.2014.05.068 PubMed PMID: 24948565.

64. Gruber S, Nickel A. Toxic or not toxic? The specifications of the standard ISO 10993-5 are not explicit enough to yield comparable results in the cytotoxicity assessment of an identical medical device. Front Med Technol. 2023;5. doi:10.3389/fmedt.2023.1195529

65. The European Committee on Antimicrobial Susceptibility Testing. Breakpoint tables for interpretation of MICs for antifungal agents. Version 12.0. 2025 Jun.

66. Kirchhoff L, Dittmer S, Weisner AK, Buer J, Rath PM, Steinmann J. Antibiofilm activity of antifungal drugs, including the novel drug olorofim, against Lomentospora prolificans. Journal of Antimicrobial Chemotherapy. 2020 Aug 1;75(8):2133–40. doi:10.1093/jac/dkaa157 PubMed PMID: 32386411.

67. Mello TP, Lackner M, Branquinha MH, Santos ALS. Impact of biofilm formation and azoles' susceptibility in Scedosporium/Lomentospora species using an in vitro model that mimics the cystic fibrosis patients' airway environment: Azole susceptibility and biofilm of Scedosporium/Lomentospora. Journal of Cystic Fibrosis. 2021 Mar 1;20(2):303–9. doi:10.1016/j.jcf.2020.12.001 PubMed PMID: 33334714.

68. Mello TP, Oliveira SSC, Branquinha MH, Santos ALS. Decoding the antifungal resistance mechanisms in biofilms of emerging, ubiquitous and multidrug-resistant species belonging to the *Scedosporium/Lomentospora* genera. Med Mycol. 2022 Jun 30;60(6). doi:10.1093/mmy/myac036

69. Johnston N, Rockliff B, Duguid R, Palasanthiran P, Bartlett AW, Willams PC, et al. Successful management of Lomentospora prolificans septic arthritis and osteomyelitis in an immunocompetent child: A case report. Med Mycol Case Rep. 2025 Jun 1;48. doi:10.1016/j.mmcr.2025.100704

70. Wu Y, Grossman N, Totten M, Memon W, Fitzgerald A, Ying C, et al. Antifungal susceptibility profiles and drug resistance mechanisms of clinical lomentospora prolificans isolates. Antimicrob Agents Chemother. 2020 Oct 1;64(11). doi:10.1128/AAC.00318-20 PubMed PMID: 32816726.

71. Borjian Boroujeni Z, Shamsaei S, Yarahmadi M, Getso MI, Salimi Khorashad A, Haghighi L, et al. Distribution of invasive fungal infections: Molecular epidemiology, etiology, clinical conditions, diagnosis and risk

factors: A 3-year experience with 490 patients under intensive care. Microb Pathog. 2021 Mar;152:104616. doi:10.1016/j.micpath.2020.104616

72. Seagle EE, Williams SL, Chiller TM. Recent Trends in the Epidemiology of Fungal Infections. Infectious Disease Clinics of North America. W.B. Saunders; 2021. p. 237–60. doi:10.1016/j.idc.2021.03.001 PubMed PMID: 34016277.

73. Mello TP, Ramos LS, Andrade V V., Torres-Santos EC, Lackner M, Branquinha MH, et al. Elucidating the augmented resistance profile of Scedosporium/Lomentospora species to azoles in a cystic fibrosis mimic environment. Journal of Antimicrobial Chemotherapy. 2025 Jan 1;80(1):106–15. doi:10.1093/jac/dkae381 PubMed PMID: 39545480.

7. Supplementary Information

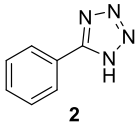

2

5-phenyl-1H-tetrazole **2** (85.03%)

White cotton-like solid, mp 216-218 °C, R.F. (MeOH:EtOAc 1:1) 0.65; FTIR v (cm^{-1}): 1562 (C=N), 3100-3010 (Ar-H); ^{1}H NMR (500 MHz, DMSO-d_6) δ 8.16 – 7.97 (m, 2H, H_{arom}), 7.67 – 7.51 (m, 3H, H_{arom}); ^{13}C NMR (500 MHz, DMSO) δ 131.75, 129.92, 127.43, 124.58. HRMS (ESI^+) *m/z* calc for $C_7H_7N_4^+$ $[M + H]^+$ 147.0665, found 147.0679.

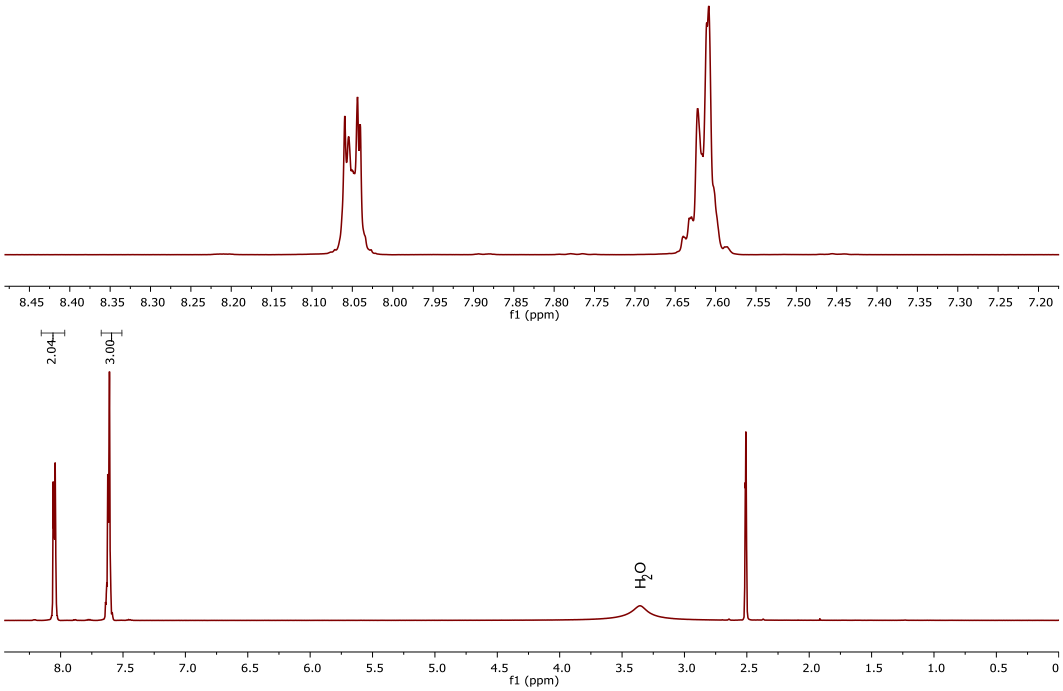

Appendix A. ^{1}H NMR (500 MHz, DMSO-*d6*) of 5-phenyl-1H-tetrazole **2**.

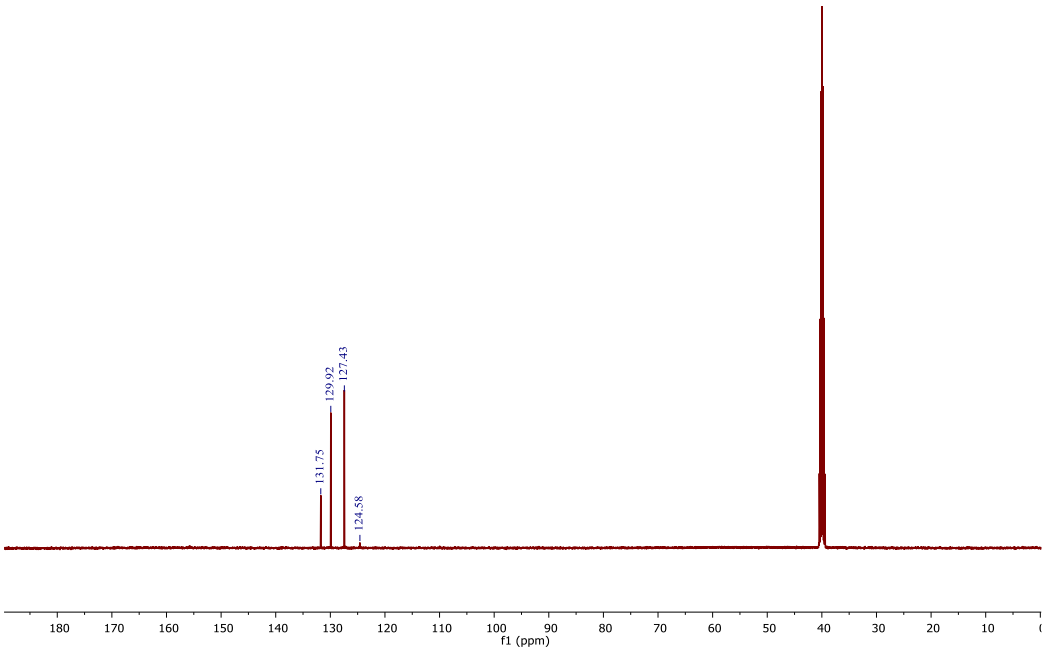

Appendix B. ^{13}C NMR (500 MHz, $CDCl_3$) of 5-phenyl-1H-tetrazole **2**.

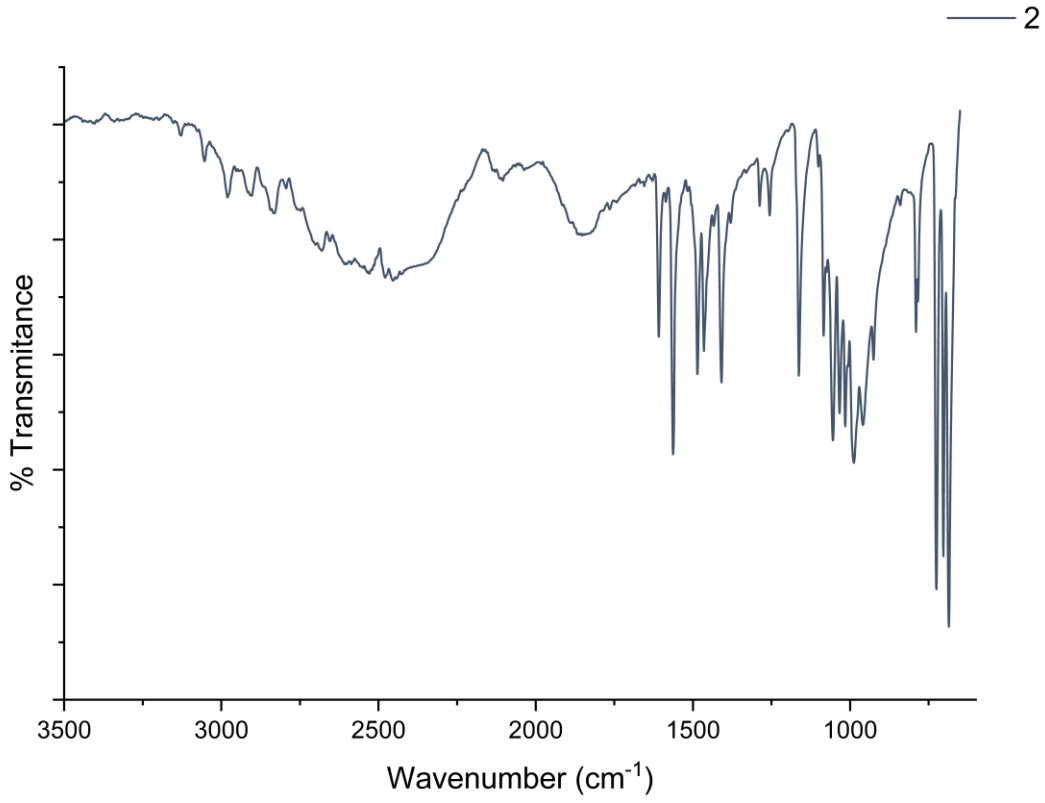

Appendix C. FT-IR of 5-phenyl-1H-tetrazole **2**.

(*E*)-3-(4-(dimethylamino)phenyl)acrylic acid **5c** (54.30%)

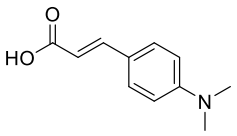

5c

Yellow solid, mp 212-214 °C, R.F. (Hex:EtOAc 7:3) 0.18; ^{1}H NMR (500 MHz, DMSO-*d6*) δ 7.49 (d, *J* = 8.8 Hz, 2H), 7.47 (d, J = 15.6 Hz, 1H), 6.70 (d, *J* = 8.9 Hz, 2H), 6.21 (d, *J* = 15.8 Hz, 1H), 2.97 (s, 6H); ^{13}C NMR (500 MHz, DMSO) δ 167.63, 150.96, 143.98, 129.10, 120.93, 112.38, 111.15, 39.10. HRMS (ESI^{+}) *m/z* calc for $C_{11}H_{14}NO_2^{+}$ [M + H]$^{+}$ 192.1019, found 192.0974.

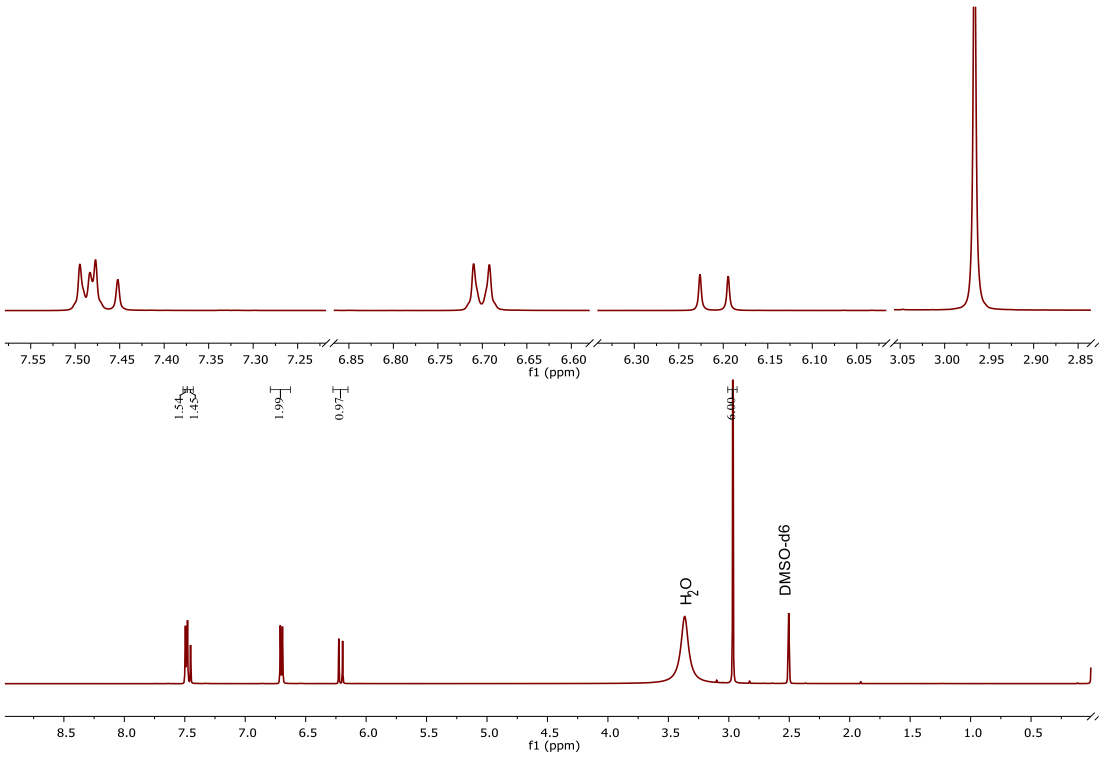

Appendix D. ^{1}H NMR (500 MHz, DMSO-*d6*) of (*E*)-3-(4-(dimethylamino)phenyl)acrylic acid **5c**.

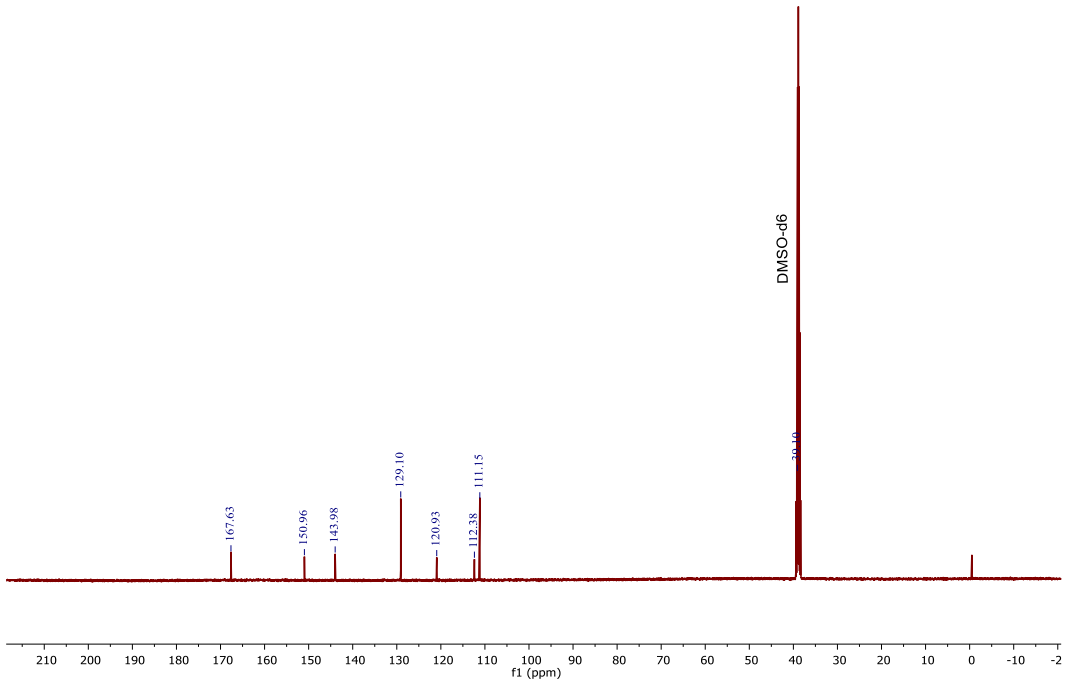

Appendix E. ^{13}C NMR (500 MHz, DMSO) of (*E*)-3-(4-(dimethylamino)phenyl)acrylic acid **5c**.

(*E*)-3-(4-(diethylamino)phenyl)acrylic acid **5d** (63.71%)

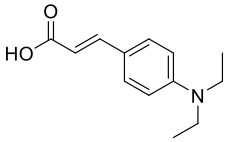

5d

Yellow solid, mp 176-178 °C, R.F. (Hex:EtOAc 7:3) 0.19; FTIR ν (cm^{-1}): 1180 (Ar-N), 1519 (C=C, Ar), 1582 (C=C), 1653 (C=O), 2730-2220 (O-H); ^{1}H NMR (500 MHz, DMSO-*d6*) δ 11.91 (s, 1H), 7.44 (d, J = 14.3 Hz, 1H), 7.44 (s, 2H), 6.65 (d, J = 8.9 Hz, 2H), 6.16 (d, J = 15.9 Hz, 1H), 3.38 (q, J = 7.0 Hz, 5H), 1.10 (t, J = 7.0 Hz, 7H); ^{13}C NMR (500 MHz, DMSO) δ 167.81, 148.25, 143.58, 129.37, 120.21, 112.30, 110.48, 43.12, 11.83. HRMS (ESI^{+}) *m/z* calc for $C_{13}H_{18}NO_2^+$ [M + H]$^+$ 220.1332, found 220.1322.

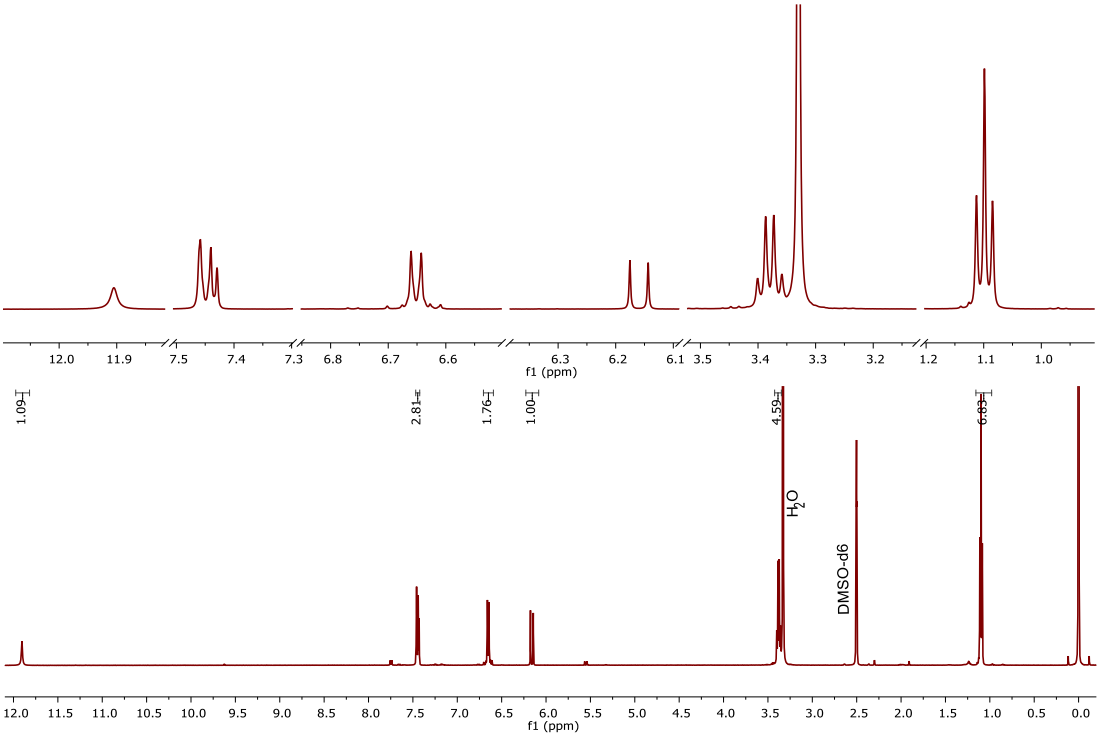

Appendix F. ^{1}H NMR (500 MHz, DMSO-d_6) of (*E*)-3-(4-(diethylamino)phenyl)acrylic acid **5d**.

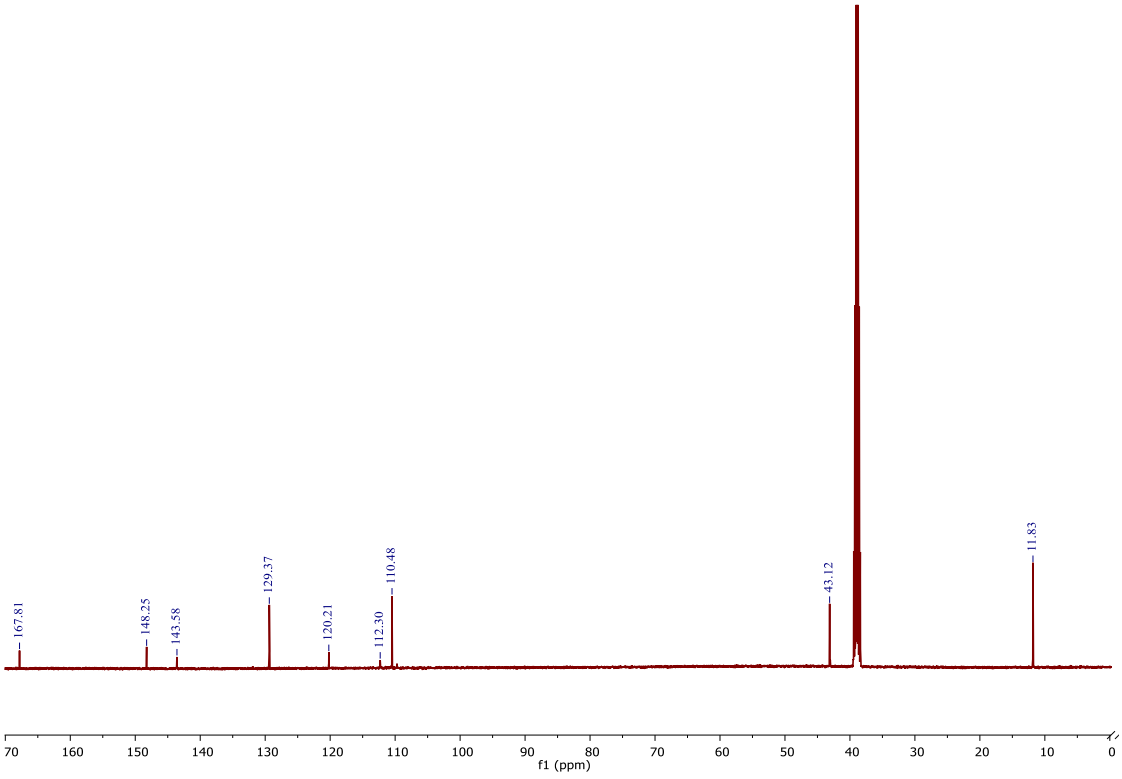

Appendix G. ^{13}C NMR (500 MHz, DMSO) of (*E*)-3-(4-(diethylamino)phenyl)acrylic acid **5d**.

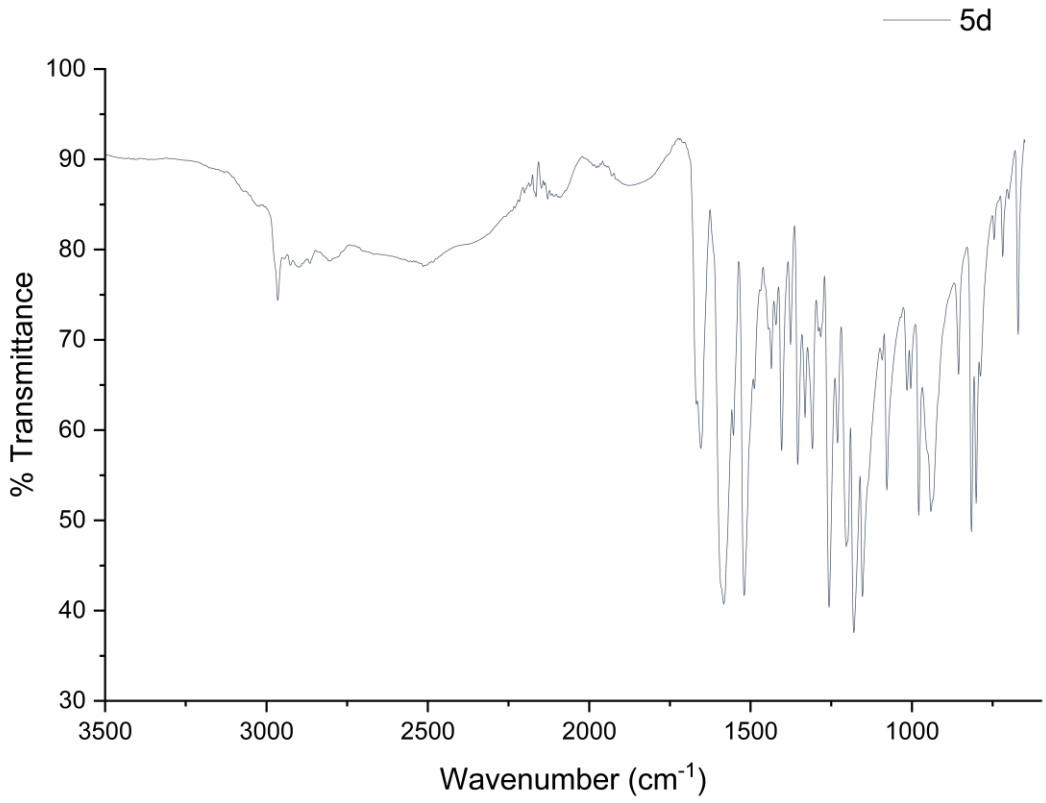

Appendix H. FTIR of (*E*)-3-(4-(diethylamino)phenyl)acrylic acid **5d**.

(*E*)-3-(4-morpholinophenyl)acrylic acid **5e** (79.13%)

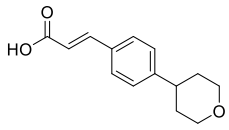

5e

White solid, mp 300°C, R.F. (Hex:EtOAc 7:3) 0.06; FTIR v (cm^{-1}): 1120 (C-O), 1234 (Ar-N), 1518 (C=C, Ar), 1605 (C=C), 1629 (C=O), 3480-3080 (O-H); ^{1}H NMR (500 MHz, DMSO-d_6) δ 7.32 (d, J = 8.8 Hz, 1H), 6.98 (d, J = 15.8 Hz, 1H), 6.89 (d, J = 8.8 Hz, 2H), 6.18 (d, J = 15.8 Hz, 1H), 3.73 (dd, J = 6.0, 3.6 Hz, 4H), 3.11 (dd, J = 6.0, 3.6 Hz, 4H); ^{13}C NMR (500z MHz, DMSO) δ 169.82, 150.01, 134.03, 127.25, 127.20, 127.07, 114.24, 65.42, 47.49. HRMS (ESI^+) *m/z* calc for $C_{13}H_{16}NO_3^+$ $[M + H]^+$ 234.1125, found 234.1116.

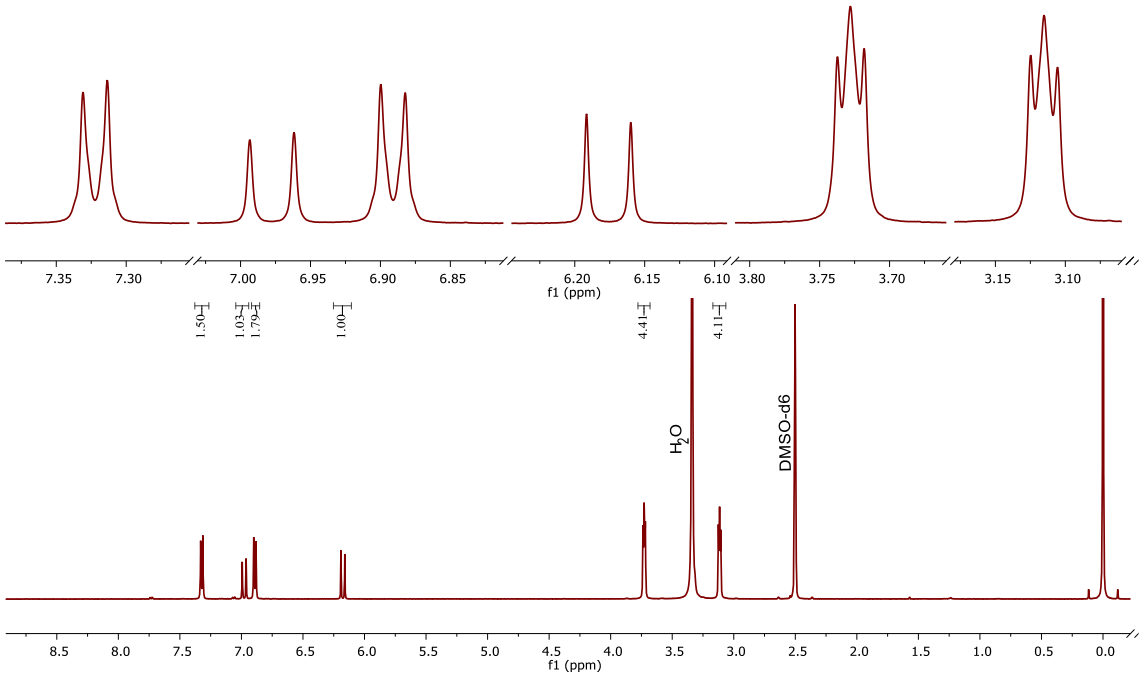

Appendix I. ^{1}H NMR (500 MHz, DMSO-d_6) of (*E*)-3-(4-morpholinophenyl)acrylic acid **5e**.

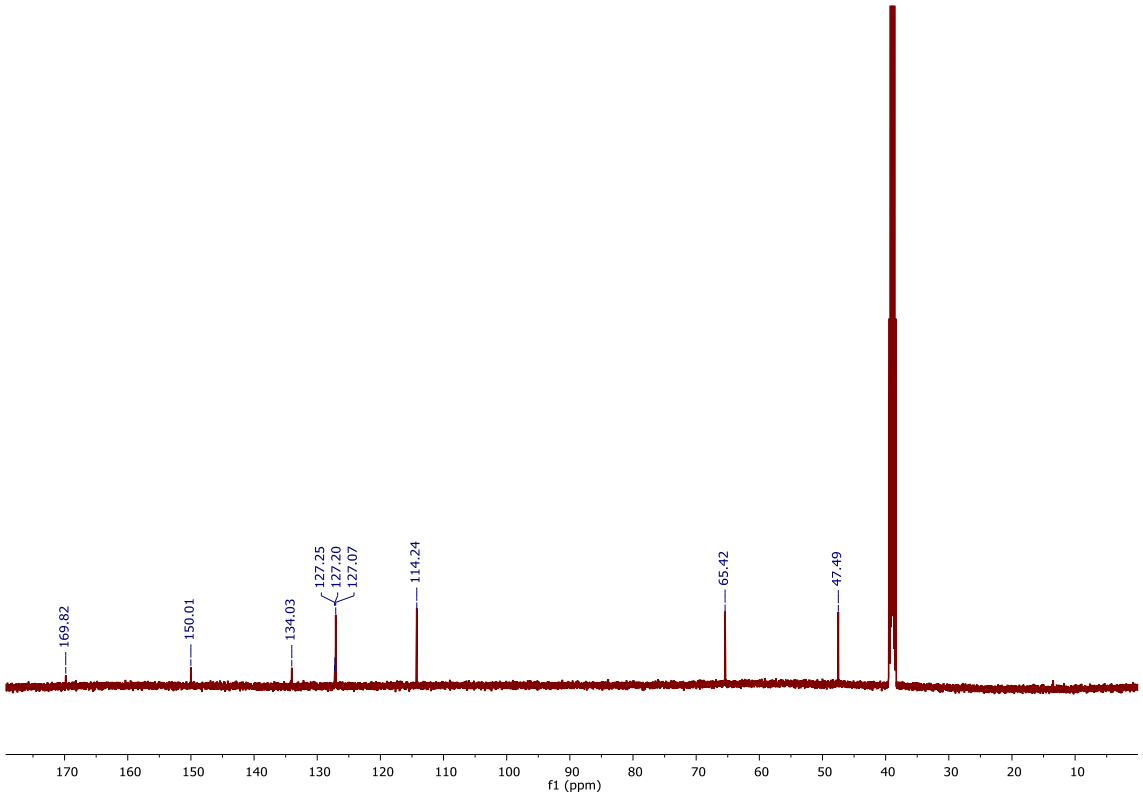

Appendix J. ^{13}C NMR (500 MHz, DMSO) of (*E*)-3-(4-morpholinophenyl)acrylic acid **5e**.

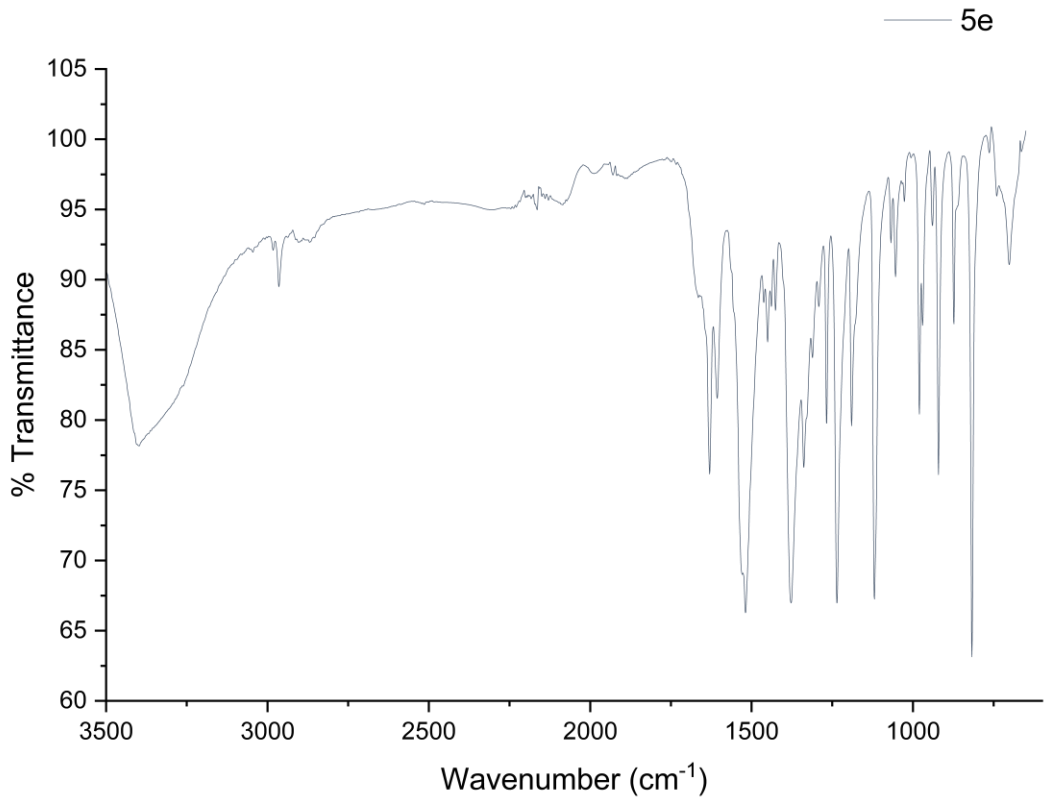

Appendix K. FTIR of (*E*)-3-(4-morpholinophenyl)acrylic acid **5e**.

(*E*)-3-(4-(pyrrolidin-1-yl)phenyl)acrylic acid **5f** (39.66%)

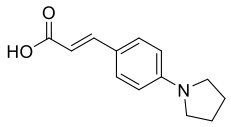

5f

Beige solid, mp 188-189°C, R.F. (Hex:EtOAc 7:3) 0.25; FTIR v (cm^{-1}): 1187 (Ar-N), 1519 (C=C, Ar), 1599 (C=C), 1661 (C=O), 2750-2260 (O-H); ^{1}H NMR (500 MHz, DMSO-d_6) δ 11.90 (s, 1H), 7.47 (d, J = 8.3 Hz, 2zH), 7.46 (d, J = 16.6 Hz, 2H), 6.54 (d, J = 8.8 Hz, 2H), 6.17 (d, J = 15.8 Hz, 1H), 3.31 – 3.25 (m, 4H), 2.00 – 1.92 (m, 4H); ^{13}C NMR (500 MHz, DMSO) δ 168.57, 152.85, 144.77, 130.13, 123.65, 114.92, 114.43, 48.73, 25.37. HRMS (ESI^+) *m/z* calc for $C_{13}H_{16}NO_2^+$ $[M + H]^+$ 218.1176, found 218.1169.

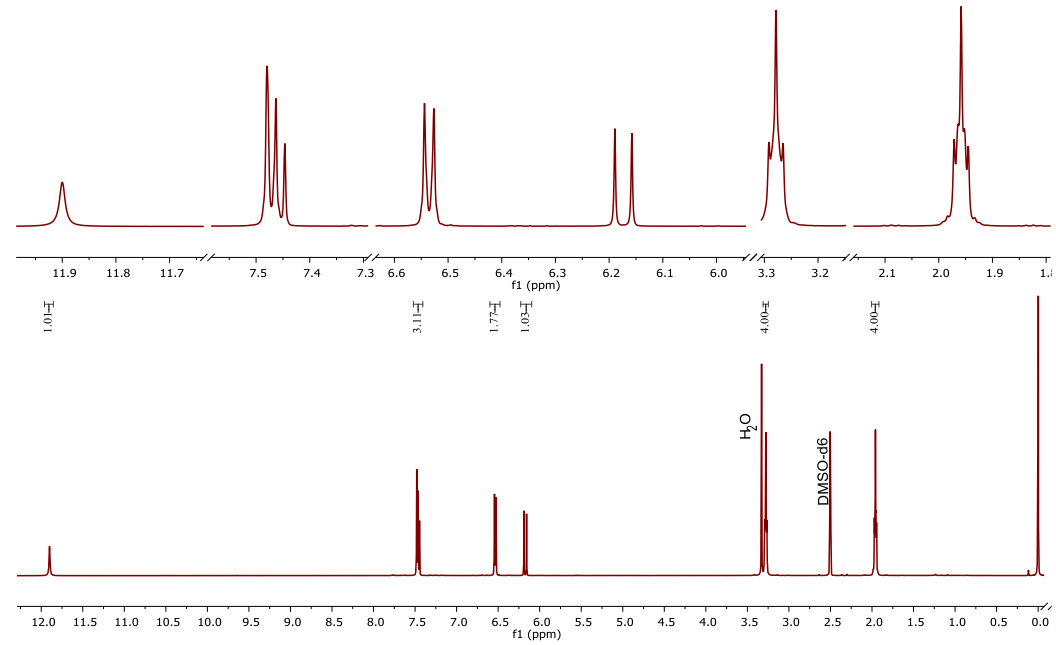

Appendix L. ^{1}H NMR (500 MHz, DMSO-d_6) of (*E*)-3-(4-(pyrrolidin-1-yl)phenyl)acrylic acid **5f**.

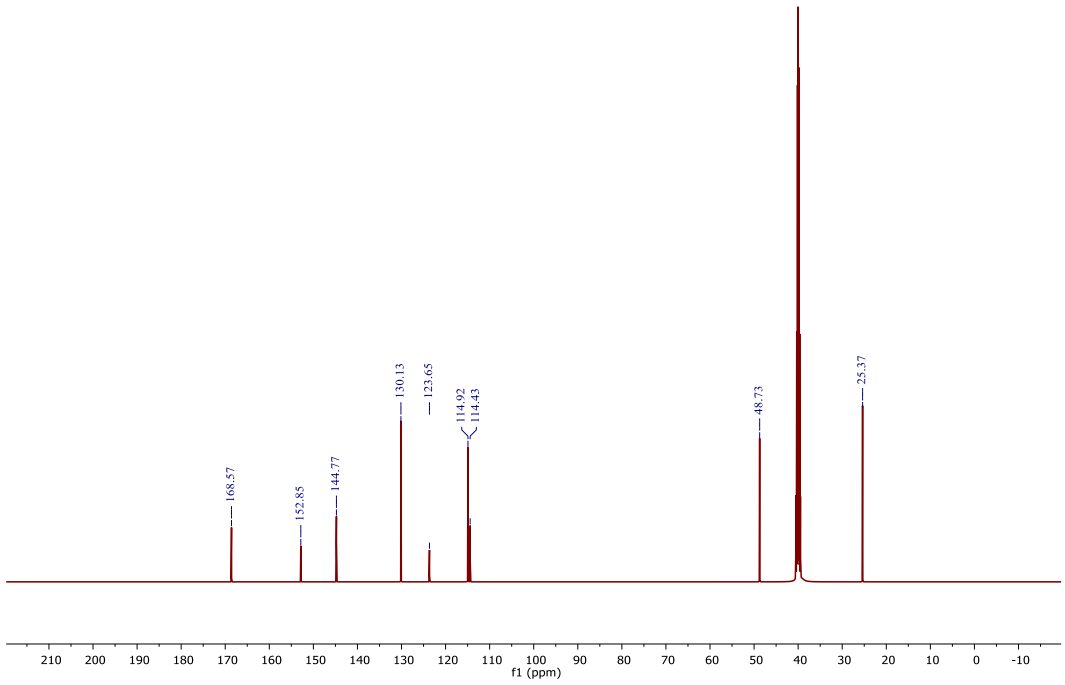

Appendix M. ^{13}C NMR (500 MHz, DMSO) of (*E*)-3-(4-(pyrrolidin-1-yl)phenyl)acrylic acid **5f**.

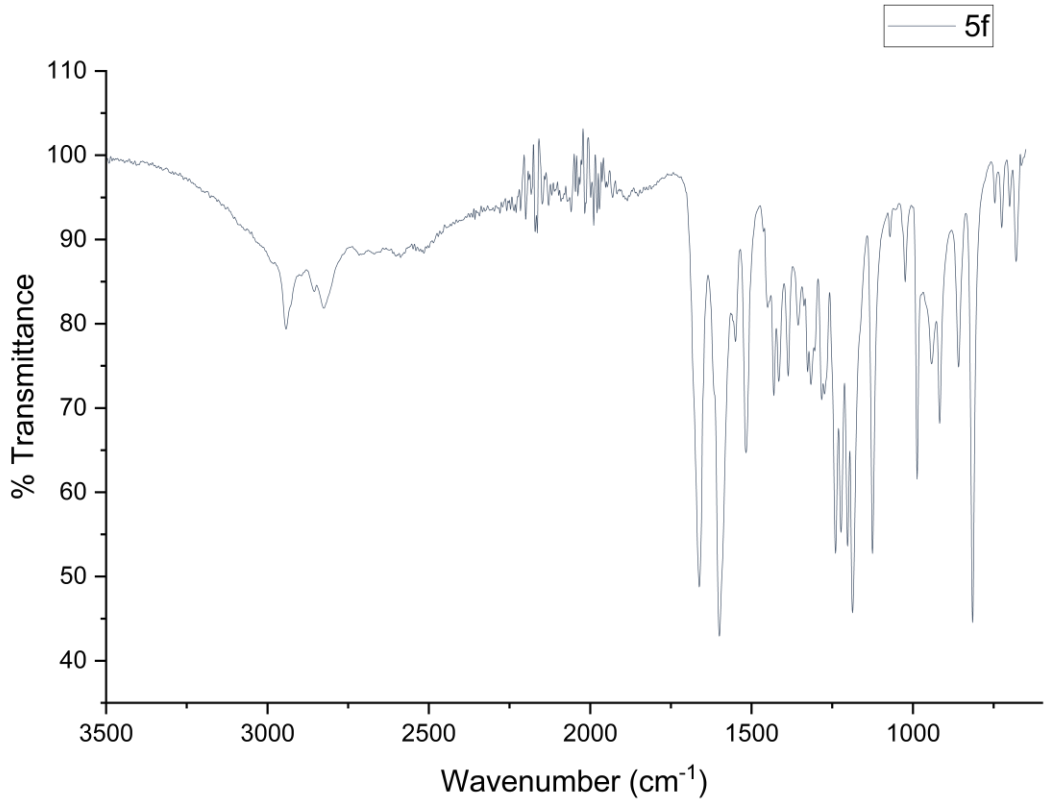

Appendix N. FTIR of (*E*)-3-(4-(pyrrolidin-1-yl)phenyl)acrylic acid **5f**.

(*E*)-3-(9-ethyl-9H-carbazol-3-yl)acrylic acid **5g** (80.63%)

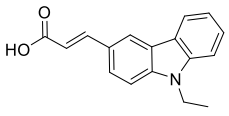

5g

Light brown solid, mp 228-229 °C, R.F. (Hex:EtOAc 7:3) 0.19; ^{1}H NMR (500 MHz, DMSO-d_6) δ 12.18 (s, 1H), 8.54 (s, 1H), 8.21 (d, J = 7.7 Hz, 1H), 7.81 (d, J = 8.62 Hz, 1H), 7.77 (d, J = 16.0 Hz, 1H), 7.64 (d, J = 8.76 Hz, 1H), 7.49 (t, J = 7.7 Hz, 1H), 7.25 (t, J = 7.4 Hz, 1H), 6.55 (d, J = 15.9 Hz, 1H), 4.47 (q, J = 7.1 Hz, 2H), 1.32 (t, J = 7.1 Hz, 3H); ^{13}C NMR (126 MHz, DMSO) δ 139.28, 136.79, 128.72, 126.16, 125.73, 122.24, 119.95, 119.62, 109.14, 45.03, 10.96. HRMS (ESI^{+}) *m/z* calc for $C_{17}H_{16}NO_2^{+}$ $[M + H]^{+}$ 266.1176, found 266.1172.

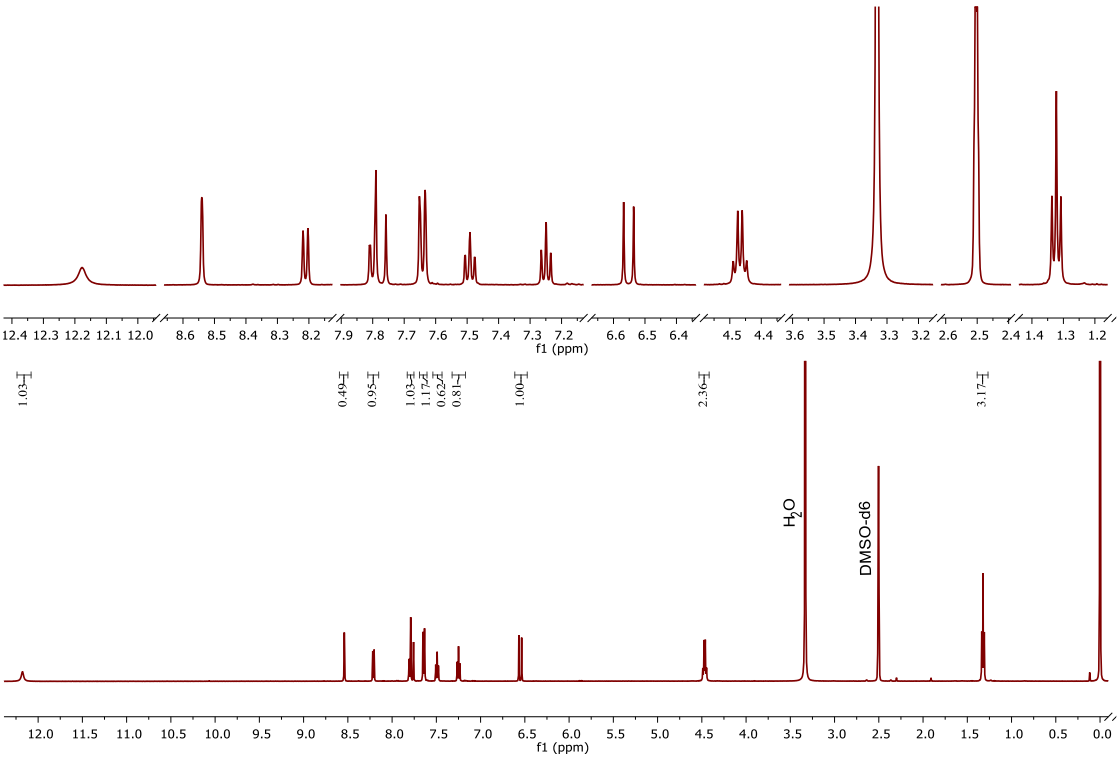

Appendix O. [1]H NMR (500 MHz, DMSO-d_6) of (*E*)-3-(9-ethyl-9H-carbazol-3-yl)acrylic acid **5g**.

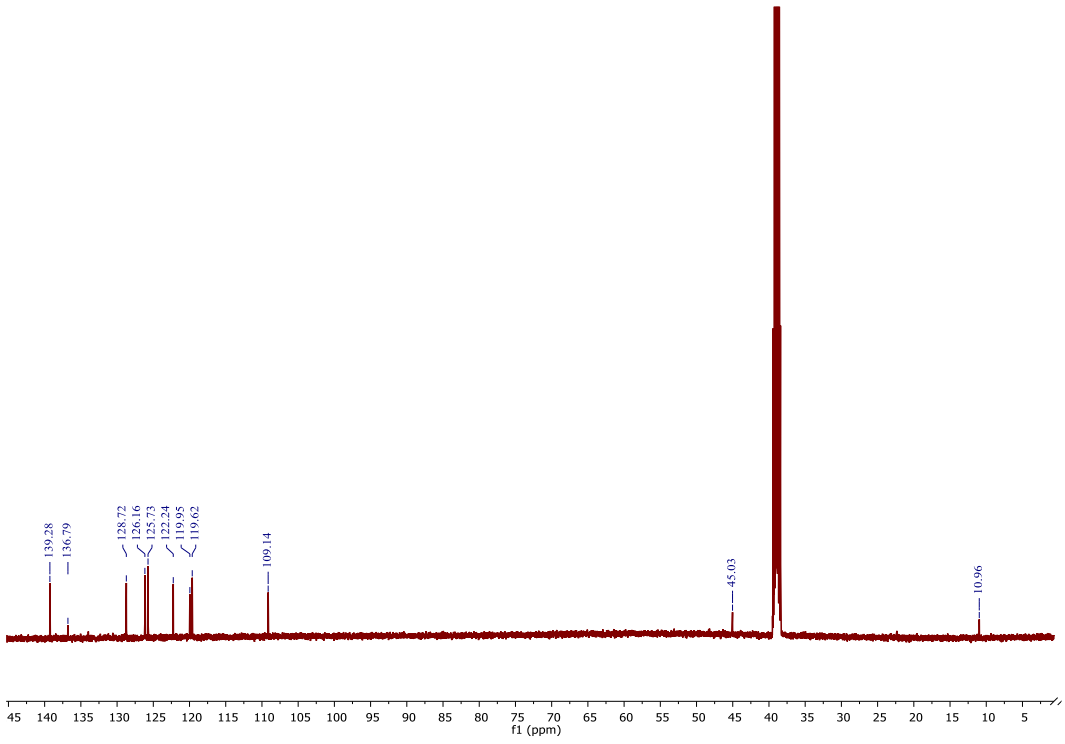

Appendix P. [13]C NMR (500 MHz, DMSO) of (*E*)-3-(9-ethyl-9H-carbazol-3-yl)acrylic acid **5g**.

(*E*)-3-(4-(9H-carbazol-9-yl)phenyl)acrylic acid **5h** (61.12%)

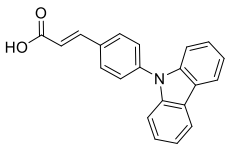

5h

Light yellow solid, mp 245-246 °C, R.F. (Hex:EtOAc 7:3) 0.12; ^{1}H NMR (500 MHz, DMSO-d_6) δ 12.50 (s, 1H), 8.26 (d, J = 7.8 Hz, 2H), 8.00 (d, J = 8.6 Hz, 2H), 7.74 (d, J = 16.0 Hz, 1H), 7.70 (d, J = 8.5 Hz, 2H), 7.48 – 7.41 (m, 4H), 7.31 (ddd, J = 7.9, 4.8, 3.3 Hz, 2H), 6.66 (d, J = 16.0 Hz, 1H); ^{13}C NMR (126 MHz, DMSO) δ 166.95, 142.35, 139.18, 137.72, 132.69, 129.37, 126.19, 125.77, 122.33, 119.99, 119.74, 119.29, 109.15. HRMS (ESI^{+}) *m/z* calc for $C_{21}H_{16}NO_2^{+}$ $[M + H]^{+}$ 314.1176, found 314.1139.

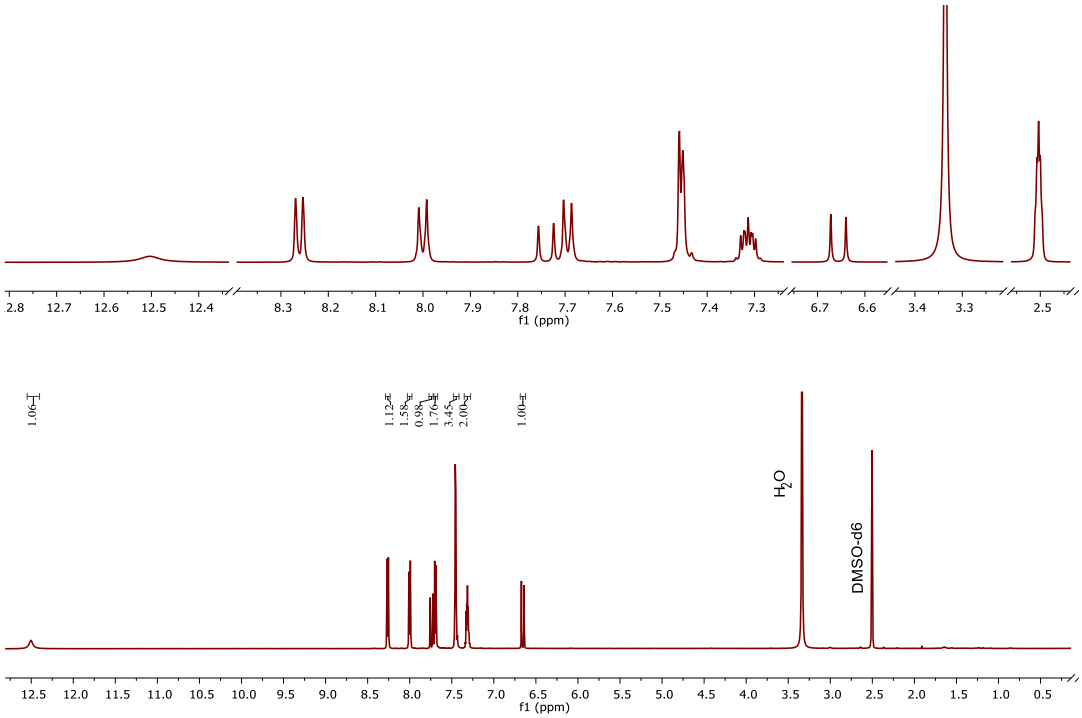

Appendix Q. ^{1}H NMR (500 MHz, DMSO-d_6) of (*E*)-3-(4-(9H-carbazol-9-yl)phenyl)acrylic acid **5h**.

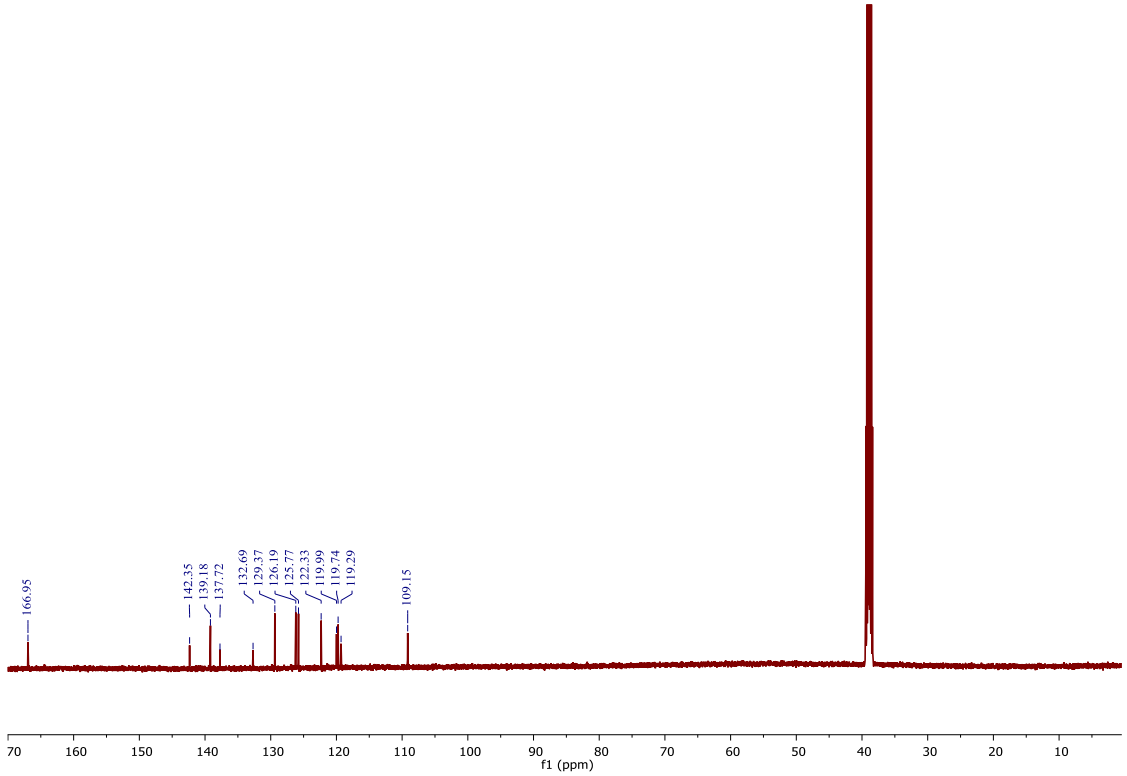

Appendix R. ^{13}C NMR (500 MHz, DMSO) of (*E*)-3-(4-(9H-carbazol-9-yl)phenyl)acrylic acid **5h**.

(*E*)-2-phenyl-5-styryl-1,3,4-oxadiazole **6a** (29.20%)

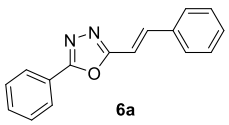

6a

White solid, mp 118-120 °C, R.F. (Hex:EtOAc 7:3) 0.59; FTIR v (cm^{-1}): 1013 (C-O), 1524 (C=C, Ar), 1549 (C=C), 1645 (C=N); ^{1}H NMR (500 MHz, Chloroform-*d*) δ 8.07 (dd, *J* = 7.8, 1.8 Hz, 2H), 7.58 (d, *J* = 16.5 Hz, 1H), 7.54 – 7.51 (m, 2H), 7.50 – 7.45 (m, 3H), 7.40 – 7.31 (m, 3H), 7.05 (d, *J* = 16.4 Hz, 1H); ^{13}C NMR (500 MHz, $CDCl_3$) δ 164.32, 164.08, 138.96, 134.81, 131.79, 130.02, 129.11, 129.07, 127.55, 127.00, 123.89, 110.06. HRMS (ESI^{+}) *m/z* calc for $C_{16}H_{13}N_2O^{+}$ $[M + H]^{+}$ 249.1022, found 249.1006.

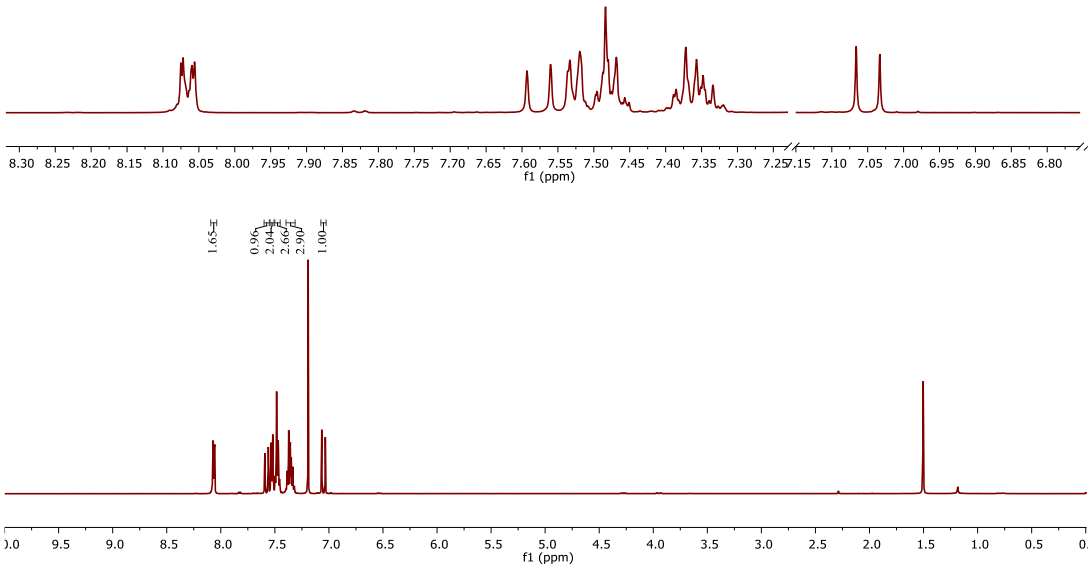

Appendix S. ^{1}H NMR (500 MHz, $CDCl_3$) of (E)-2-phenyl-5-styryl-1,3,4-oxadiazole **6a**.

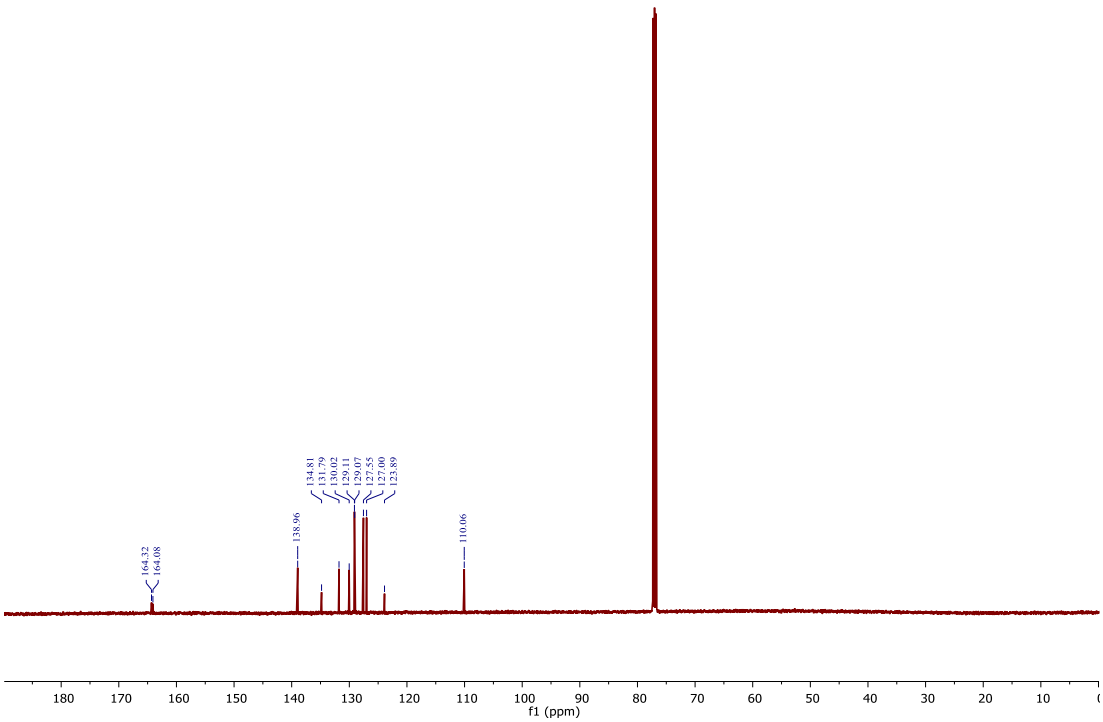

Appendix T. ^{13}C NMR (500 MHz, $CDCl_3$) of (*E*)-2-phenyl-5-styryl-1,3,4-oxadiazole **6a**.

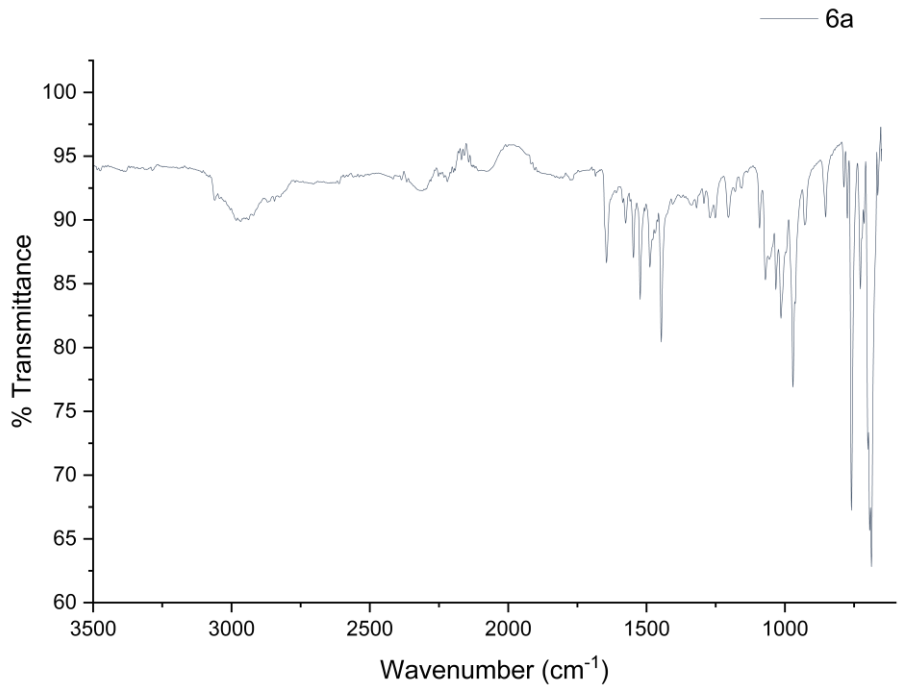

Appendix U. FTIR of (*E*)-2-phenyl-5-styryl-1,3, 4-oxadiazole **6a**

(*E*)-2-phenyl-5-(4-(trifluoromethyl)styryl)-1,3,4-oxadiazole **6b** (21.44%)

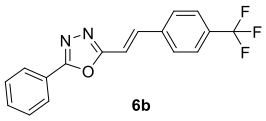

6b

Beige solid, mp 168-170 °C, R.F. (Hex:EtOAc 7:3) 0.58; FTIR v (cm^{-1}): 1063 (C-O), 1107 (C-F), 1613 (C=C, Ar), 1648 (C=C), 1645 (C=N); ^{1}H NMR (500 MHz, Chloroform-*d*) δ 8.07 (dd, *J* = 8.1, 1.6 Hz, 2H), 7.63 (s, 4H), 7.59 (d, *J* = 16.4 Hz, 1H), 7.53 – 7.45 (m, 3H), 7.13 (d, *J* = 16.5 Hz, 1H); ^{13}C NMR (500 MHz, $CDCl_3$) δ 164.39, 163.78, 138.14, 137.08, 132.00, 131.39, 129.17, 127.67, 127.07, 126.07, 126.04, 123.68, 122.77, 112.52. HRMS (ESI^+) *m/z* calc for $C_{17}H_{12}F_3N_2O^+$ $[M + H]^+$ 317.0896, found 317.0873.

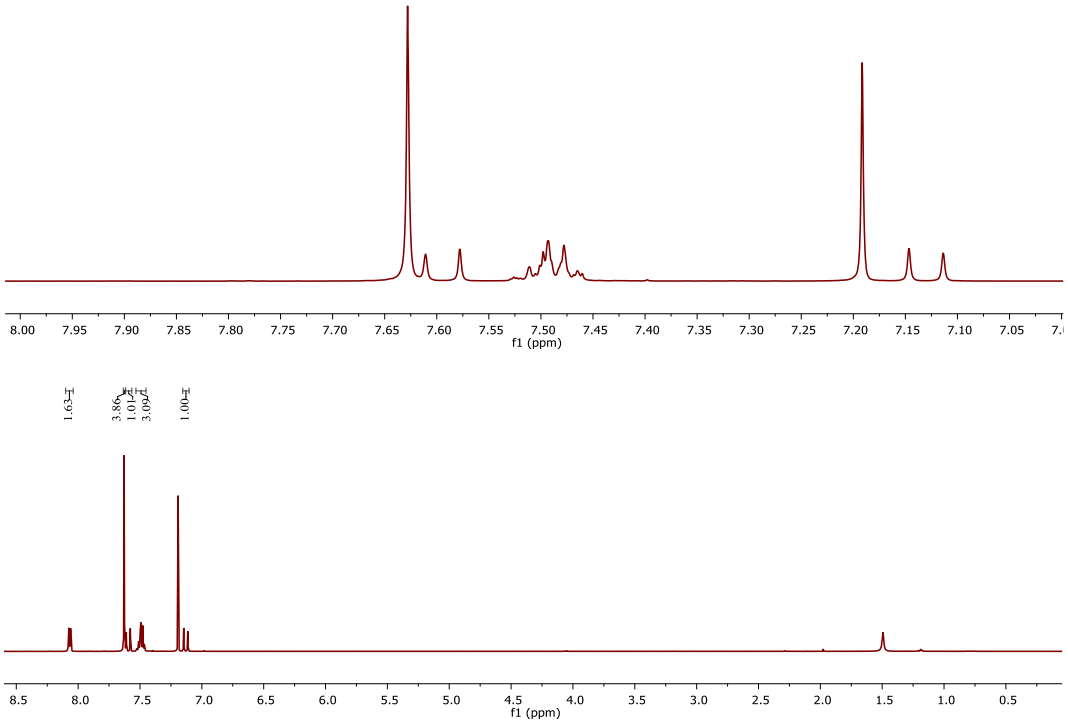

Appendix V. ^{1}H NMR (500 MHz, $CDCl_3$) of ((*E*)-2-phenyl-5-(4-(trifluoromethyl)styryl)-1,3,4-oxadiazole **6b**.

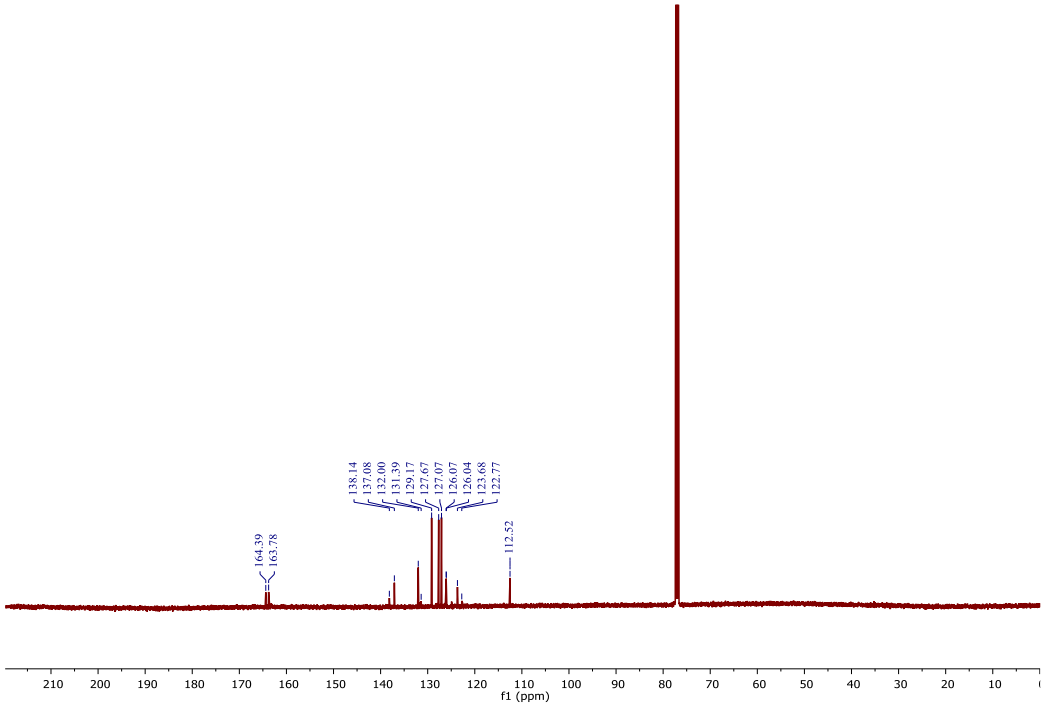

Appendix W. ^{13}C NMR (500 MHz, $CDCl_3$) of ((E)-2-phenyl-5-(4-(trifluoromethyl)styryl)-1,3,4-oxadiazole **6b**.

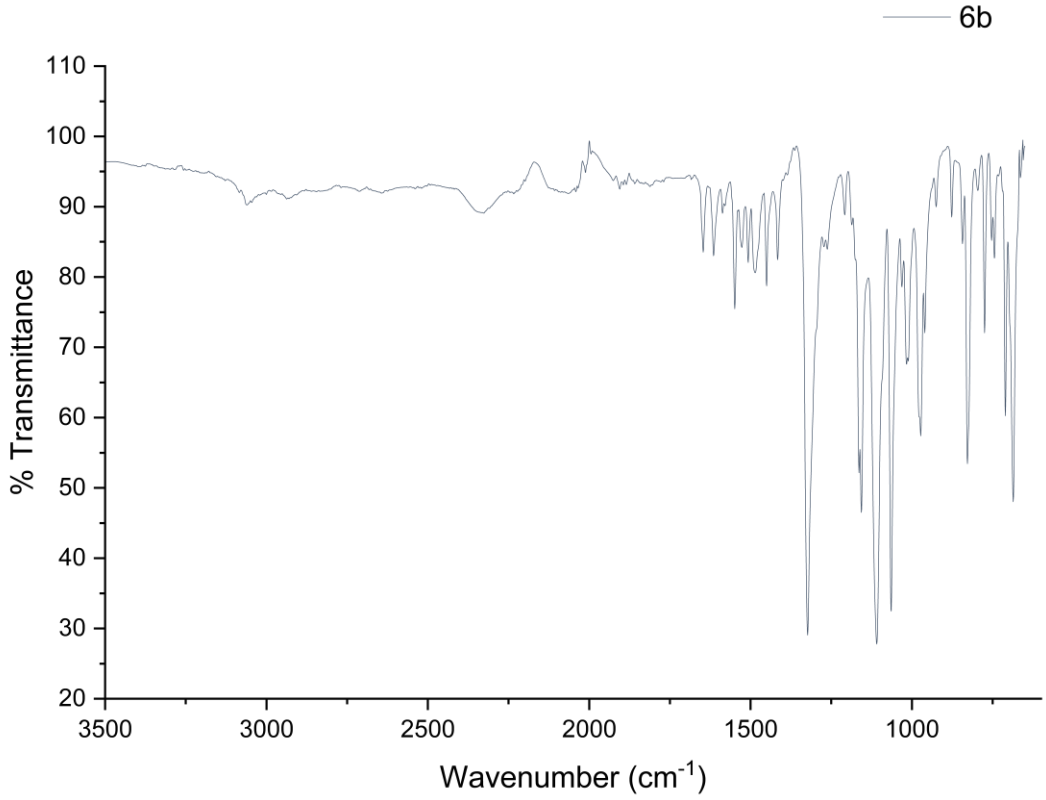

Appendix X. FTIR of ((E)-2-phenyl-5-(4-(trifluoromethyl)styryl)-1,3,4-oxadiazole **6b**.

(*E*)-N,N-dimethyl-4-(2-(5-phenyl-1,3,4-oxadiazol-2-yl)vinyl)aniline **6c** (41.39%)

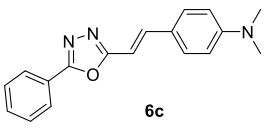

6c

Yellow solid, mp 158-160 °C, R.F. (Hex:EtOAc 7:3) 0.37; FTIR v (cm^{-1}): 1015 (C-O), 1177 (Ar-N), 1532 (C=C, Ar), 1601 (C=C), 1631 (C=N); ^{1}H NMR (500 MHz, Chloroform-*d*) δ 8.04 (dd, *J* = 7.3, 2.3 Hz, 2H), 7.48 (d, *J* = 16.4 Hz, 2H), 7.48 – 7.43 (m, 3H), 7.41 (d, *J* = 8.9 Hz, 1H), 6.80 (d, *J* = 16.3 Hz, 1H), 6.66 (d, *J* = 8.3 Hz, 2H), 2.97 (s, 6H); ^{13}C NMR (126 MHz, $CDCl_3$) δ 165.22, 163.47, 151.49, 139.28, 131.42, 129.06, 129.01, 126.83, 124.18, 122.70, 111.99, 104.60, 40.19. HRMS (ESI^+) *m/z* calc for $C_{18}H_{18}N_3O^+$ $[M + H]^+$ 292.1444, found 292.1423.

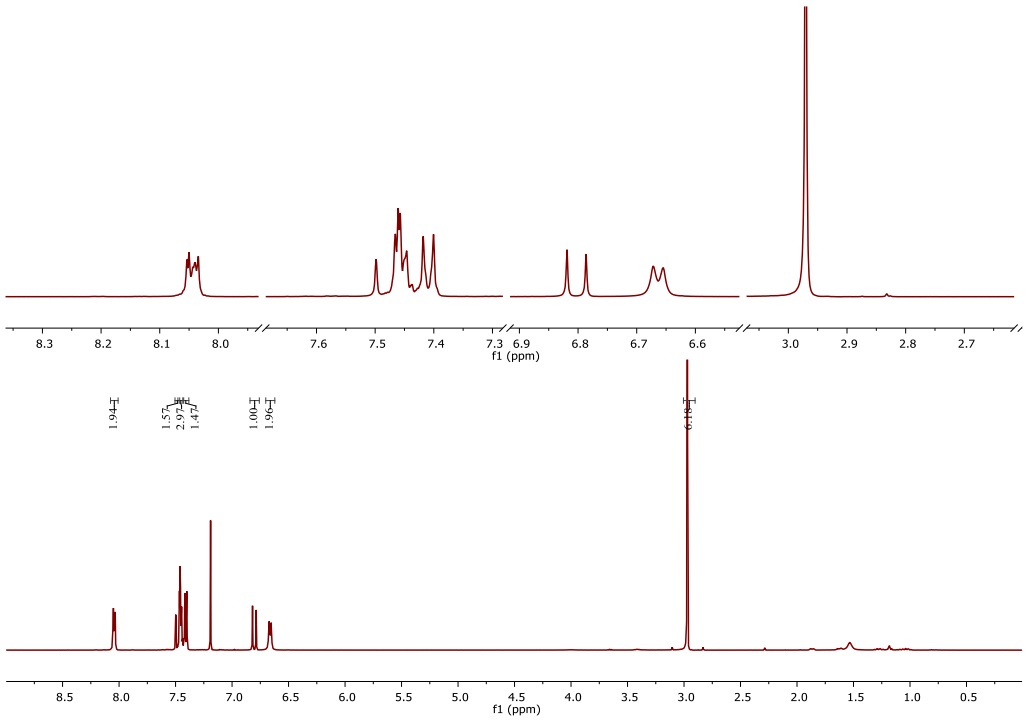

Appendix Y. ^{1}H NMR (500 MHz, $CDCl_3$) of (E)-N,N-dimethyl-4-(2-(5-phenyl-1,3,4-oxadiazol-2-yl)vinyl)aniline **6c**.

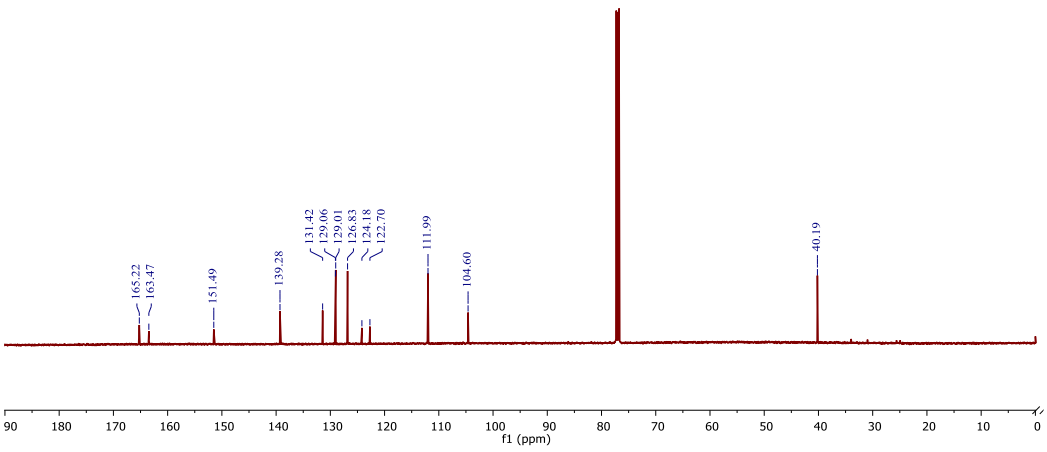

Appendix Z. ^{13}C NMR (500 MHz, $CDCl_3$) of (*E*)-N,N-dimethyl-4-(2-(5-phenyl-1,3,4-oxadiazol-2-yl)vinyl)aniline **6c**.

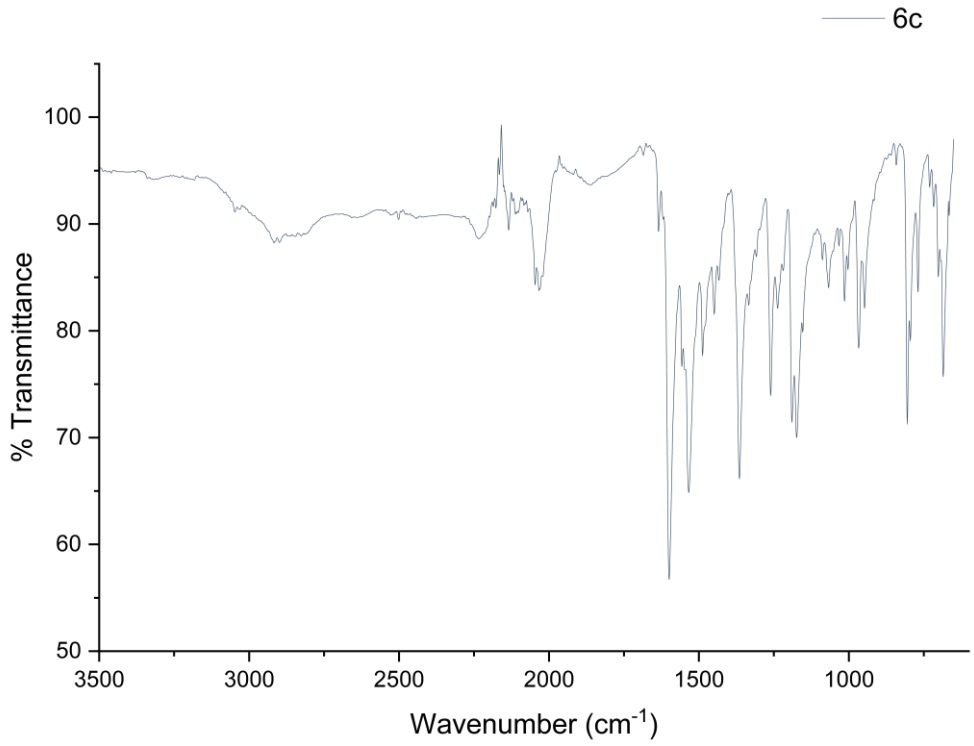

Appendix AA. FTIR of (*E*)-N,N-dimethyl-4-(2-(5-phenyl-1,3,4-oxadiazol-2-yl)vinyl)aniline **6c**.

(*E*)-N,N-diethyl-4-(2-(5-phenyl-1,3,4-oxadiazol-2-yl)vinyl)aniline **6d** (37.17%)

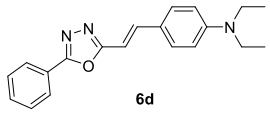

Orange solid, mp 178-180 °C, R.F. (Hex:EtOAc 7:3) 0.45; FTIR v (cm^{-1}): 1012 (C-O), 1155 (Ar-N), 1527 (C=C, Ar), 1594 (C=C), 1639 (C=N); ^{1}H NMR (400 MHz, Chloroform-*d*) δ 8.13 (dd, *J* = 7.2, 2.7 Hz, 1H), 7.57 – 7.51 (m, 3H), 7.55 (d, *J* = 16.7 Hz, 1H), 7.47 (d, *J* = 8.9 Hz, 2H), 6.86 (d, *J* = 16.3 Hz, 1H), 6.70 (d, *J* = 8.9 Hz, 2H), 3.43 (q, *J* = 7.1 Hz, 4H), 1.22 (t, *J* = 7.1 Hz, 6H); ^{13}C NMR (500 MHz, $CDCl_3$) δ 165.36, 163.39, 149.03, 139.31, 131.38, 129.38, 129.00, 126.81, 124.22, 121.81, 111.36, 103.92, 44.48, 12.61. HRMS (ESI^+) *m/z* calc for $C_{20}H_{22}N_3O^+$ $[M + H]^+$ 320.1757, found 320.1733.

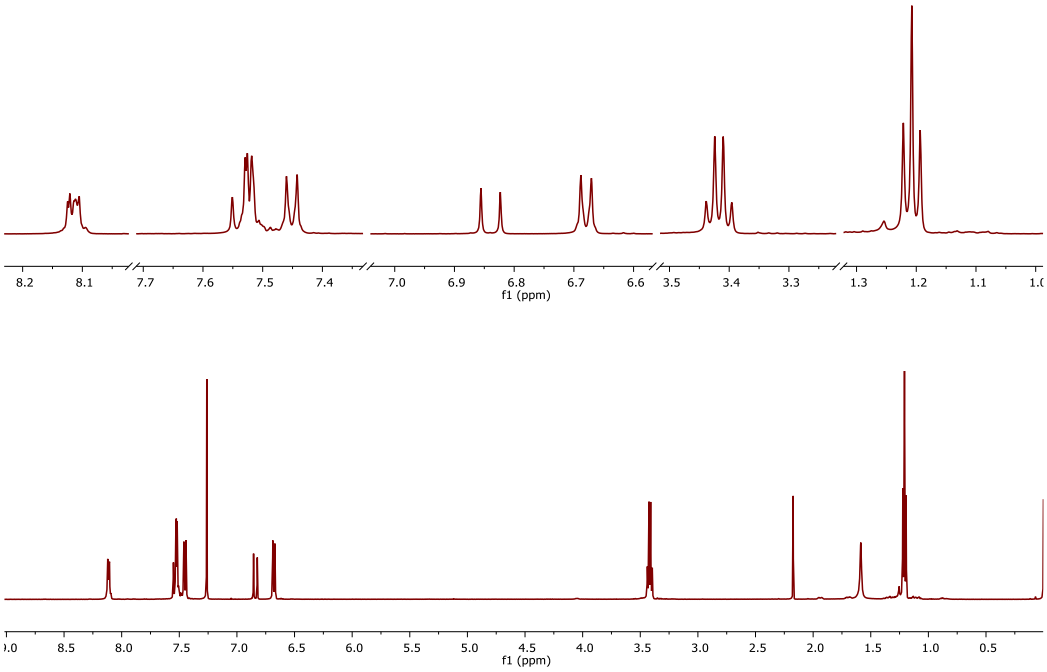

Appendix BB. ^{1}H NMR (500 MHz, $CDCl_3$) of (*E*)-N,N-diethyl-4-(2-(5-phenyl-1,3,4-oxadiazol-2-yl)vinyl)aniline **6d**.

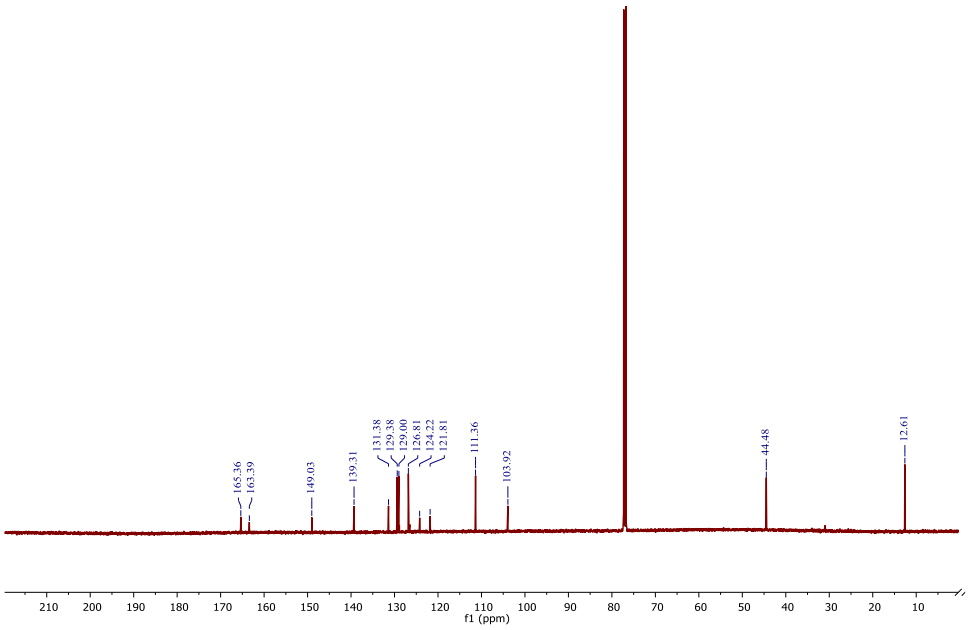

Appendix CC. ^{13}C NMR (500 MHz, $CDCl_3$) of (E)-N,N-diethyl-4-(2-(5-phenyl-1,3,4-oxadiazol-2-yl)vinyl)aniline **6d**.

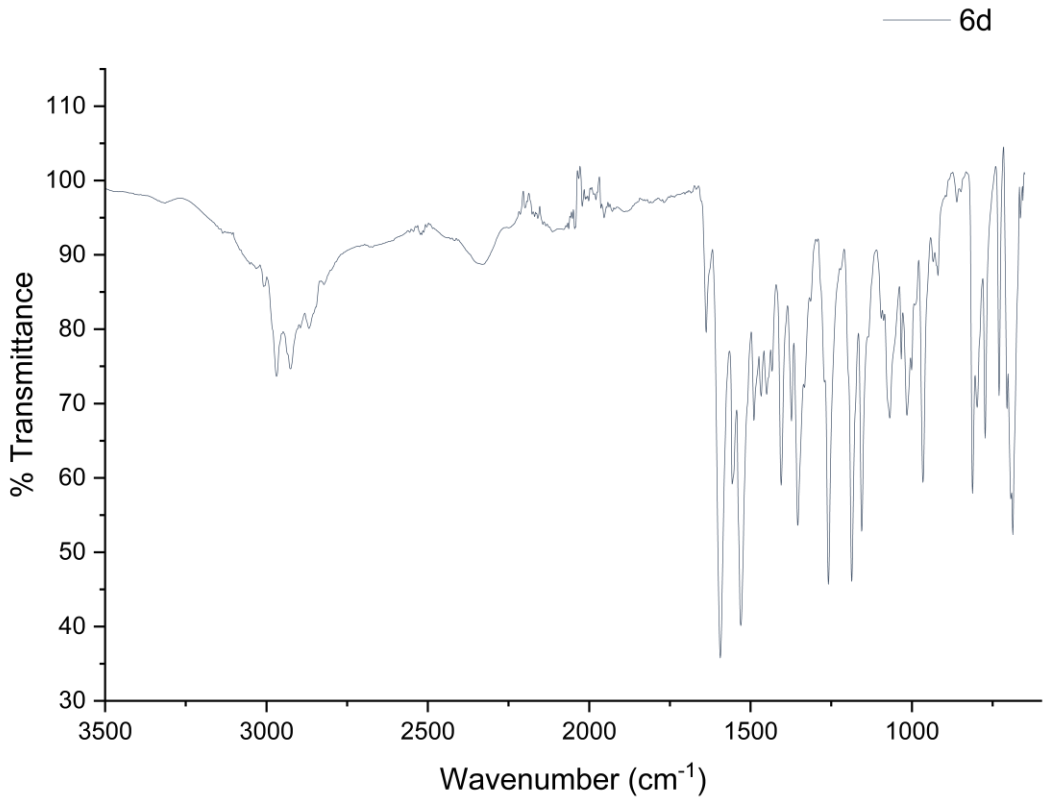

Appendix DD. FTIR of (*E*)-N,N-diethyl-4-(2-(5-phenyl-1,3,4-oxadiazol-2-yl)vinyl)aniline **6d**.

(*E*)-4-(4-(2-(5-phenyl-1,3,4-oxadiazol-2-yl)vinyl)phenyl)morpholine **6e** (38.92%)

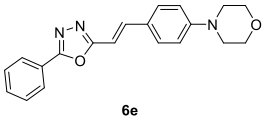

6e

Yellow solid, mp 198-200 °C, R.F. (Hex:EtOAc 7:3) 0.21; FTIR v (cm^{-1}): 1016 (C-O), 1176 (Ar-N), 1532 (C=C, Ar), 1597 (C=C), 1637 (C=N); ^{1}H NMR (500 MHz, Chloroform-*d*) δ 8.05 (dd, *J* = 7.5, 2.0 Hz, 2H), 7.50 (d, *J* = 16.4 Hz, 1H), 7.48 – 7.45 (m, 3H), 7.45 (d, *J* = 7.1 Hz, 2H), 6.90 (d, *J* = 8.7 Hz, 2H), 6.88 (d, *J* = 16.3 Hz, 1H), 3.83 (dd, *J* = 6.0, 3.6 Hz, 4H), 3.20 (dd, *J* = 6.0, 3.6 Hz, 4H); ^{13}C NMR (500 MHz, $CDCl_3$) δ 164.76, 163.77, 158.82, 138.48, 131.62, 129.07, 128.95, 126.91, 124.04, 115.53, 107.11, 66.47, 48.77. HRMS (ESI^+) *m/z* calc for $C_{20}H_{20}N_3O_2^+$ $[M + H]^+$ 334.1550, found 334.1526.

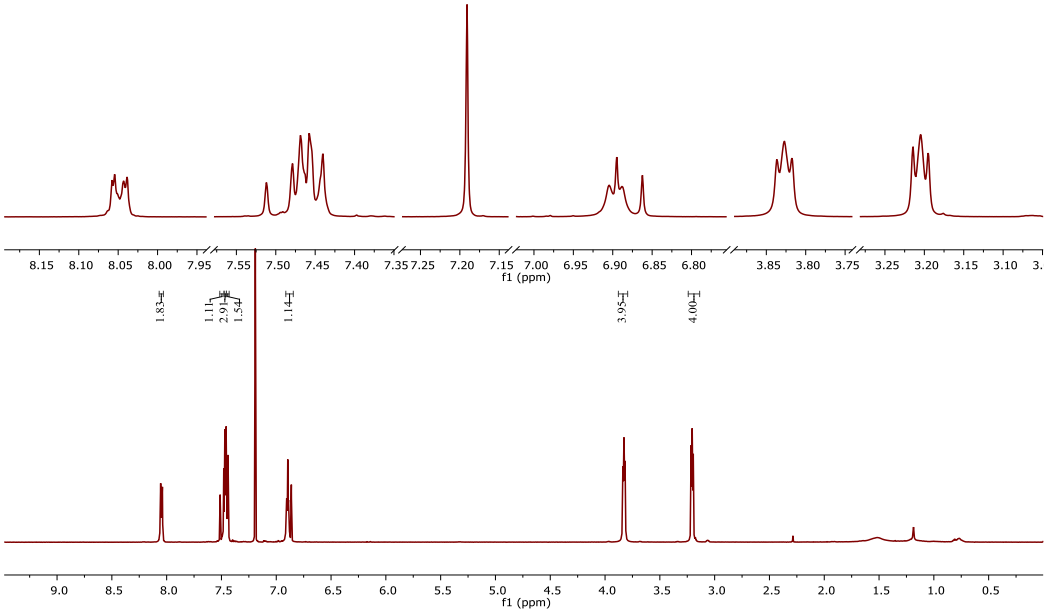

Appendix EE. ^{1}H NMR (500 MHz, $CDCl_3$) of (E)-4-(4-(2-(5-phenyl-1,3,4-oxadiazol-2-yl)vinyl)phenyl)morpholine **6e**.

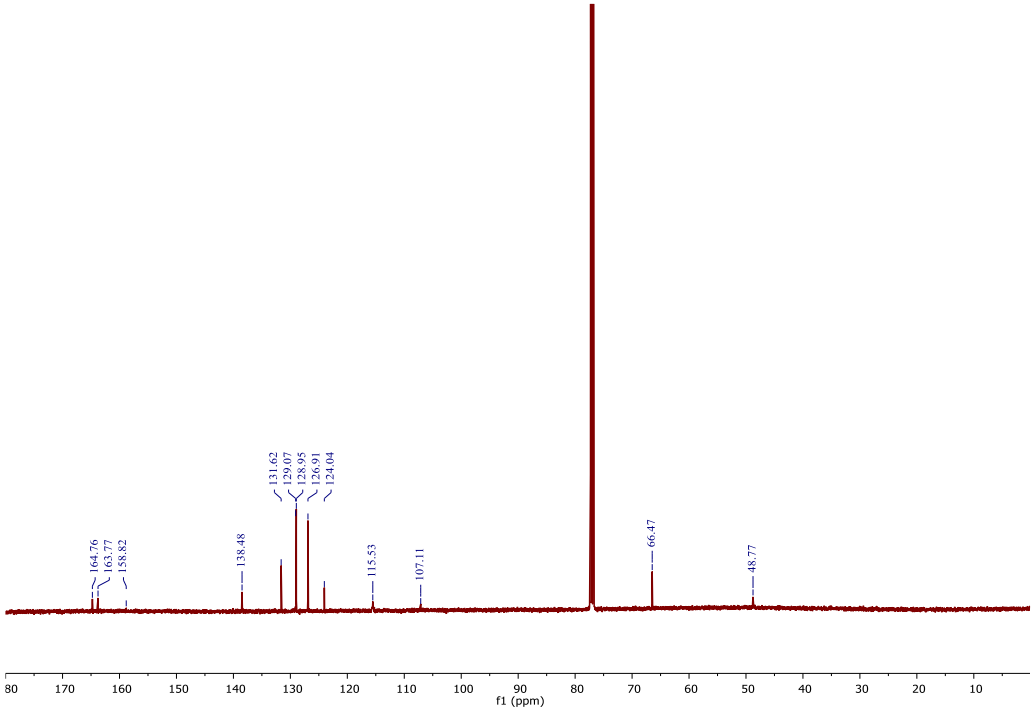

Appendix FF. ^{13}C NMR (500 MHz, $CDCl_3$) of (*E*)-4-(4-(2-(5-phenyl-1,3,4-oxadiazol-2-yl)vinyl)phenyl)morpholine **6e**.

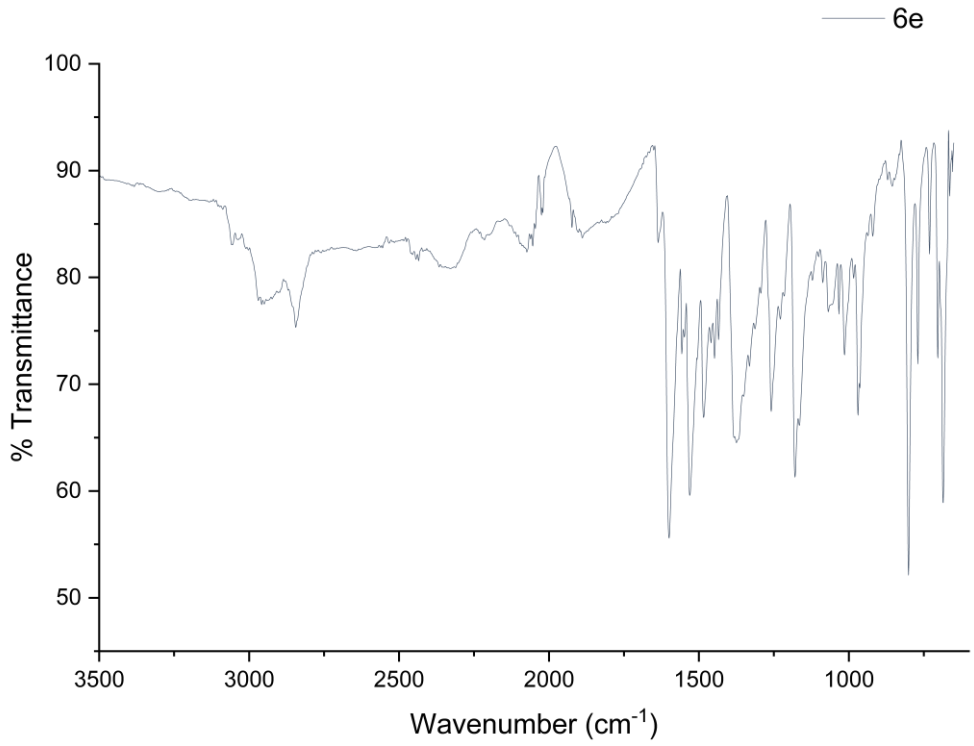

Appendix GG. FTIR of (*E*)-4-(4-(2-(5-phenyl-1,3,4-oxadiazol-2-yl)vinyl)phenyl)morpholine **6e**.

(*E*)-2-phenyl-5-(4-(pyrrolidin-1-yl)styryl)-1,3,4-oxadiazole **6f** (35.89%)

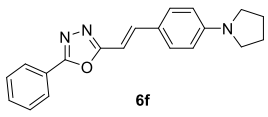

6f

Brown solid, mp 118-120 °C, R.F. (Hex:EtOAc 7:3) 0.43; FTIR v (cm^{-1}): 1056 (C-O), 1184 (Ar-N), 1524 (C=C, Ar), 1590 (C=C), 1633 (C=N); ^{1}H NMR (500 MHz, Chloroform-*d*) δ 8.11 (dd, *J* = 7.2, 2.6 Hz, 2H), 7.55 (d, *J* = 16.7 Hz, 2H), 7.53 – 7.50 (m, 3H), 7.47 (d, *J* = 8.7 Hz, 2H), 6.84 (d, *J* = 16.2 Hz, 1H), 6.57 (d, *J* = 8.7 Hz, 2H), 3.44 – 3.25 (m, 4H), 2.11 – 1.98 (m, 4H). ^{13}C NMR (500 MHz, $CDCl_3$) δ 165.36, 163.38, 149.03, 139.55, 131.37, 129.23, 128.99, 126.80, 124.24, 122.02, 111.77, 103.86, 47.57, 25.48. HRMS (ESI^+) *m/z* calc for $C_{20}H_{20}N_3O^+$ $[M + H]^+$ 318.1601, found 318.1573.

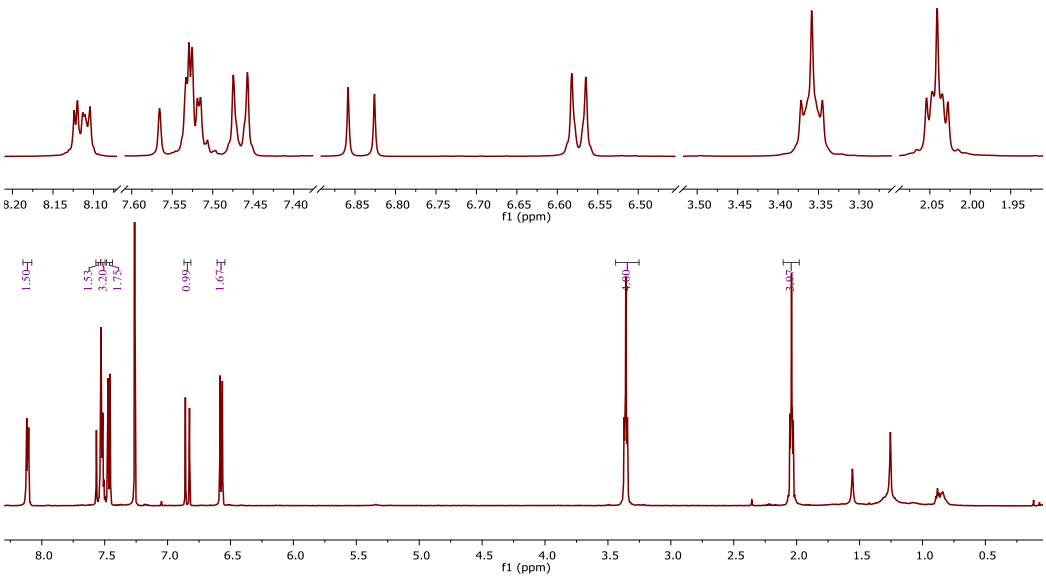

Appendix HH. ^{1}H NMR (500 MHz, $CDCl_3$) of (E)-2-phenyl-5-(4-(pyrrolidin-1-yl)styryl)-1,3,4-oxadiazole **6f**.

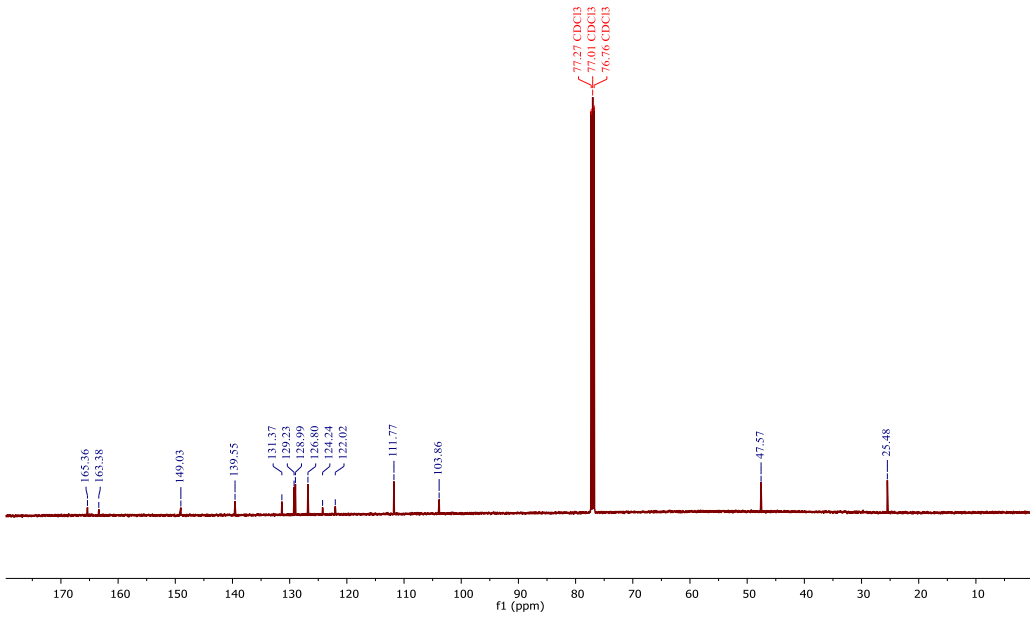

Appendix II. ^{13}C NMR (500 MHz, $CDCl_3$) of (*E*)-2-phenyl-5-(4-(pyrrolidin-1-yl)styryl)-1,3,4-oxadiazole **6f**.

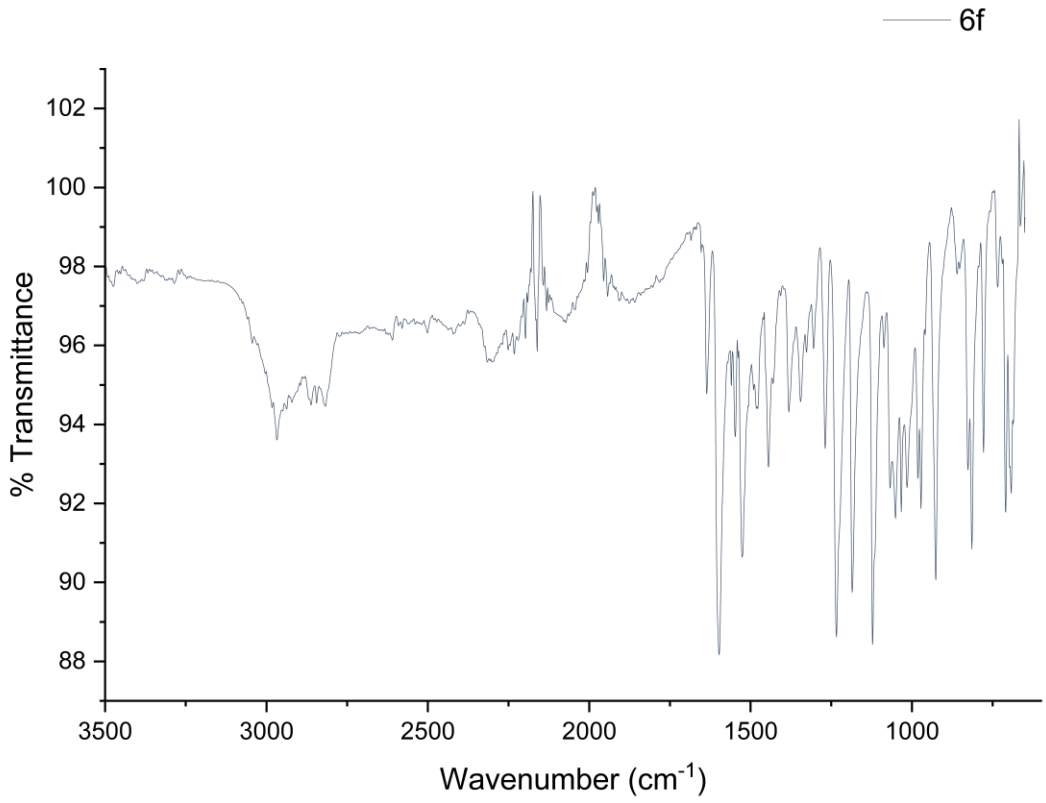

Appendix JJ. FTIR de of (*E*)-2-phenyl-5-(4-(pyrrolidin-1-yl)styryl)-1,3,4-oxadiazole **6f**.

(*E*)-2-(2-(9-ethyl-9H-carbazol-3-yl)vinyl)-5-phenyl-1,3,4-oxadiazole **6g** (38.21%)

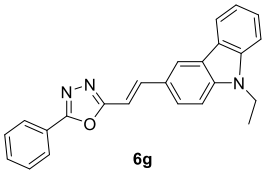

Beige solid, mp 178-180 °C, R.F. (Hex:EtOAc 7:3) 0.34; FTIR v (cm^{-1}): 1016 (C-O), 1158 (Ar-N), 1591 (C=C, Ar), 1622 (C=C), 1643 (C=N); ^{1}H NMR (500 MHz, Chloroform-*d*) δ 8.24 (s, 0H), 8.10 – 8.04 (m, 3H), 7.78 (d, *J* = 16.3 Hz, 1H), 7.68 (dd, *J* = 8.5, 1.7 Hz, 1H), 7.50 – 7.42 (m, 4H), 7.38 (dd, *J* = 8.3, 3.6 Hz, 2H), 7.22 (t, *J* = 7.5 Hz, 1H), 7.06 (d, *J* = 16.3 Hz, 1H), 4.33 (q, *J* = 7.3 Hz, 2H), 1.40 (t, *J* = 7.2 Hz, 3H). ^{13}C NMR (126 MHz, $CDCl_3$) δ 164.22, 140.48, 139.22, 137.79, 133.66, 131.89, 129.16, 128.98, 127.32, 127.05, 126.13, 123.84, 123.68, 120.45, 120.38, 110.64, 109.79, 44.48, 12.61. HRMS (ESI^+) *m/z* calc for $C_{24}H_{20}N_3O^+$ $[M + H]^+$ 366.1601, found 366.1575.

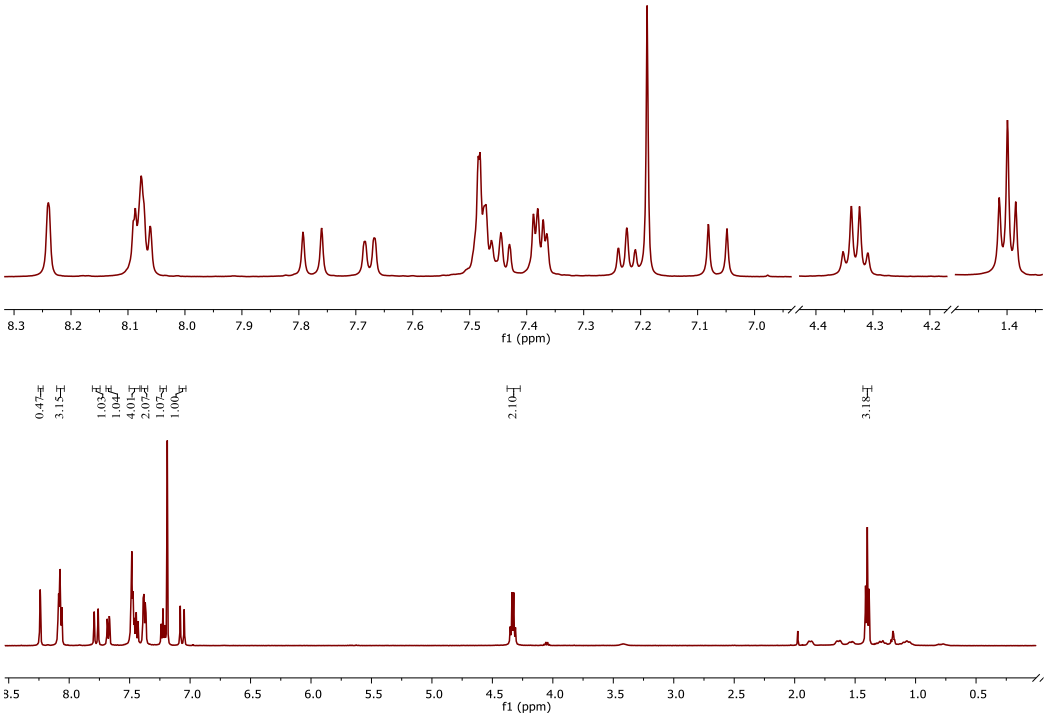

Appendix KK. ^{1}H NMR (500 MHz, $CDCl_3$) of (E)-2-(2-(9-ethyl-9H-carbazol-3-yl)vinyl)-5-phenyl-1,3,4-oxadiazole **6g**.

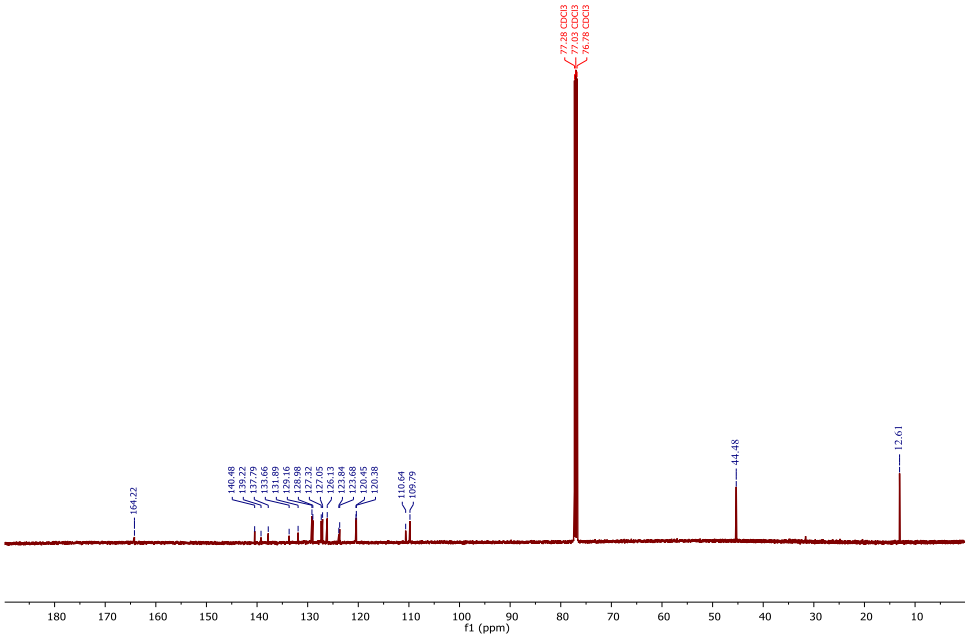

Appendix LL. ^{13}C NMR (500 MHz, $CDCl_3$) of (*E*)-2-(2-(9-ethyl-9H-carbazol-3-yl)vinyl)-5-phenyl-1,3,4-oxadiazole **6g**.

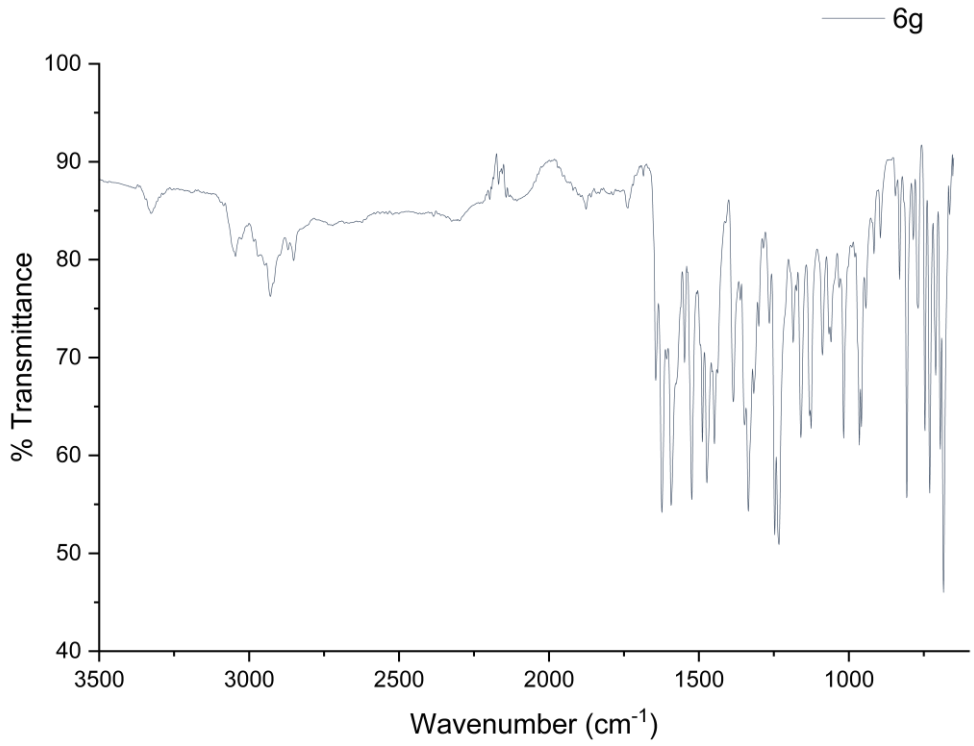

Appendix MM. FTIR of (*E*)-2-(2-(9-ethyl-9H-carbazol-3-yl)vinyl)-5-phenyl-1,3,4-oxadiazole **6g**.

(*E*)-2-(4-(9H-carbazol-9-yl)styryl)-5-phenyl-1,3,4-oxadiazole **6h** (41.38%)

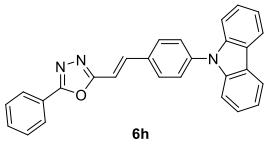

Light yellow solid, mp 180-182 °C, R.F. (Hex:EtOAc 7:3); FTIR v (cm^{-1}): 1008 (C-O), 1169 (Ar-N), 1532 (C=C, Ar), 1606 (C=C), 1637 (C=N); ^{1}H NMR (500 MHz, Chloroform-*d*) δ 8.11 – 8.07 (m, 4H), 7.76 (d, *J* = 8.4 Hz, 2H), 7.68 (d, *J* = 16.5 Hz, 1H), 7.61 (d, *J* = 8.4 Hz, 2H), 7.53 – 7.46 (m, 3H), 7.44 – 7.40 (m, 2H), 7.37 (ddd, *J* = 8.2, 6.9, 1.3 Hz, 2H), 7.25 (ddd, *J* = 7.9, 6.9, 1.1 Hz, 2H), 7.14 (d, *J* = 16.3 Hz, 1H); ^{13}C NMR (126 MHz, $CDCl_3$) δ 164.22, 140.48, 139.22, 137.79, 133.66, 131.89, 129.16, 128.98, 127.32, 127.05, 126.13, 123.84, 123.68, 120.45, 120.38, 110.64, 109.79. HRMS (ESI^+) *m/z* calc for $C_{28}H_{20}N_3O^+$ $[M + H]^+$ 414.1601, found 414.1571.

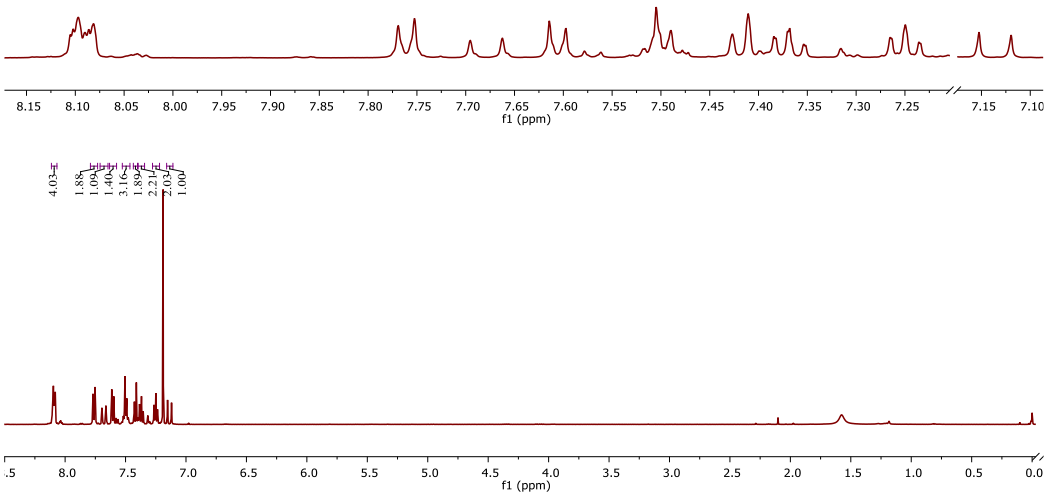

Appendix NN. ^{1}H NMR (500 MHz, $CDCl_3$) of (E)-2-(4-(9H-carbazol-9-yl)styryl)-5-phenyl-1,3,4-oxadiazole **6h**.

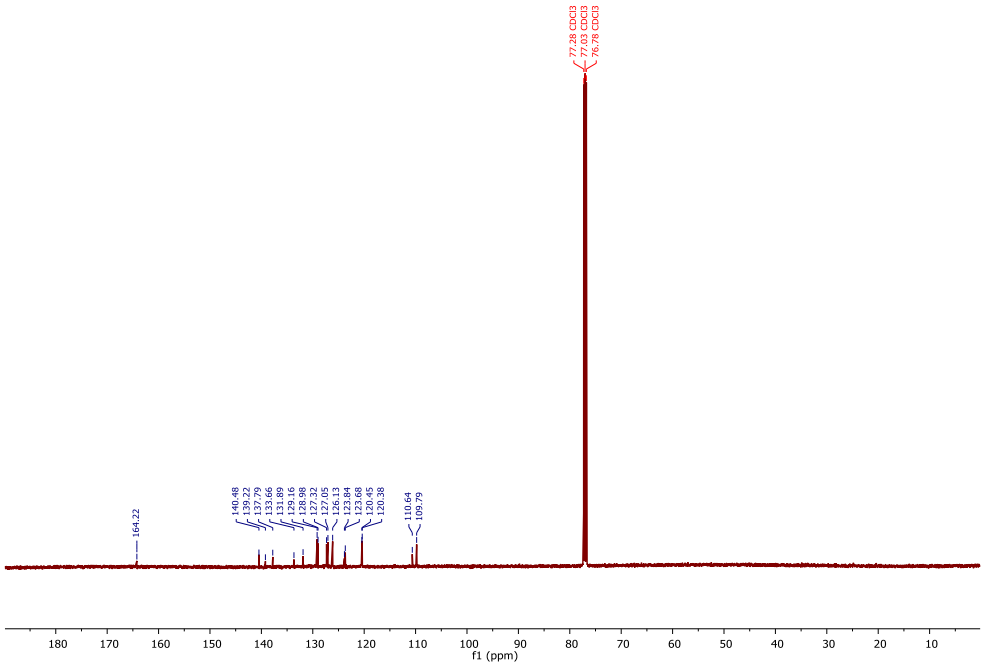

Appendix OO. ^{13}C NMR (500 MHz, $CDCl_3$) of (*E*)-2-(4-(9H-carbazol-9-yl)styryl)-5-phenyl-1,3,4-oxadiazole **6h**.

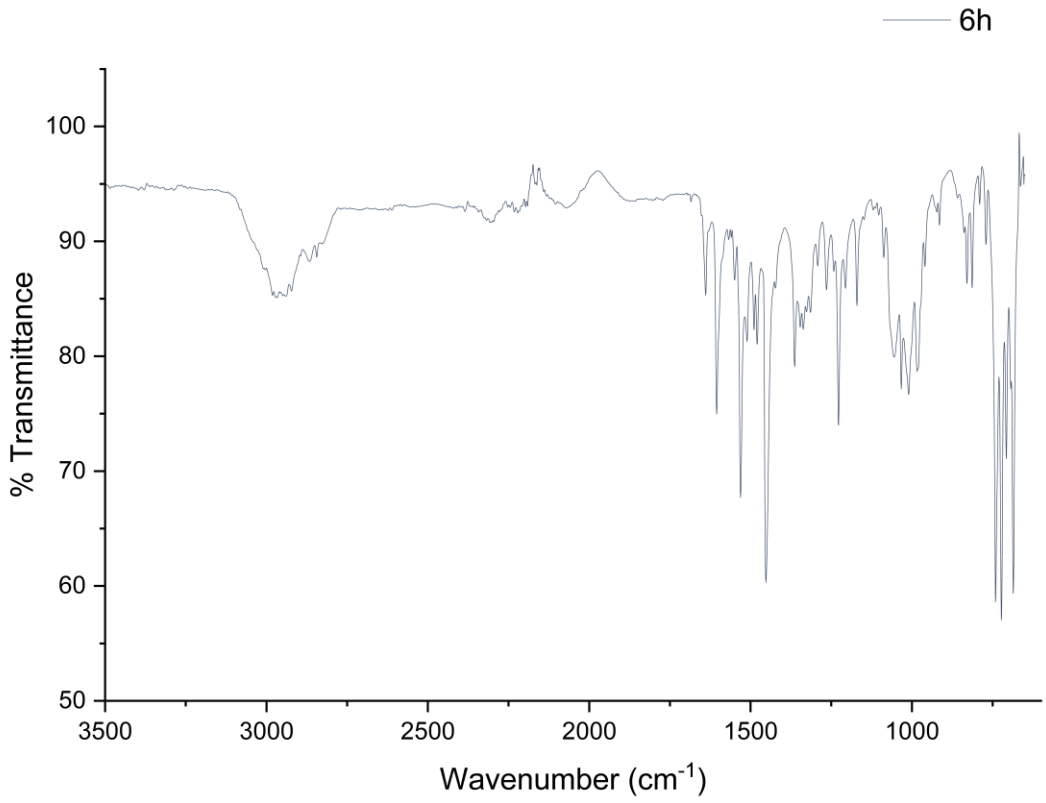

Appendix PP. FTIR of (*E*)-2-(4-(9H-carbazol-9-yl)styryl)-5-phenyl-1,3,4-oxadiazole **6h**.